Title
Cdc20 Autoubiquitination in the Spindle Assembly Checkpoint

Author
Foster, Scott Andrew

Publication Date
2013

Peer reviewed|Thesis/dissertation

Cdc20 Autoubiquitination in the Spindle Assembly Checkpoint

by

Scott Andrew Foster

DISSERTATION

Submitted in partial satisfaction of the requirements for the degree of

DOCTOR OF PHILOSOPHY

in

Biochemistry and Cellular Biology

in the

GRADUATE DIVISION

of the

UNIVERSITY OF CALIFORNIA, SAN FRANCISCO

Acknowledgements

First and foremost, I would like to thank my thesis advisor Dave Morgan. I am very grateful for the opportunity to work with Dave. He, probably against his better judgment, was willing to take three new students (and I realize I was the third he accepted) in the same year. While at the time I was torn between two labs, in hindsight the decision was clear and I have absolutely no regrets. Dave as a mentor has provided the ideal environment for me. He has given me space to figure out my own path, while at the same time ensuring that I continued moving forward. I have learned many things from Dave, but two skills really stand out. First, he has helped me to think about scientific questions from a big picture perspective. Second, he has contributed significantly in the development of my writing skills. I leave the lab feeling well prepared for my next scientific journey.

I am very grateful for the guidance throughout graduate school from my thesis committee members, Sandy Johnson and Jonathan Weissman. Thank you as well to Dave Toczyski, pseudo-committee member and collaborator, who I have worked closely with throughout graduate school.

I would also like to thank the Morgan lab. The Morgan Lab, despite consisting of an ever-changing group, has always been a supportive and fun place to work. In particular, I am very grateful for the mentoring I received in the early years from Liam Holt, Mary Matyskiela, Monica Rodrigo-Brenni, and Jon Schaefer. I am also very grateful for the support and friendship of Mike Lopez and Gilad Yaakov who have helped make the last many years much easier and more enjoyable.

I would like to thank my support group outside of lab. My classmates Ken Finn and Ian Foe are great friends and have made the last many years a lot of fun. Having my family close by has been invaluable, and they have provided tremendous support throughout the years. Last but not least, I would like to thank Stef. She has been incredibly supportive and without her I would not have made it through graduate school.

The text of Chapter 2 is a reprint of the material as it appears in Current Biology, Volume 21, Issue 22, "Ubiquitination of Cdc20 by the APC Occurs through an Intramolecular Mechanism", pages 1870-1877, copyright 2011, with permission from Elsevier. The coauthors David O. Morgan and David P. Toczyski listed in this publication co-directed and co-supervised the research that forms the basis for this Chapter. The research was performed in close collaboration with the co-first author Ian T. Foe. Ian performed the experiments found in figures 1C, 2A, 2C, 3A, 3D, 4, S1B, S1C, and S2. A few initial results that helped guide future experiments were performed by the coauthors Stephanie K. Cheung and Steven Z. DeLuca.

The text of Chapter 3 is a reprint of the material as it appears in Molecular Cell, Volume 47, Issue 6, "The APC/C Subunit Mnd2/Apc15 Promotes Cdc20 Autoubiquitination and Spindle Assembly Checkpoint Inactivation", pages 921-932, copyright 2012, with permission from Elsevier. The coauthor listed in this publication directed and supervised the research that forms the basis for this Chapter.

Cdc20 Autoubiquitination in the Spindle Assembly Checkpoint

Scott Andrew Foster

Abstract

The critical event of mitosis is the equal segregation of duplicated chromosomes to opposite poles of the cell. As would be expected for such a significant event in the life of a cell, this process is highly regulated. We explored how the regulation of the protein Cdc20 through ubiquitination contributes to proper mitotic progression in budding yeast. Cdc20 is an activating subunit of the Anaphase Promoting Complex (APC/C), the E3 ubiquitin ligase that promotes anaphase by ubiquitinating, and thereby targeting for destruction, specific mitotic inhibitors. We found that Cdc20 is also a substrate of the APC/C, which occurs through an autoubiquitination mechanism while Cdc20 is bound to the APC/C in its activator binding orientation. This activity is cell cycle regulated, and peaks in late mitosis. Using a Cdc20 mutant that is poorly ubiquitinated throughout the cell cycle, we found that this turnover is required to reset Cdc20 levels to allow cells to establish a Spindle Assembly Checkpoint (SAC) in the subsequent cell cycle. Cdc20 has also been observed to be an unstable protein during an SAC arrest, although the mechanism has largely been unexplored. Using purified components, we found that two essential SAC components, Mad2 and Mad3 (which is found in a complex with Bub3), have opposite effects on Cdc20 autoubiquitination. Mad2 inhibits full binding of Cdc20 to the APC/C, thereby inhibiting Cdc20 autoubiquitination. The Mad3-Bub3 complex increases Cdc20 binding to the APC/C, an effect that is enhanced by the presence of Mad2, effectively stimulating Cdc20 autoubiquitination. Specific inhibition of this mechanism, by deletion of the APC/C subunit Mnd2/Apc15, allowed cells to establish and SAC arrest, but delay release from the arrest. Together these results show that Cdc20 autoubiquitination has two opposing functions on mitotic progression: Cdc20

autoubiquitination is required in late mitosis to allow cells to establish an SAC arrest in the subsequent cell cycle, and Cdc20 autoubiquitination in the arrest is required for SAC inactivation.

Table of Contents

List of Figures

Chapter 3

Chapter 4

Chapter 1

Introduction

The Cell Cycle

Fundamental to the existence of life is the ability of cells to generate a copy of themselves. In the context of a single-celled organism, such as *Saccharomyces cerevisiae* (commonly referred to as budding yeast), cell division results in a whole new organism. In multi-celled organisms like us, multiple divisions result in the complex architecture of a human being. The cell cycle is the intricate process by which a cell accomplishes this feat (Morgan, 2007). The cell cycle is divided into distinct phases (see figure 1): gap phase or G1, in which an increase in cellular components and cell size occurs to support the resulting two cells; DNA replication or S phase, in which the genetic material is duplicated; and M Phase, which consists of both mitosis and cytokinesis, in which cells segregate the duplicated copies of their genetic material at the metaphase to anaphase transition and then physically split the mother cell into the two resulting daughter cells. In most cell types an additional gap phase (G2) occurs after DNA replication and before cellular division.

The cell must ensure that the distinct cell cycle stages occur in the correct order. Ordering of the cell cycle is largely accomplished by the oscillation in the activity of cyclin-dependent kinases (Cdks) (Bloom and Cross, 2007). Cdk activity requires the association of cyclin proteins, and promotes the transfer of a phosphate group from ATP to specific serine or threonine residues within a substrate. Phosphorylation can have varying effects on a given substrate, ranging from changes in localization, ability to associate with binding partners, stability, or enzymatic activity.

The periodicity of Cdk activity is accomplished through the formation of specific cyclin-Cdk complexes (Bloom and Cross, 2007). These cell cycle specific cyclin-Cdk

complexes phosphorylate unique sets of substrates that result in the characteristic cell cycle events (see figure 2): G1/S cyclin-Cdks target substrates required for cells to exit G1 and enter S phase, S phase cyclin-Cdks target substrates required for DNA replication, and mitotic cyclin-Cdks target substrates required for spindle assembly and required to drive cells to a metaphase state. Dephosphorylation of mitotic substrates by phosphatase enzymes is required for cells to exit mitosis and to maintain a G1 state.

An important feature of this system, which ensures the unidirectionality and irreversibility of the cell cycle, is the coupling of the activities of subsequent cyclin-Cdk complexes (Bloom and Cross, 2007). For example, G1/S cyclin-Cdks promote the activity of S phase cyclin-Cdks. Several mechanisms control these transitions, including regulation of gene expression, inhibitory or activating proteins, and most importantly, protein degradation. Together these regulatory mechanisms help generate the rapid transitions between subsequent cell cycle stages.

In addition to ensuring the order of each cell cycle stage, cells must also ensure that each stage is completed before the next stage is initiated. This is largely achieved by checkpoints (Morgan, 2007). Three main checkpoints exist at critical transition points in the cell cycle (see figure 2): the G1 to S transition (also called Start) monitors the cellular environment and cell size and commits cells to enter the cell cycle; the G2/M checkpoint regulates mitotic Cdk levels and commits cells to enter mitosis only when DNA replication has been completed correctly; and the metaphase to anaphase transition is regulated by a checkpoint ensuring that the critical event of mitosis, chromosome segregation, is initiated at the proper time.

Mitosis

The process of mitosis is a visually compelling event in which the duplicated genetic material is separated and equally segregated to opposite poles of the cell (Morgan, 2007). Essential to the process of equal segregation is the ability of cells to distinguish between duplicate copies of a specific chromosome from another chromosome. This is achieved through physically tethering duplicates. Upon DNA replication, duplicate chromosomal copies, referred to as sister chromatids, are held tightly together by a protein complex known as cohesin (Oliveira and Nasmyth, 2010). The tethering of sisters during DNA replication is essential for the cells to keep track of the genome and ensure that upon segregation daughter cells receive the correct chromosomal composition.

The process of mitosis occurs in discrete steps (Morgan, 2007). Initially, during prophase, chromosomes condense in order to become compact and more easily maneuvered. During prometaphase, the nuclear envelope breaks down (in the majority of organisms that undergo an 'open' mitosis), which allows sister chromatids to begin interacting with the mitotic spindle. The mitotic spindle is formed from an organelle known as the centrosome, which nucleates microtubules, providing the physical link between the sister chromatids and the poles of the cell. Budding yeast does not undergo nuclear envelope breakdown, and spindle microtubules originate in spindle pole bodies, similar to centrosomes, that are embedded in the nuclear envelope. Spindle microtubules are polymers, consisting of ordered repeats of tubulin dimers. Microtubules can undergo rapid polymerization or depolymerization mechanisms, generating the dynamics required for the movement of the chromatids.

In metaphase, a signaling system known as the Spindle Assembly Checkpoint or Mitotic Checkpoint ensures that each sister chromatid pair is properly attached to microtubules from opposite poles of the spindle (Lara-Gonzalez et al., 2012). This results in the positioning of sister chromatids in a tight line at the center of the cell, referred to as the metaphase plate. When this bi-orientation is achieved, the Anaphase-Promoting Complex (or APC/C) is activated, thereby initiating anaphase (Pines, 2011). The process of anaphase occurs through two major physical activities. First, cohesin complexes are cleaved, which allows the initial separation of sister chromatids (Oliveira and Nasmyth, 2010). Second, sister chromatid pairs are rapidly pulled in opposite directions by the dramatic depolymerization of spindle microtubules. Once sister chromatids are fully segregated, the nuclear envelope can reassemble around each complete set of the genome (in organisms with an open mitosis) or the nucleus is pinched in half in organisms with a closed mitosis. Cellular division, or cytokinesis, then splits the mother cell into two daughter cells.

The Anaphase-Promoting Complex

The APC/C is a large, unusually complex ubiquitin ligase consisting of 13 subunits in budding yeast and as many as 17 subunits in humans (Barford, 2011; Pines, 2011). The function of the APC/C is to attach the small protein ubiquitin to target proteins, resulting in the destruction of the substrate by the proteasome. The essential APC/C substrates are securin and S-phase/mitotic cyclins. Securin destruction leads to activation of the protease separase, which cleaves a subunit of the cohesin complex, relieving cohesion between sister chromatids. Cyclin destruction leads to Cdk

inactivation, allowing for the dephosphorylation of Cdk substrates required for mitotic exit.

The APC/C facilitates the transfer of ubiquitin to a substrate through the coordinated action of two additional enzymes (Barford, 2011) (see figure 3). First, free ubiquitin is activated by an E1 enzyme in an ATP-dependent reaction. Activated ubiquitin is subsequently transferred to an active site cysteine residue within the E1. Ubiquitin covalently attached to an E1 can then be transferred to an active site cysteine residue of an E2 enzyme. E2 enzymes conjugated with ubiquitin can interact with E3 enzymes, such as the APC/C, promoting the transfer of ubiquitin from the active site of the E2 to the ε-amine of lysine residues within the substrate or ubiquitin itself. The APC/C interacts with two E2s, Ubc4 and Ubc1, each with distinct properties. Ubc4 functions to initiate the ubiquitination reaction by specifically targeting lysine residues within the substrate. Ubc1 has specificity towards ubiquitinated substrates, specifically modifying lysine 48 of ubiquitin. Multiple conjugated Ubc1 molecules can bind and transfer ubiquitin per substrate-binding event, resulting in the formation of lysine 48-linked polyubiquitin chains. Lysine 48 polyubiquitin chains composed of a minimal of 4 ubiquitins are required for recognition by the proteasome.

The APC/C is the largest member of the cullin-RING ubiquitin ligase family (Barford, 2011; Pines, 2011). It is composed of two subcomplexes held together by the largest subunit Apc1 (see figure 4). One subcomplex contains the catalytic core of the APC/C, consisting of the cullin-homology subunit Apc2 and RING-finger subunit Apc11. Apc11 binds the E2 and facilitates the transfer of ubiquitin from the E2 to the substrate. Also within the catalytic subcomplex is the Doc1/Apc10 subunit, which is thought to

directly bind the substrate, increasing the affinity of the substrate and therefore increasing the processivity of the ubiquitination reaction. The other subcomplex of the APC/C, commonly referred to as the scaffolding complex, is mostly composed of three tetratricopeptide repeat (TPR) subunits Cdc16, Cdc23, and Cdc27. These subunits are tethered to Apc1 through the subunits Apc4 and Apc5. Also within this scaffolding subcomplex are the non-essential subunits Cdc26, Apc9, and Swm1/Apc13, which are thought to stabilize the three TPR subunits. Mnd2/Apc15 is also within this complex and was originally thought to function specifically in meiosis.

APC/C activity requires the association of substrate-specific activating proteins (Barford, 2011; Pines, 2011). Cdc20 is the essential APC/C activator required for cells to undergo anaphase. Cdc20 is replaced in late mitosis by Cdh1, which maintains APC/C activity into G1. The activator proteins contain highly conserved WD40 domains within their C-termini, which directly recognize destruction sequences within substrates. The two most common recognition sequences, typically found within unstructured N-terminal regions of substrates, are the "Destruction box" (D box) and "KEN box". The activators interact with the APC/C through multiple interaction motifs: The N-terminal "C box" motif is thought to interact with Apc2, and the extreme C-terminus of the activator contains a highly conserved Isoleucine-Arginine ("IR") motif that directly interacts with Cdc27. Additional interaction motifs likely exist and the combined effect of all motifs results in a very high affinity of the activator for the APC/C. Cdc20 is a substrate of the APC/C, originally thought to be recognized by Cdh1 through and N-terminal D box sequence within Cdc20. How Cdc20 is recognized and ubiquitinated by the APC/C was an open question, which we addressed.

The APC/C and the Spindle Assembly Checkpoint

How do cells ensure the sister chromatids are equally segregated? The Spindle Assembly Checkpoint (SAC) ensures equal segregation by preventing activation of the APC/C until all sister chromatids have achieved bi-orientation (Lara-Gonzalez et al., 2012).

At the center of the SAC signaling network is the kinetochore (Gascoigne and Cheeseman, 2011). The kinetochore is a large protein complex that contains both DNA-binding and microtubule-binding proteins, therefore providing the link between the chromosomes and the mitotic spindle. In addition to providing this critical link, the kinetochore must also sense whether each kinetochore is properly attached to the spindle, as errors in attachment can have catastrophic results for the cell. If improper attachments are not sensed and corrected, cells undergoing anaphase with attachment errors will result in abnormal chromosomal numbers, or aneuploidy, a common characteristic of many human diseases including cancer.

An essential molecular target of the SAC is APC/C-Cdc20 (Lara-Gonzalez et al., 2012). By inhibiting Cdc20, the SAC prevents mitotic progression when sister chromatids are improperly attached to the mitotic spindle. The key SAC components in this pathway are Mad1, Mad2, Mad3 (BubR1 in vertebrates), and Bub3. All of these components are recruited to and activated at unattached kinetochores.

The most upstream component is Mad1, which upon localization to unattached kinetochores becomes hyperphosphorylated. Activated Mad1 recruits and induces a conformational change in Mad2, which results in the reorientation of the C-terminal

region of Mad2. This region, commonly referred to as the "seatbelt", wraps around a region within Mad1 upon activation. The Mad1-Mad2 complex is stably associated with unattached kinetochores and provides a binding site for soluble molecules of Mad2. Binding of soluble Mad2 to this complex activates the soluble molecule of Mad2, promoting the "seatbelt" region to bind to Cdc20. Two additional checkpoint proteins, Mad3 and Bub3, form a stable complex, which also binds to Cdc20 and binds preferentially to Cdc20 already bound to Mad2. The final output of the checkpoint is an inhibitory complex known as the mitotic checkpoint complex (MCC), which contains Cdc20, Mad2, Mad3, and Bub3. Little was known about how this complex inhibits APC/C activity, although there is evidence that Mad3 functions as a pseudosubstrate. We addressed how the various components of the MCC inhibit the APC/C.

Cdc20 has also been observed to be an unstable protein during a SAC arrest (Lara-Gonzalez et al., 2012). The mechanism of this instability had largely been unexplored and here we addressed the mechanism by which the SAC regulates this turnover. We further explored this question using Cdc20 mutants and APC/C mutants that allowed us to better characterize the role of this turnover.

Figure 1. Distinct phases of the cell cycle

The key events of the cell cycle are highlighted. Reproduced with permission from The Cell Cycle, Principle of Control (Morgan, 2007).

Figure 1

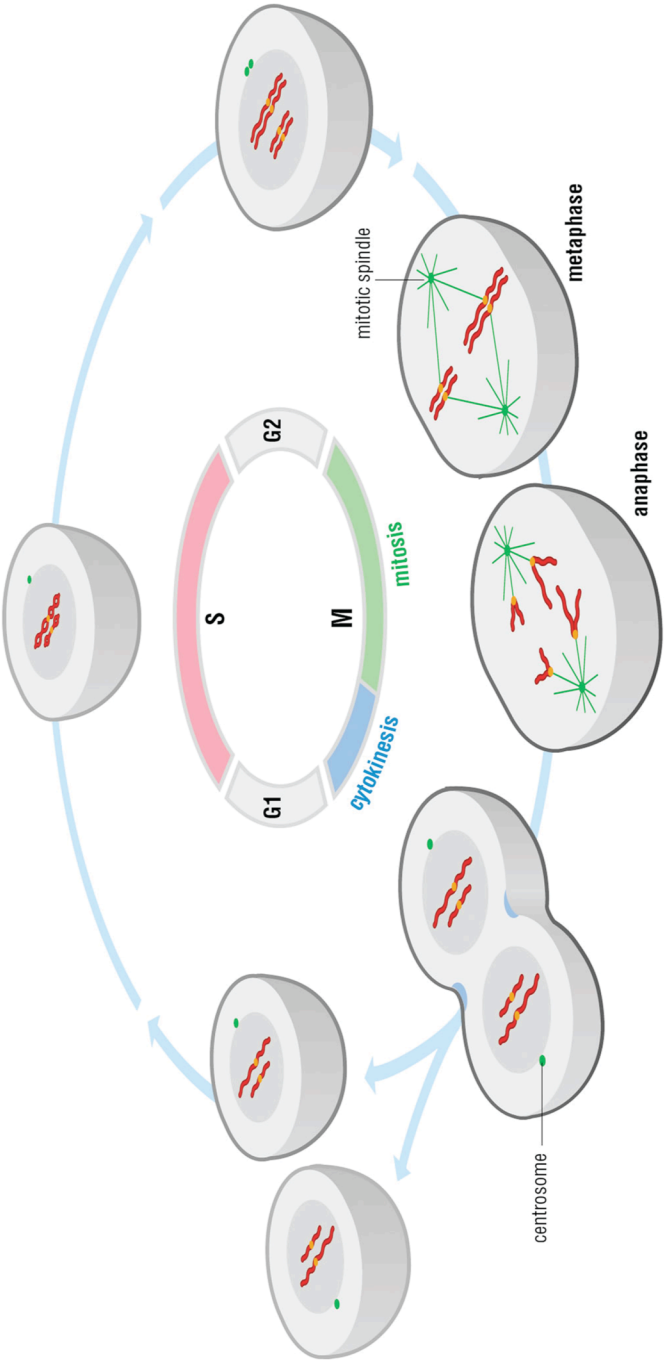
metaphase
mitotic spindle
anaphase
G2
S
M
mitosis
cytokinesis
G1
centrosome

Chapter 2. Schematic of the cell cycle control system

The cell cycle is driven by the oscillations in Cyclin-Dependent Kinase (Cdk) activity, with overall low Cdk activity in G1 and higher Cdk activity throughout the rest of the cell cycle. Specific Cyclin (either G1/S, S, or M)-Cdk complexes target distinct sets of substrates, contributing to the characteristic events of a given cell cycle stage. Transition between these cell cycle stages is controlled by the checkpoints: 'Start', 'G2/M', and 'metaphase-anaphase'. The Anaphase-Promoting Complex (APC/C) promotes transition past the 'metaphase-anaphase' checkpoint, known as the Spindle Assembly Checkpoint, and resets Cdk activity for the subsequent cell cycle. Reproduced with permission from The Cell Cycle, Principle of Control (Morgan, 2007).

Figure 2

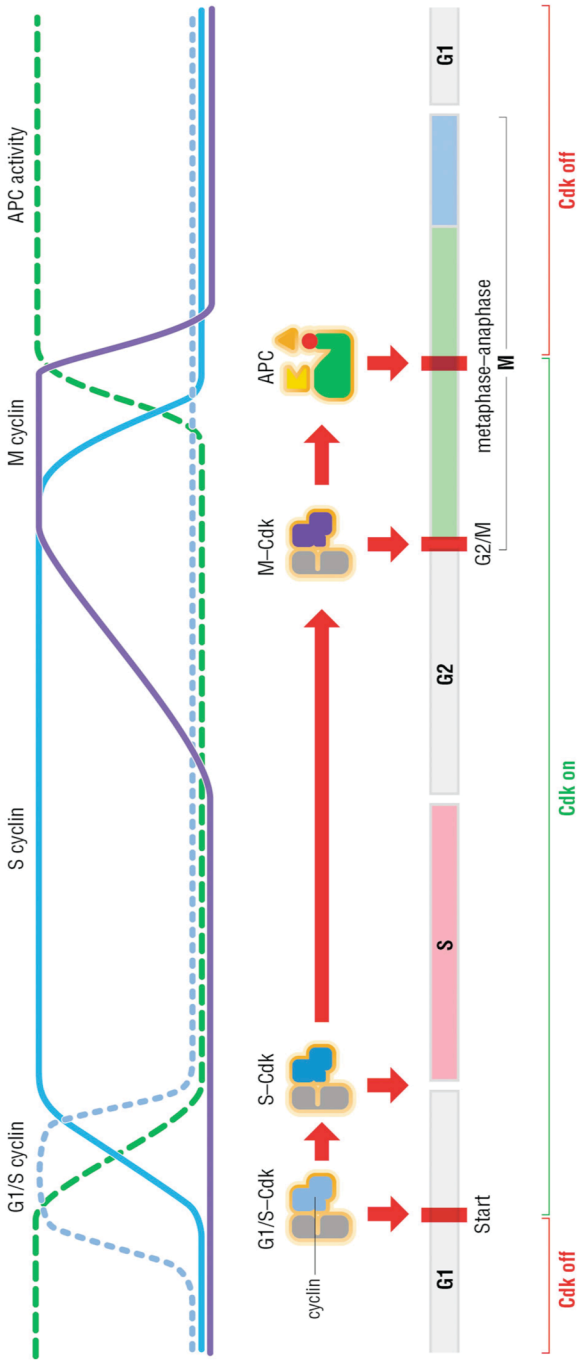
APC activity
M cyclin
S cyclin
G1/S cyclin
APC
M–Cdk
S–Cdk
G1/S–Cdk
cyclin
G1
S
G2
G2/M
metaphase–anaphase
M
Start
G1
Cdk off
Cdk on
Cdk off

Figure 3. The ubiquitination cascade

The ubiquitination cascade begins with the activation and transfer of ubiquitin to an active site cysteine within the E1 enzyme. Ubiquitin is subsequently transferred to an active site cysteine of one of many E2 enzymes. E2s bind to E3 enzymes, in this case the Anaphase-Promoting Complex, and transfer the ubiquitin to the substrate. Depending upon the specificity of the E2, either a lysine within the substrate or a lysine within ubiquitin itself will be modified. Specific E2s build ubiquitin chains linked through lysine 48, which results in the recognition of the polyubiquitinated substrate by the proteasome.

Figure 3

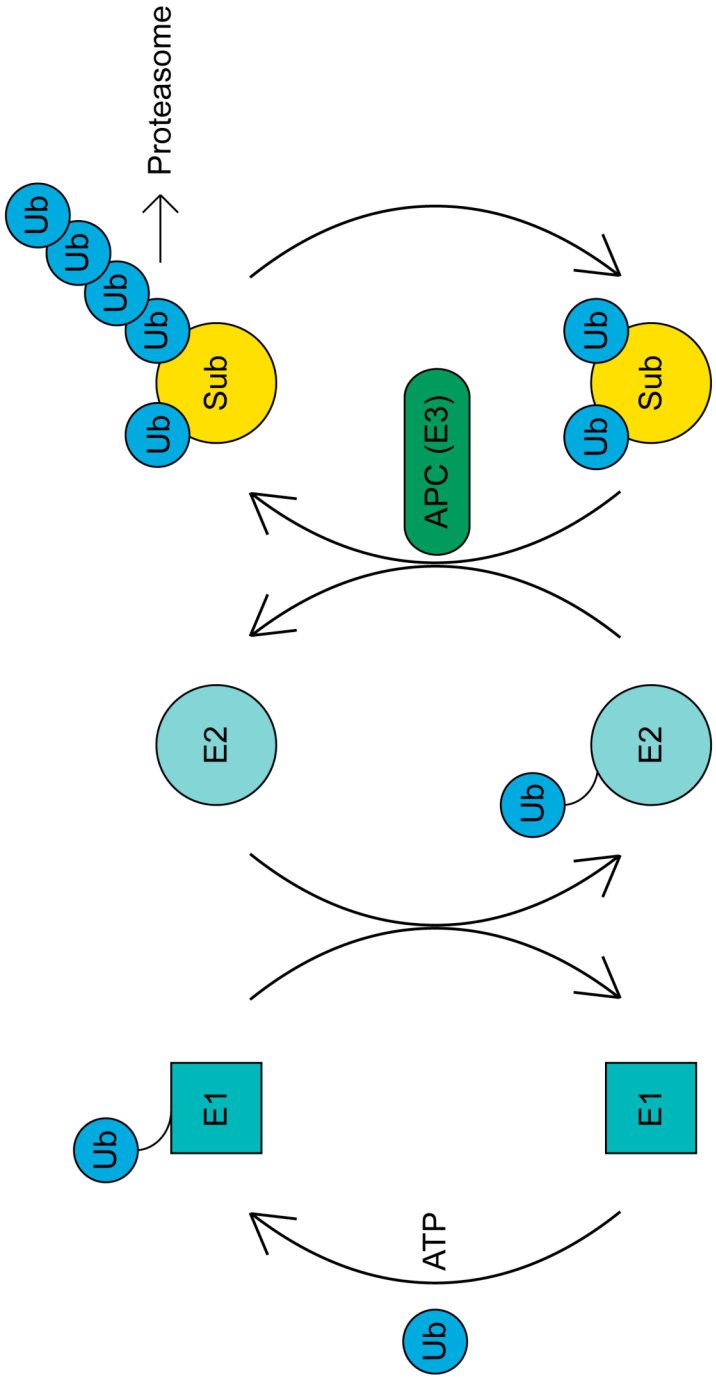
Proteasome
Ub
Ub
Ub
Ub
Sub
Ub
APC (E3)
Ub
Sub
Ub
E2
E2
Ub
Ub
E1
E1
ATP
Ub

Figure 4. The Anaphase-Promoting Complex (APC/C)

The APC/C is a large, complex E3 ubiquitin ligase, with the budding yeast subunits highlighted. The APC/C can be subdivided into two subcomplexes, the catalytic subcomplex and the scaffolding subcomplex, held together by the largest subunit Apc1. The catalytic subcomplex consists of Apc2, Apc11, and Doc1/Apc10. The E2-ubiquitin conjugate binds to Apc11. The scaffolding complex consists of Cdc16, Cdc23, Cdc27, Apc4, Apc5, and Mnd2. The activating subunit Cdc20 interacts with Cdc27 through its C-terminal IR motif and likely interacts with Apc2 through its N-terminal C box motif. Three non-essential subunits, Cdc26, Apc9, and Swm1/Apc13 are not shown.

Figure 4

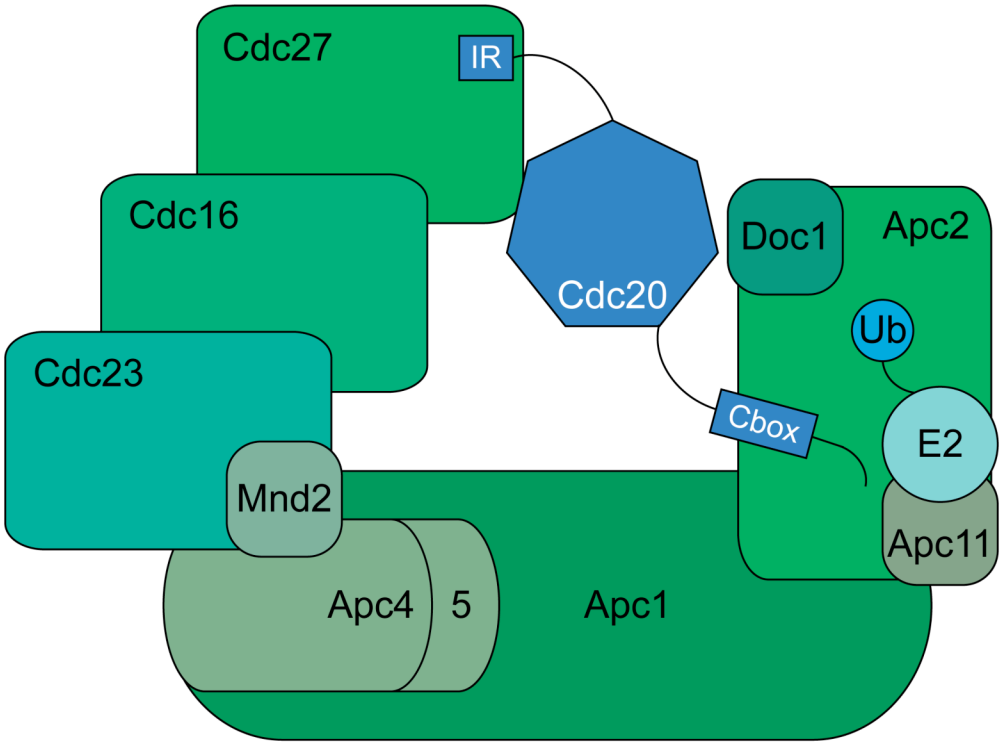
Cdc27
IR
Cdc16
Cdc20
Doc1
Apc2
Ub
Cdc23
Cbox
E2
Mnd2
Apc11
Apc4
5
Apc1

REFERENCES

Barford, D. (2011). Structure, function and mechanism of the anaphase promoting complex (APC/C). Q Rev Biophys *44*, 153-190.

Bloom, J., and Cross, F.R. (2007). Multiple levels of cyclin specificity in cell-cycle control. Nat Rev Mol Cell Biol *8*, 149-160.

Gascoigne, K.E., and Cheeseman, I.M. (2011). Kinetochore assembly: if you build it, they will come. Curr Opin Cell Biol *23*, 102-108.

Lara-Gonzalez, P., Westhorpe, F.G., and Taylor, S.S. (2012). The spindle assembly checkpoint. Curr Biol *22*, R966-980.

Morgan, D.O. (2007). The Cell Cycle: Principles of Control (London: New Science Press).

Oliveira, R.A., and Nasmyth, K. (2010). Getting through anaphase: splitting the sisters and beyond. Biochemical Society transactions *38*, 1639-1644.

Pines, J. (2011). Cubism and the cell cycle: the many faces of the APC/C. Nat Rev Mol Cell Biol *12*, 427-438.

Chapter 2

Ubiquitination of Cdc20 by the APC occurs through an intramolecular mechanism

Ian T. Foe*, Scott A. Foster*, Stephanie K. Cheung, Steven Z. DeLuca, David O. Morgan, and David P. Toczyski

Departments of Physiology and Biochemistry & Biophysics, University of California, San Francisco, San Francisco, CA.

Published: November 22, 2011 *Current Biology*, 21(22): 1870-7.

SUMMARY

Background: Cells control progression through late mitosis by regulating Cdc20 and Cdh1, the two mitotic activators of the Anaphase Promoting Complex (APC). The control of Cdc20 protein levels during the cell cycle is not well understood.

Results: Here, we demonstrate that Cdc20 is degraded in budding yeast by multiple APC-dependent mechanisms. We find that the majority of Cdc20 turnover does not involve a second activator molecule, but instead depends on *in cis* Cdc20 autoubiquitination while it is bound to its activator-binding site on the APC core. Unlike *in trans* ubiquitination of Cdc20 substrates, the APC ubiquitinates Cdc20 independent of APC activation by Cdc20's C-box. Cdc20 turnover by this intramolecular mechanism is cell cycle-regulated, contributing to the decline in Cdc20 levels that occurs after anaphase. Interestingly, high substrate levels *in vitro* significantly reduce Cdc20 autoubiquitination.

Conclusion: We show here that Cdc20 fluctuates through the cell cycle via a distinct form of APC-mediated ubiquitination. This *in cis* autoubiquitination may preferentially occur in early anaphase, following depletion of Cdc20 substrates. This suggests that distinct mechanisms are able to target Cdc20 for ubiquitination at different points during the cell cycle.

INTRODUCTION

Chromosome segregation is one of the most tightly regulated events in the dividing cell. Incorrect entry into anaphase can have catastrophic cellular consequences ranging from genomic instability to cell death. Anaphase is initiated by the Anaphase-Promoting Complex/Cyclosome (APC) (Sudakin et al., 1995; King et al., 1995), an E3 ubiquitin ligase composed of at least 13 core subunits (Yoon et al., 2002; Thornton and Toczyski, 2006). APC function is regulated by association with one of two activator subunits, Cdc20 or Cdh1 (also known as Hct1) (Visintin et al., 1997; Schwab et al., 1997; Dawson et al., 1995). These proteins are thought to function both in the binding of substrates to the APC (Schwab et al., 2001) and APC activation (Kimata et al., 2008). Cdc20 associates with the APC in early mitosis, and triggers anaphase onset by promoting the destruction of a subset of mitotic cyclins and Securin (also known as Pds1) (Shirayama et al., 1999; Cohen-Fix et al., 1996), resulting in the activation of Esp1, and the separation of sister chromatids through cleavage of cohesion (Oliveira and Nasmyth, 2010). In late mitosis and G1, Cdh1 associates with the APC, promoting mitotic exit and maintaining low Cdk activity.

Both activators contain well-conserved motifs involved in APC and substrate binding (Figure 1A). APC binding is mediated by both a C-box motif within the activator's N-terminus (Schwab et al., 2001) and a C-terminal Isoleucine-Arginine (IR) motif (Vodermaier et al., 2003; Passmore et al., 2003) (Figure 1A). Substrate binding is mediated by a WD40 domain that is likely to interact directly with degradation signals found within substrates (Kraft et al., 2005), the most common being the Destruction box

(D-box) (Glotzer et al., 1991) and KEN-box (Pfleger and Kirschner, 2000). Processive substrate ubiquitination has also been shown to require the core APC subunit Doc1 (Passmore et al., 2003; Carroll and Morgan, 2002), which is thought to function as a co-receptor for the D-box in conjunction with the WD40 of Cdc20/Cdh1 (Carroll et al., 2005; da Fonseca et al., 2011).

The two mitotic APC activators are thought to function analogously, but they are regulated in distinct ways. While Cdh1 protein and transcript levels are constitutive, Cdc20 transcription and protein levels both oscillate throughout the cell cycle (Prinz et al., 1998). Cdc20 is absent in G1, but begins to accumulate in late S phase, its peak coinciding with the initiation of anaphase. Cdh1 is thought to bind an N-terminal D-box within Cdc20, leading to the destruction of Cdc20 in late mitosis and G1 (Yu, 2007; Manchado et al., 2010; Pesin and Orr-Weaver, 2008). However, while Cdh1-mediated turnover of Cdc20 is likely important, several studies have suggested that Cdc20 is also turned over by Cdh1-independent mechanisms (Prinz et al., 1998; Thornton et al., 2006; Robbins and Cross, 2011). Regulation of Cdc20 levels is very important, as high-level over-expression of Cdc20 is lethal (Lim and Surana, 1996) and as little as three-fold over-expression of Cdc20 is sufficient to override the spindle assembly checkpoint (Pan and Chen, 2004).

Previously, we found that deletion of Cdc20's IR domain caused a strong accumulation of Cdc20 *in vivo* (Thornton et al., 2006), which is inconsistent with Cdc20 simply being a passive Cdh1 substrate. Here, we show that Cdc20 turnover is fully APC-dependent, but does not depend on a second activator molecule. While Cdc20 can be targeted by the APC associated with either Cdh1 or, more poorly, by a second Cdc20

molecule (i.e. *in trans* turnover), we find that most turnover *in vivo,* and ubiquitination *in vitro,* is promoted by direct association with the APC (*in cis* turnover) (Figure 1B). Consistent with this model, we show that processive ubiquitination of Cdc20 does not require Doc1. Importantly, we find that Cdc20 levels oscillate independently of *CDC20* transcription and Cdh1 activity, implying that the *in cis* autoregulation of Cdc20 turnover changes during the cell cycle. Additionally this regulation can be influenced by the presence of APC^{Cdc20} substrates. These findings uncover another mechanism by which the activity of the APC is tightly controlled during the cell cycle.

RESULTS

Cdc20 turnover depends on the APC

Cdc20 is thought to be destroyed by both APC-dependent mechanisms (Prinz et al., 1998; Shirayama et al., 1998; Goh et al., 2000) and APC-independent mechanisms (Goh et al., 2000). However, previous experiments suggesting APC-independent Cdc20 turnover were performed with temperature-sensitive APC mutants, which do not necessarily eliminate all APC function. While the APC is normally essential, we have previously shown that deletion of genes encoding two Cdc20 substrates, Pds1 and Clb5, combined with 10-fold over-expression of the Cdk inhibitor Sic1 (*SIC1*^{10x}), allows cells to survive in the absence of the APC (Thornton and Toczyski, 2003). To determine whether Cdc20 turnover is dependent upon a functional APC, we examined Cdc20 turnover in an *apc11Δ pds1Δ clb5Δ SIC1*^{10x} strain. Deletion of *APC11*, which encodes the essential RING finger subunit of the APC (Zachariae et al., 1998), abolishes APC activity in the cell. We found that, as with the known APC substrate Clb2 (Amon et al., 1994), turnover of Cdc20 was eliminated in the *apc11*Δ strain (Figure 1C). This strongly suggests that, under normal conditions, the majority of Cdc20 turnover depends on APC activity.

We postulated that there could be three modes of APC-dependent Cdc20 turnover (Figure 1B). First, as previously suggested, Cdh1 bound to the APC as an activator could recognize Cdc20 as a substrate through Cdc20's D-box (Cdh1^{trans}) (Yu, 2007); (Manchado et al., 2010; Pesin and Orr-Weaver, 2008). However, we found previously that while Cdc20 levels were slightly increased in *cdh1Δ* cells, they were more

dramatically increased in Apc$^-$ cells (Thornton et al., 2006), suggesting that the APC targets Cdc20 by Cdh1-independent mechanisms as well. Consistent with this, we observed APC-dependent ubiquitination of Cdc20 both in the presence and absence of Cdh1 *in vitro* (Figure 1D).

There are two distinct mechanisms by which Cdh1-independent ubiquitination could occur. The first is similar to the Cdh1^{trans} mechanism. Here, one molecule of Cdc20 associates with the APC as an activator and this APC-Cdc20 complex binds a second Cdc20 molecule as a substrate through a WD40/D-box interaction (Cdc20^{trans}, Figure 1B). Alternatively, a single Cdc20 molecule bound to the APC as an activator could be ubiquitinated directly by the APC (Cdc20^{cis}, Figure 1B).

Contribution of the Cdh1-dependent and independent mechanisms to Cdc20 turnover

We found previously that mutation of Cdc20's IR motif increased steady-state Cdc20 levels (Thornton et al., 2006), consistent with a Cdh1-independent mechanism for Cdc20 turnover. This increase in steady-state level is higher than that observed for wildtype Cdc20 in a *cdh1Δ* strain, suggesting that the Cdh1-independent mechanism is responsible for the majority of Cdc20 turnover (Figure 2A, lanes 5&9) (Thornton et al., 2006). The IRΔ and *cdh1*Δ double mutant was more stable than either single mutant, consistent with multiple mechanisms controlling Cdc20 stability (Figure 2A lanes 5-16). Since mutation of the IR decreases Cdc20 binding to the APC (data not shown), both Cdc20^{trans} and Cdc20^{cis} could, in principle, be affected. Consistent with this idea, we

found that mutation of the IR had no effect on Cdh1-dependent ubiquitination *in vitro* (Supplementary Fig. 1A) but greatly inhibited autoubiquitination (Figure 2B, lanes 9-12).

To further assess the contribution of the $Cdh1^{trans}$ mechanism in isolation, we sought to create a Cdc20 mutant that was defective in binding to the APC as an activator, but could be bound as a substrate through its D-boxes. The observation that mutation of Cdc20's IR motif has no obvious growth phenotypes is consistent with it only having a partial effect on Cdc20 binding to the APC. Mutation of C-box, however, is lethal and decreases Cdc20 binding to the APC (Schwab et al., 2001; Thornton et al., 2006), suggesting that C-box mutations greatly reduce interaction with the APC. Therefore, we expected a C-box mutation to eliminate $Cdc20^{cis}$ and $Cdc20^{trans}$ mediated turnover. The minimal conserved sequence of the C-box in both Cdc20 and Cdh1 is DRYIP (Schwab et al., 2001). Previously, we characterized two C-box mutants, a weaker *cdc20-I147A,P148A* allele and a stronger *cdc20-R145D* allele (which did not translate well *in vitro*) (Thornton et al., 2006). We examined the turnover of Cdc20-R145D in a *cdh1Δ* strain. Surprisingly, while the known Cdc20 substrate Dbf4 was stabilized, the Cdc20-R145D protein was still turned over rapidly, although there was an increase in steady-state levels (Figure 2C lanes 4-9 and Supplementary Fig. 1B). It was possible that this mutation did not entirely eliminate C-box function, so we also analyzed a *cdc20-D144R, R145D* double mutant. This mutant turned over with similar kinetics to the *cdc20-R145D* allele (Supplementary Fig. 1C).

We also observed that the *I147A, P148A* C-Box mutant had a larger effect than the IR mutation on securin ubiquitination *in vitro* (Figure 2D, lanes 7-12). Yet the defect observed with the same C-box mutation is less severe than that observed with the IR

mutant in autoubiquitination activity (Figure 2B, lanes 5-12). Thus, while the C-Box is essential for APC function *in vivo*, considerable Cdc20 turnover occurs when the C-box is mutated. Our results, together with previous evidence that the C-box, but not the IR, is essential for viability, indicates that the C-box is more important than the IR motif for substrate turnover and less critical for Cdc20 autoubiquitination.

Since neither the IR nor C-box mutation alone eliminated Cdh1-independent turnover, we generated a C-box, IR double mutant. Cdc20-IR, R145D should not be able to interact with the APC as an activator and therefore should eliminate both the $Cdc20^{trans}$ and $Cdc20^{cis}$ mechanisms of turnover. Consistent with this, the Cdc20-IR, R145D mutant was strongly stabilized in a *cdh1Δ* strain, but could be turned over in a *CDH1* strain (Figure 3A, lanes 7-9 and 13-15). Similarly, we detected ubiquitination of a Cdc20-C-box-IR mutant in the presence of Cdh1 *in vitro* and this activity was entirely D-box-dependent (Figure 3B, lanes 1-6). These results are consistent with previously suggested model that Cdh1 can target Cdc20 (Yu, 2007; Manchado et al., 2010; Pesin and Orr-Weaver, 2008). However, the dramatic increase in steady-state levels and the relatively slow rate of turnover in the $Cdh1^{trans}$-only strain suggests that Cdh1-dependent turnover likely contributes to a small portion of normal Cdc20 turnover (Figure 3A, lanes 7-9).

We next sought to investigate if the $Cdc20^{trans}$ mechanism makes any contribution to Cdh1-independent turnover. We generated a *cdh1Δ* strain containing a wildtype copy of *CDC20* and the *cdc20-IR, R145D* allele at a second locus. Turnover of Cdc20-IR, R145D should be defective in both the $Cdh1^{trans}$ and $Cdc20^{cis}$ mechanisms in this strain and should therefore be turned over exclusively by $Cdc20^{trans}$. This Cdc20-IR, R145D mutant was slightly more stable than that observed in the $Cdh1^{trans}$-only strain, suggesting

that the Cdc20^{trans} mechanism does occur, but likely contributes very little to Cdh1-independent turnover (Figure 3A, lanes 10-12). To further characterize the Cdc20^{trans} mechanism, we tested whether a wildtype copy of Cdc20 can ubiquitinate this double mutant *in vitro*. We detected very little ubiquitination of this mutant in the presence of a wildtype copy of Cdc20 and the little stimulation seen over background was D-box-dependent (Figure 3C, lanes 4-6 & 10-12). Interestingly, while this D-box appears Cdh1-specific in terms of targeting Cdc20 as a substrate *in vitro*, we did see a slight defect with this mutant both in direct binding to the APC and in targeting Securin for ubiquitination *in vitro,* suggesting that Cdc20's D-box may have an additional function (data not shown).

Given that total Cdc20 turnover appeared significantly faster than turnover via either Cdc20^{trans} or Cdh1^{trans}, we examined the contribution of the Cdc20^{cis} mechanism using an allele of Cdc20 that could only be bound to the APC as an activator and not as a substrate. We generated a *cdh1Δ* strain in which the only copy of Cdc20 is mutated at its first D-box (*cdc20-DB*), and thus cannot function as a substrate in a Cdc20^{trans} reaction. In this strain, where only Cdc20^{cis} turnover occurs, Cdc20 turnover is quite fast, and steady-state Cdc20 levels are low, similar to those in a *cdh1Δ* strain where both Cdh1-independent mechanisms can occur (Fig. 3D, lanes 1-8). These data suggest that Cdc20^{cis} is the dominant form of Cdc20 turnover, with the contribution of Cdc20^{trans} being very small (Figure 3D, lanes 9-12).

To determine the extent to which the first D-box mutation eliminates Cdc20^{trans} turnover *in vivo*, we examined its effect in our strain that uses Cdc20^{trans} exclusively (see Figure 3A, lanes 10-12). We found that Cdc20-IR, R145D, DB was extremely stable in a

CDC20 cdh1Δ strain, although a very low level of turnover did occur (Figure 3D, lanes 13-16). Mutation of a second N-terminal D-box had no additional effect (data not shown). Thus, the D-box mutation eliminated *in trans* turnover, consistent with previous reports (Prinz et al., 1998; Shirayama et al., 1998). These data suggest that $Cdc20^{cis}$ is the dominant form of Cdc20 turnover, with the contribution of $Cdc20^{trans}$ being very small (Figure 3D, lanes 5-8 & 9-12).

The nonessential APC subunit Doc1 (APC10) is thought to interact directly with the D-box of substrates and enhance processivity by limiting the dissociation rate of the substrate (Passmore et al., 2003; Carroll and Morgan, 2002; Carroll et al., 2005). Deletion of this subunit or mutation of 4 residues (Doc1-4A) within its putative substrate-binding site leads to a decrease in the number of ubiquitins conjugated to the substrate, as visualized by a significant decrease in higher molecular weight substrate-ubiquitin bands and accumulation of mono-ubiquitinated substrate (Figure 3E, lanes 1-8) (Carroll et al., 2005). Cdc20 contains a D-box that has been shown to be important in Cdh1-dependent ubiquitination (Prinz et al., 1998). We tested whether a Doc1/D-box interaction was required for processive ubiquitination of Cdc20 *in vitro* in the absence of Cdh1. Unlike our results with all other substrates tested, mutation of Doc1 had no effect on the processivity of this reaction. Doc1 and Doc1-4A had nearly identical activity towards Cdc20 (Figure 3E, lanes 9-16), implying that Doc1 is not required for Cdh1-independent ubiquitination of Cdc20. These data strongly suggest that Cdc20 is not ubiquitinated by the APC as a canonical substrate, and can best be explained by the $Cdc20^{cis}$ mechanism of autoubiquitination.

Cdc20 levels oscillate independently of Cdh1 and Cdc20 transcriptional oscillation

Cdh1 activity is cell-cycle regulated, which contributes to Cdc20 periodicity. We sought to determine if Cdh1-independent mechanisms are also important for oscillations in Cdc20 levels. Since *cdh1*Δ cells do not arrest well in alpha factor, we examined Cdc20 levels through the cell cycle using *cdh1Δ cdc15-2* cells. Cells were arrested at the non-permissive temperature in anaphase and released into the permissive temperature. Consistent with a recent report, we found that Cdh1 is not necessary for Cdc20 levels to fluctuate with the cell cycle (Figure 4A, Supplementary Fig. 3A) (Robbins and Cross, 2011).

To examine the extent to which oscillations in *CDC20* transcription contribute to the fluctuation of Cdc20 levels, we generated a strain with *CDC20* under the control of a constitutive promoter (*TEF1p*). Cdc20 levels were still periodic in this strain. Moreover, Cdh1 was not required for this periodicity (Figure 4B, Supplementary Fig. 3B). While Cdh1-dependent turnover of Cdc20 and cell cycle-regulated transcription both contribute to Cdc20 cycling, Cdh1-independent turnover mechanisms appear to add significantly to Cdc20 oscillation.

Substrates inhibit Autoubiquitination

If Cdc20 targets itself while bound to the APC as an activator, then how does the cell maintain Cdc20 levels sufficient to trigger anaphase? We tested the possibility that the binding of substrates to Cdc20 might inhibit autoubiquitination, maintaining Cdc20 stability until its targets are depleted in anaphase. We generated an N-terminal fragment (aa 1-110) of budding yeast securin, containing the characterized destruction motif

(Cohen-Fix et al., 1996). As expected for a competitive inhibitor, this fragment potently inhibited securin ubiquitination (IC_{50} ~ 200 nM) (Figure 5A). A 10 μM concentration of the securin fragment completely inhibited ubiquitination of securin (Figure 5A). This concentration of the fragment also inhibited the total activity and processivity of Cdc20 autoubiquitination (Figure 5B). These results support the notion that substrate blocks autoubiquitination, prolonging Cdc20 levels in the cell until substrates are depleted (Figure 6).

DISCUSSION

One of the first APC substrates to be identified was its own activator, Cdc20, hinting at the existence of autoregulation (Prinz et al., 1998; Shirayama et al., 1998). Initial reports suggested that Cdc20 behaved similarly to other APC substrates, being targeted in part via a different activator (Cdh1) through Cdc20's D-box (Yu, 2007; Manchado et al., 2010; Pesin and Orr-Weaver, 2008). Interestingly, we show here that, unlike other APC substrates, Cdc20 is largely targeted for destruction by the APC through an autoubiquitination mechanism that occurs when Cdc20 is bound to the APC as an activator. Importantly, this mechanism appears to be regulated throughout the cell cycle, and may be influenced by the presence or absence of substrates.

The observation that Cdc20 turnover was only partially reduced in conditional APC mutants led some authors to speculate that the residual turnover observed might be mediated by an APC-independent pathway. Our work in a strain that permits the deletion of the *APC11* gene shows that in unperturbed cells, Cdc20 is turned over solely by the APC. This discrepancy is likely due to the fact that conditional alleles may not be completely null for APC activity, whereas deletion of the gene encoding the catalytic subunit (*APC11*) eliminates activity completely.

APC^{Cdh1} has long been assumed to be the APC complex that targets Cdc20 for destruction ($Cdh1^{trans}$, Figure 1B) (Pfleger and Kirschner, 2000; Yu, 2007; Manchado et al., 2010; Pesin and Orr-Weaver, 2008). However, deletion of *APC11* leads to much greater steady-state levels of Cdc20 than deletion of *CDH1*, suggesting the existence of other APC-mediated mechanisms (Thornton et al., 2006). This suggests two obvious

models for turnover. First, Cdc20 bound to the APC as an activator could recognize another molecule of Cdc20 leading to ubiquitination of the substrate Cdc20 ($Cdc20^{trans}$, Figure 1B). In this case, the substrate Cdc20 should behave similarly to other Cdc20 substrates. Alternatively, Cdc20 may bind to the APC as an activator and this binding alone may be sufficient for autoubiquitination ($Cdc20^{cis}$, Figure 1B). To evaluate the relative contributions of the three possible modes of Cdc20 turnover, we generated strains in which only one mechanism of turnover was possible and performed *in vitro* experiments with similar perturbations. These experiments strongly suggested that $Cdc20^{cis}$ is the predominant form of Cdc20 turnover.

Previous work showed that Cdc20 not only recruits substrates to the APC, but also serves to activate the APC, since its presence was also required for the ubiquitination of the APC substrate Nek2A, which can bind the APC independently of an activator (Kimata et al., 2008; Hayes et al., 2006). Importantly, these results suggested that an N-terminal fragment of Cdc20 containing the C-box was sufficient to activate the APC toward Nek2A, and that the C-box was required for this activation (Kimata et al., 2008). Interestingly, we find that a Cdc20 C-box mutant, which does not support viability and is unable to drive Dbf4 turnover in vivo (Fig. 2C) (Thornton et al., 2006), is still targeted for turnover by the APC, although its turnover is compromised. This result suggests that the C-box is not absolutely required for APC activity, but is specifically required for stimulating APC activity towards other APC substrates, potentially by properly orientating either the substrate and or the catalytic arm of the APC so substrate ubiquitination can occur. Interestingly, deletion of the C-terminal IR domain, which does not result in a growth defect, has a significant effect on Cdc20 turnover, slightly greater

than the defect seen for the lethal C-box mutant. The IR domain has been shown to interact with Cdc27, the terminal subunit of the TPR arm (Vodermaier et al., 2003; Thornton et al., 2006; Matyskiela and Morgan, 2009). The non-essential nature of the IR-Cdc27 interaction could suggest that it is an intermediate in the reaction mechanism when Cdc20 is particularly susceptible to autoubiquitination. Consistent with this observation, this interaction is not required for the processive ubiquitination of other APC substrates (Matyskiela and Morgan, 2009). However, the lack of affinity provided by the Cdc27-IR interaction is compensated by an interaction between the activator, substrate, and Doc1 on the APC core. However, autoubiquitination does not use Doc1, possibly, making the affinity provided by the Cdc27-IR interaction more important.

The discovery that Cdc20 is targeted for turnover by Cdh1, which is itself cell-cycle regulated, suggested a mechanism by which Cdc20's cyclical expression could be achieved. Work from the Cross lab (Robbins and Cross, 2011) and from experiments presented here suggests that Cdh1 may contribute to but is not necessary for Cdc20's cell cycle oscillation. However, previous work (Prinz et al., 1998) suggested that oscillation in Cdc20 levels is also achieved by transcriptional regulation. *CDC20* is a member of the *CLB2* cluster of genes (Spellman et al., 1998), whose transcription is under the control of Fkh2/Ndd1 (Zhu et al., 2000; Koranda et al., 2000). The observation that Cdc20 levels still oscillate in cells that express *CDC20* under a constitutive promoter (*TEF1p*) in the absence of Cdh1 implies an additional cell cycle regulated mechanism. This is strong evidence that regulation of the $Cdc20^{cis}$ mechanism we observe is sufficient to drive the oscillatory behavior of Cdc20 through out the cell cycle.

Previous work has shown that phosphorylation of the TPR subunits (Cdc27, Cdc16, and Cdc23) by the Cyclin-Dependent Kinase (CDK) increases the affinity of Cdc20 for the APC (Rudner and Murray, 2000). It is possible that these phosphorylations are regulating the $Cdc20^{cis}$ mechanism. However, these phosphorylations promote Cdc20 binding to the APC, and occur when CDK activity is high. If these phosphorylations are promoting the $Cdc20^{cis}$ turnover during the cell cycle, we would expect to see the lowest Cdc20 levels when CDK activity is highest. However, we observe that the lowest Cdc20 levels occur during the G1 phase of the cell cycle, when CDK activity is lowest. Alternatively, phosphorylation of the TPR proteins may cause Cdc20 to bind in a slightly different position on the APC, which may inhibit the $Cdc20^{cis}$ mechanism.

These data suggest the following model. The APC is hyperphosphorylated in early mitosis, which increases its affinity for Cdc20. As APC^{Cdc20} runs out of substrates, Cdc20 begins to autoubiquitinate, constituting the majority of the late mitotic turnover. This model for the regulation of Cdc20 stability by the presence of substrates (Figure 6) is similar to that put forth for the ubiquitin conjugase Ube2C (Rape and Kirschner, 2004). As cells exit mitosis, APC becomes dephosphorylated and Cdh1 becomes active, thus removing residual Cdc20. Additionally, our model for substrate inhibition of Cdc20 turnover may explain why it is advantageous for the cell to have Cdc20 binding to the APC strongly enhanced by the presence of substrates (Matyskiela and Morgan, 2009; Burton et al., 2005). In this way, Cdc20 would be unlikely to be prematurely degraded when substrates are present.

Interestingly, Cdc20 turnover has been shown to increase in the presence of spindle poisons. This turnover is dependent on an intact Spindle Assembly Checkpoint

(SAC) (Pan and Chen, 2004). The exact mechanism for this turnover is unknown, but it will be interesting to determine the mechanism for Cdc20 turnover during SAC activation.

EXPERIMENTAL PROCEDURES

Yeast Methods

Yeast were grown in Ym-1 media (Benanti et al., 2007) and 2% dextrose. All cells were grown at 23°C unless otherwise noted. Cdc20 integrating plasmid was created by cloning Cdc20 and its promoter into pRS306 using standard techniques. Mutations to pRS306-Cdc20 were accomplished using quick change mutagenesis. Cdc20 plasmids were integrated at the *URA3* locus into derivations of 3 strains: *pds1Δ clb5Δ SIC1^{10x} cdc20Δ cdh1Δ, pds1Δ clb5Δ SIC1^{10x} cdc20Δ CDH1,* or *pds1Δ clb5Δ SIC1^{10x} CDC20 cdh1Δ*. All strains created in this manner were checked for single integration by southern blot. Replacement of the *CDC20* promoter with *TEF1p* was accomplished using standard PCR-based techniques, as was deletion of *CDH1* and mutation of Cdc20's IR motif in Figure 2A.

Half-life assays

Cells were grown to saturation, diluted and allowed to grow for at least 2 doublings to an OD between 0.6 and 1.0. 6 ODs of cells were collected for the zero time point. Cell pellets were washed with 1 ml cold H_2O and frozen on dry ice. Cycloheximide was added to cultures for a final concentration of 50 μg/ml media. 6 ODs of cells were collected for each time point as indicated. Cell pellets processed as described below.

cdc15-2 arrest and release

Cells were grown to saturation, then diluted to an OD of 0.3 and allowed to grow to an OD between 0.6 and 1.0. 6 ODs of cells were collected as described above for an asynchronous sample. Cells were diluted to an OD of 0.5 and placed at 37°C for 3 h. Cells were examined under a microscope to confirm anaphase arrest. 6 ODs of cells were collected for the zero time point, as described above. Cells were then released into media at 23°C at an OD of 0.6, and 6 ODs of cells were collected at time points indicated. Cells were collected for flow cytometry at every time point and processed (Lopez-Mosqueda et al., 2010).

Western blots

Cell pellets were processed as follows. Cell pellets were thawed in boiling sample buffer (50mM Tris pH 7.5, 5% SDS, 5 mM EDTA, 10% Glycerol, 0.5% BME, 0.1 µg/ml pepstatin A, 0.1 µg/ml leupeptin, 0.1 µg/ml bestatin, 0.1 mM Benzamidine, 5 mM NaF, 0.5 mM Na_3VO_4, 40 mM β-glycerophosphate, 1 mM PMSF). Cells were boiled for 5 min, followed by bead-beating three times, 30 s each, and then boiled again for 5 min for SDS-PAGE and transfer to nitrocellulose. Western blots were performed with low salt PBST (15 mM NaCl, 1.3 mM NaH_2PO_4, 5.4 mM Na_2HPO_4, 0.05% Tween pH 6.8). All primary antibody incubations were performed overnight in 5% milk and low salt PBST unless otherwise noted. Antibodies were used as follows: Cdc20 (yC-20) from Santa Cruz at 1:1000, Cdc28 from Santa Cruz (yC-20) at 1:1000, Dbf4 (yN-15) from Santa Cruz at 1:500, Clb2 (y180) from Santa Cruz 1:1000 (Figure 4B), Cdc6 9H8/5 from Abcam at 1:2000.

APC Assays

APC was purified from a *TAP-CDC16, cdh1Δ* strain. E1, E2 (Ubc4), APC, and Cdh1 were expressed and purified as previously described (Carroll et al., 2005; Carroll and Morgan, 2005). ZZ-tagged Cdc20 wildtype and mutants were transcribed and translated *in vitro* with TnT Quick Coupled Transcription/Translation Systems (Promega) either in the presence of ^{35}S-methionine or unlabeled methionine. Briefly, APC assays were performed by first charging the E2 in the presence of E1 (Uba1, 300 nM), E2 (Ubc4, 50 μM), Methyl-Ubiquitin (Boston Biochem, 150 μM), and ATP (1 mM) for 20 min. E1/E2(Ubc4)/Methyl-Ubiquitin mix was added to APC (1-5 nM), ZZ-Cdc20 purified from reticulocyte lysate using IgG beads and cleaved using TEV protease, and Securin purified similarly from reticulocyte lysate. In Figure 2D, APC, Cdc20 and Securin were preincubated to increase the amount of activity observed for the mutants. For Figure 5A & B, His-tagged Securin (aa1-110) was expressed in bacteria and purified using Ni-NTA resin. After TEV protease cleavage to remove the His6-tag, the protein was further purified using cation exchange and size exclusion chromatography. APC, Cdc20, and Securin (aa1-110) were preincubated before adding IVT Securin and E1/E2(Ubc4)/Methyl-Ubiquitin mix or E1/E2(Ubc4)/Methyl-Ubiquitin mix alone. All reactions were stopped by the addition of sample buffer, separated by SDS-PAGE, and visualized and quantified with a Molecular Dynamics PhosphorImager and ImageQuant (Amersham Biosciences/GE Healthcare).

Figure 1. Cdc20 is turned over by the APC by Cdh1-dependent and Cdh1-independent mechanisms

(A) Diagrams of Cdc20 and Cdh1. Red, purple, blue and green boxes represent the D-boxes, the C-box, the WD40, and the C-terminal IR, respectively.

(B) Three possible mechanisms of Cdc20 turnover: $Cdh1^{trans}$, $Cdc20^{trans}$, $Cdc20^{cis}$.

(C) Asynchronous *pds1Δ clb5Δ* $SIC1^{10x}$ cells were collected at indicated time points after cycloheximide addition. Blots were probed with antibodies against Cdc20, Clb2 and Cdc28, which served as a loading control.

(D) APC immunopurified from TAP-Cdc16 lysates in a *cdh1Δ* background was used in ubiquitination reactions using *in vitro* translated (IVT) ZZ-tagged ^{35}S-Metionine-Cdc20 purified from rabbit reticulocyte lysates using IgG beads. APC (++) and (+) are 5 nM and 1 nM final concentrations, respectively. Controls show the dependence on the presence of exogenous E1/E2(Ubc4)/Methyl-Ubiquitin mix and the APC.

Figure 1

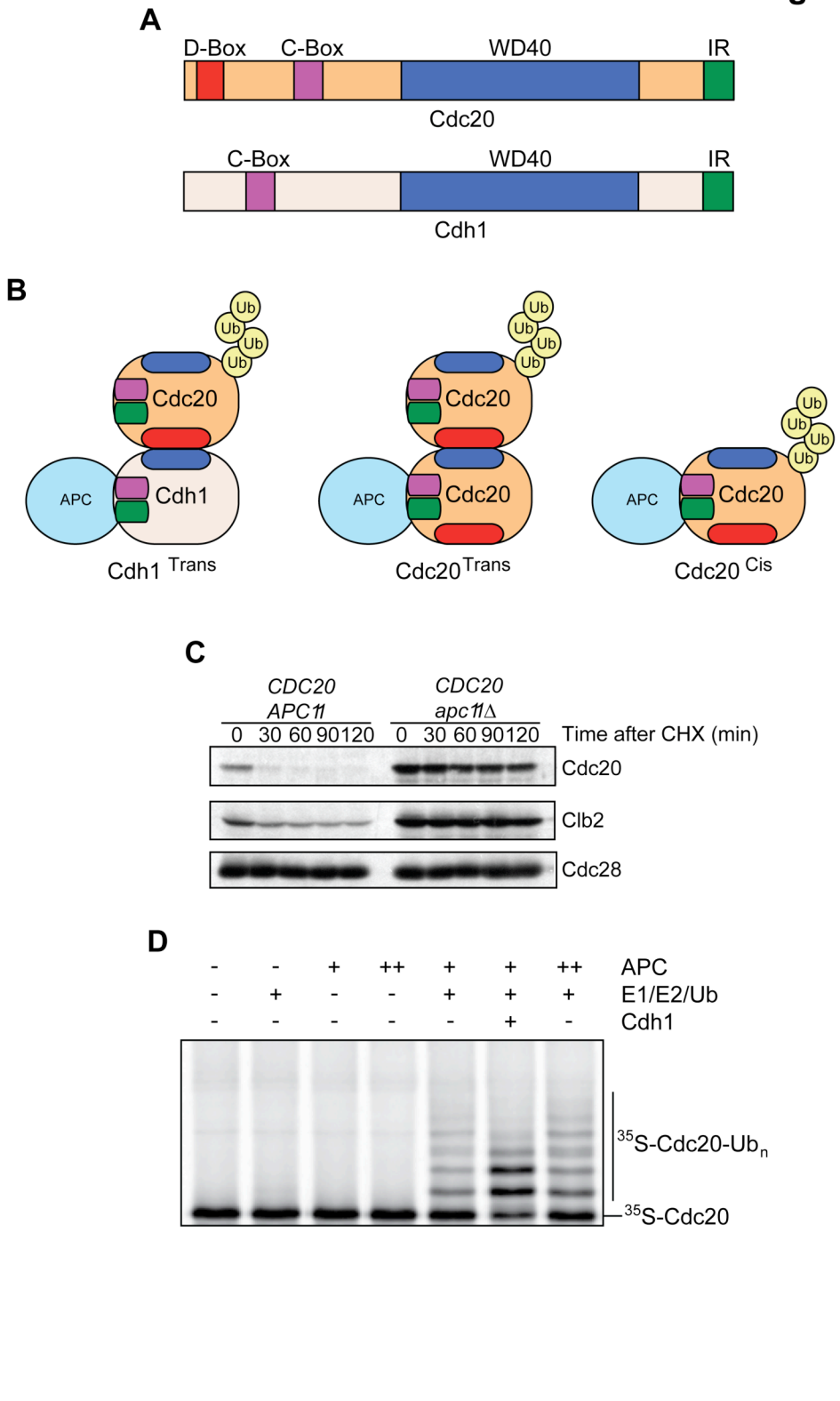
A
D-Box
C-Box
WD40
IR
Cdc20
C-Box
WD40
IR
Cdh1
B
Ub
Cdc20
APC
Cdh1
Cdh1 Trans
Cdc20
APC
Cdc20
Cdc20 Trans
Cdc20
APC
Cdc20
Cdc20 Cis
C
CDC20
APC11
CDC20
apc11Δ
0 30 60 90120 0 30 60 90120
Time after CHX (min)
Cdc20
Clb2
Cdc28
D
- - + ++ + + ++ APC
- + - - + + + E1/E2/Ub
- - - - - + - Cdh1
35S-Cdc20-Ubn
35S-Cdc20

Figure 2. Cdc20 ubiquitination and turnover in *CDC20*, *CDH1* mutants

(A) Asynchronous *PDS1 CLB5 SIC1* cells were treated with cycloheximide and samples were analyzed as in Figure 1C. Cdc20-IR denotes the Cdc20-ΔIR allele.

(B) ZZ-tagged ^{35}S-Cdc20 wildtype, C-Box mutant (I147A, P148A) or IR mutant (I609A, R610A) were generated by IVT and incubated with APC (5 nM) and E1/E2(Ubc4)/Methyl-Ubiquitin mix for the indicated times. Quantifications are shown below.

(C) Asynchronous *pds1Δ clb5Δ SIC1^{10x}* cells were treated with cycloheximide, and analyzed as in Figure 1C. Cdc20-CB denotes the Cdc20-R145D allele. Cdc20-R145D (Cdc20-CB) protein migrates more slowly on an electrophoretic gel as compared to wild type Cdc20.

(D) ZZ-tagged unlabeled Cdc20 wildtype, C-Box mutant I147A, P148A (Cdc20-CB) or IR mutant I609A, R610A (Cdc20-IR) or a mock purification from IVT lysate with no Cdc20 (-) was pre-incubated with APC (5 nM) and ZZ-tagged ^{35}S-Securin generated by IVT. After a 15 min preincubation, E1/E2(Ubc4)/Methyl-Ubiquitin mix was added and ubiquitination reactions were performed for the indicated times. See also Figure S1.

Figure 2

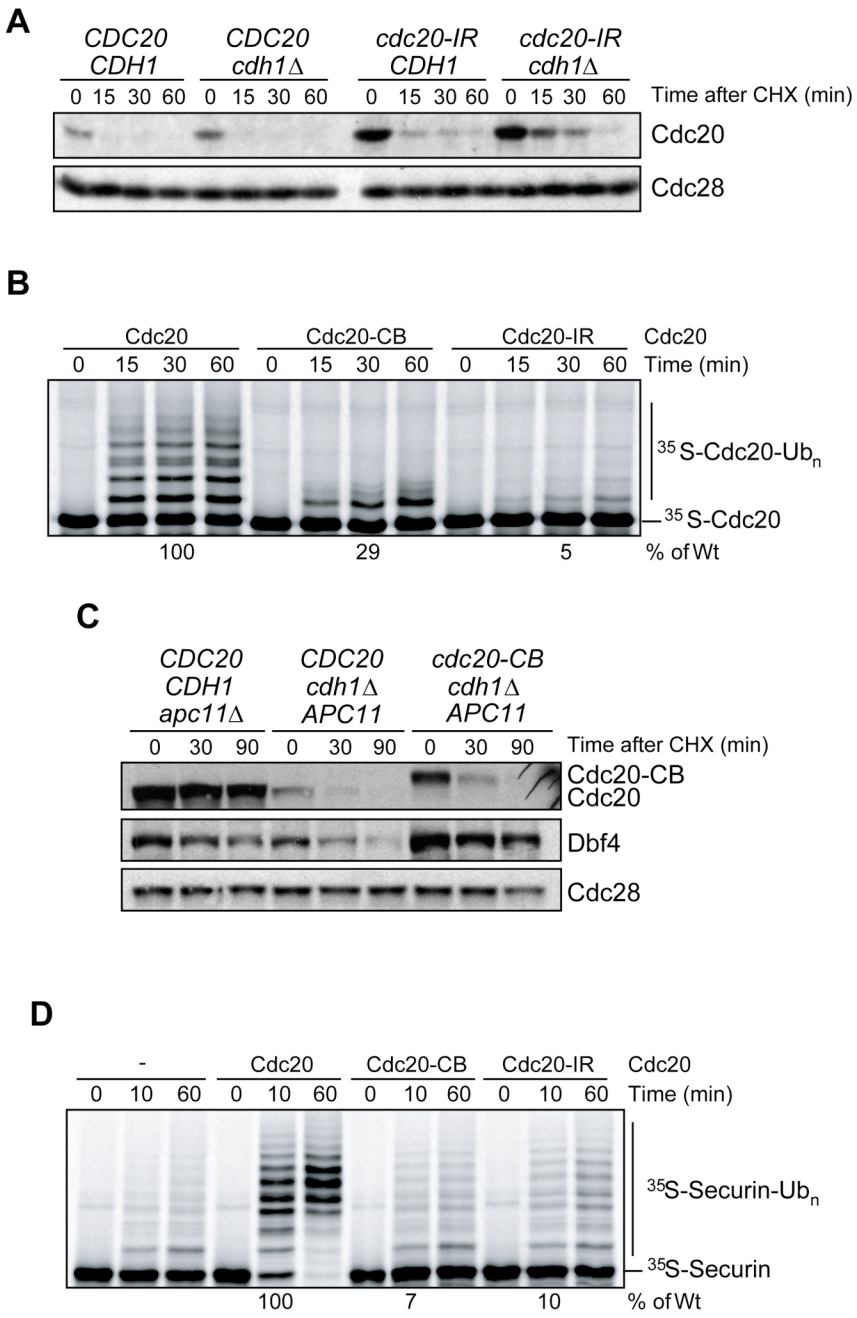
A
CDC20 CDH1
CDC20 cdh1Δ
cdc20-IR CDH1
cdc20-IR cdh1Δ
0 15 30 60 0 15 30 60 0 15 30 60 0 15 30 60
Time after CHX (min)
Cdc20
Cdc28
B
Cdc20
Cdc20-CB
Cdc20-IR
Cdc20
0 15 30 60 0 15 30 60 0 15 30 60
Time (min)
35S-Cdc20-Ubn
35S-Cdc20
100
29
5
% of Wt
C
CDC20 CDH1 apc11Δ
CDC20 cdh1Δ APC11
cdc20-CB cdh1Δ APC11
0 30 90 0 30 90 0 30 90
Time after CHX (min)
Cdc20-CB
Cdc20
Dbf4
Cdc28
D
-
Cdc20
Cdc20-CB
Cdc20-IR
Cdc20
0 10 60 0 10 60 0 10 60 0 10 60
Time (min)
35S-Securin-Ubn
35S-Securin
100
7
10
% of Wt

Figure 3. The majority of Cdc20 turnover occurs by the Cdc20^{cis} mechanism

(A) Asynchronous *pds1Δ clb5Δ SIC1^{10x}* cells were analyzed as in Figure 2C. Cdc20-CB denotes the Cdc20-R145D, IRΔ allele. Bands represented by Cdc20 and Cdc20-CB are indicated. Two exposures are shown.

(B) ZZ-tagged ^{35}S-Cdc20 C-Box, IR mutant (I147A, P148A, I609A, R610A) or ^{35}S-Cdc20 C-Box, IR, D-box mutant (I147A, P148A, I609A, R610A, R17A, L20A) mutant was incubated with recombinant Cdh1, APC (1 nM), and E1/E2(Ubc4)/Methyl-Ubiquitin mix for the indicated times.

(C) IVT generated ZZ-tagged ^{35}S-Cdc20 mutants, as in Figure 3B, were incubated with APC (5 nM), E1/E2(Ubc4)/Methyl-Ubiquitin mix, and with or without IVT-generated ZZ-Tagged unlabeled Cdc20 for the indicated times.

(D) Asynchronous *pds1Δ clb5Δ SIC1^{10x}* cells were treated with cycloheximide and examined as in Figure 2C. Bands labeled Cdc20* are Cdc20 or Cdc20-D-box allele (cdc20-R17A, L20A), whereas Cdc20-CB* indicates the Cdc20-IRΔ, R145D allele or Cdc20-R145D, IRΔ, D-box (R17A, L20A) allele.

(E) Securin and Cdc20 ubiquitination assays as in Figure 2B, except that APC was purified from *DOC1 cdh1*Δ or *doc1-4A cdh1*Δ strains.

Figure 3 Part 1

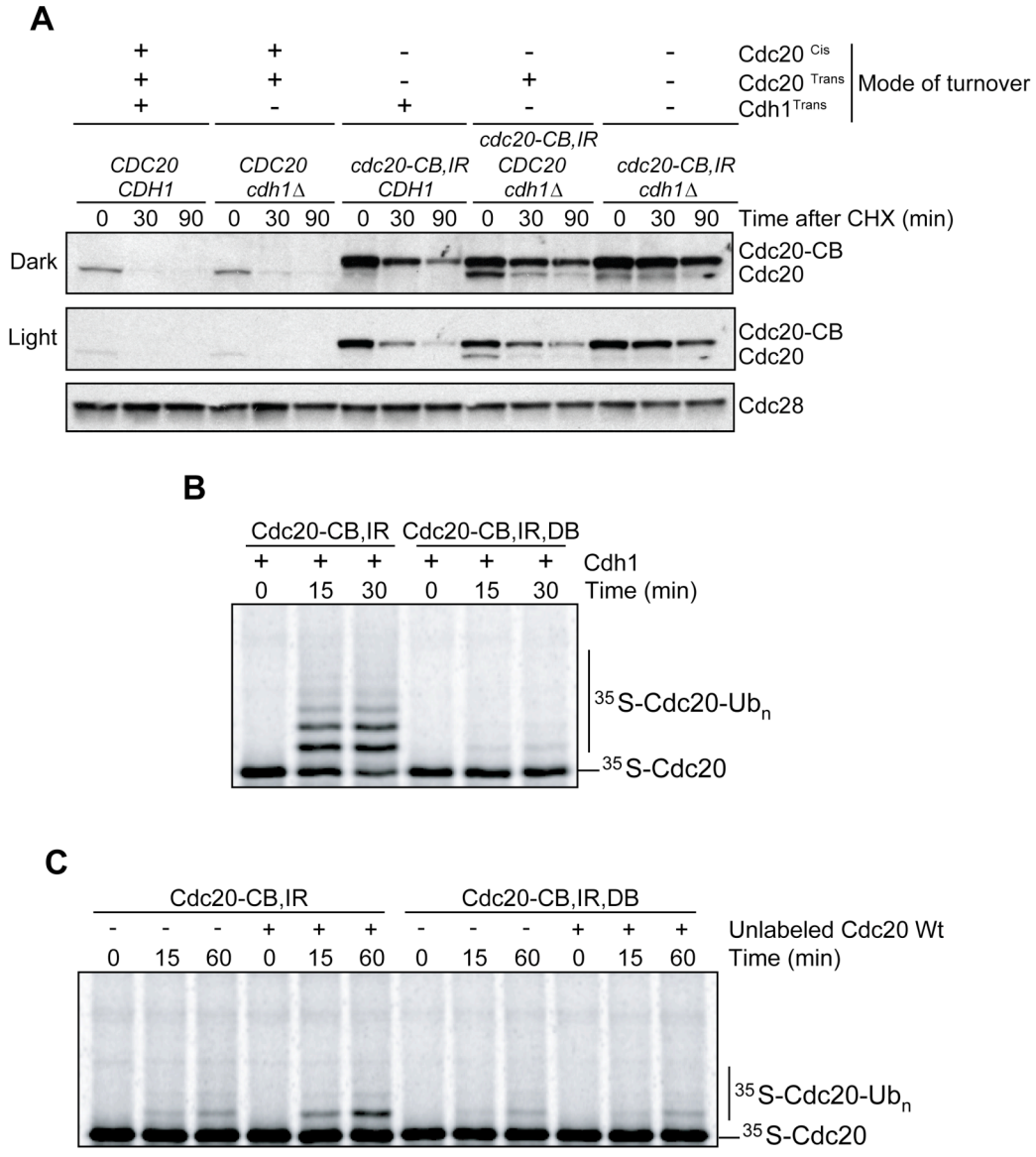

Figure 3 Part 2

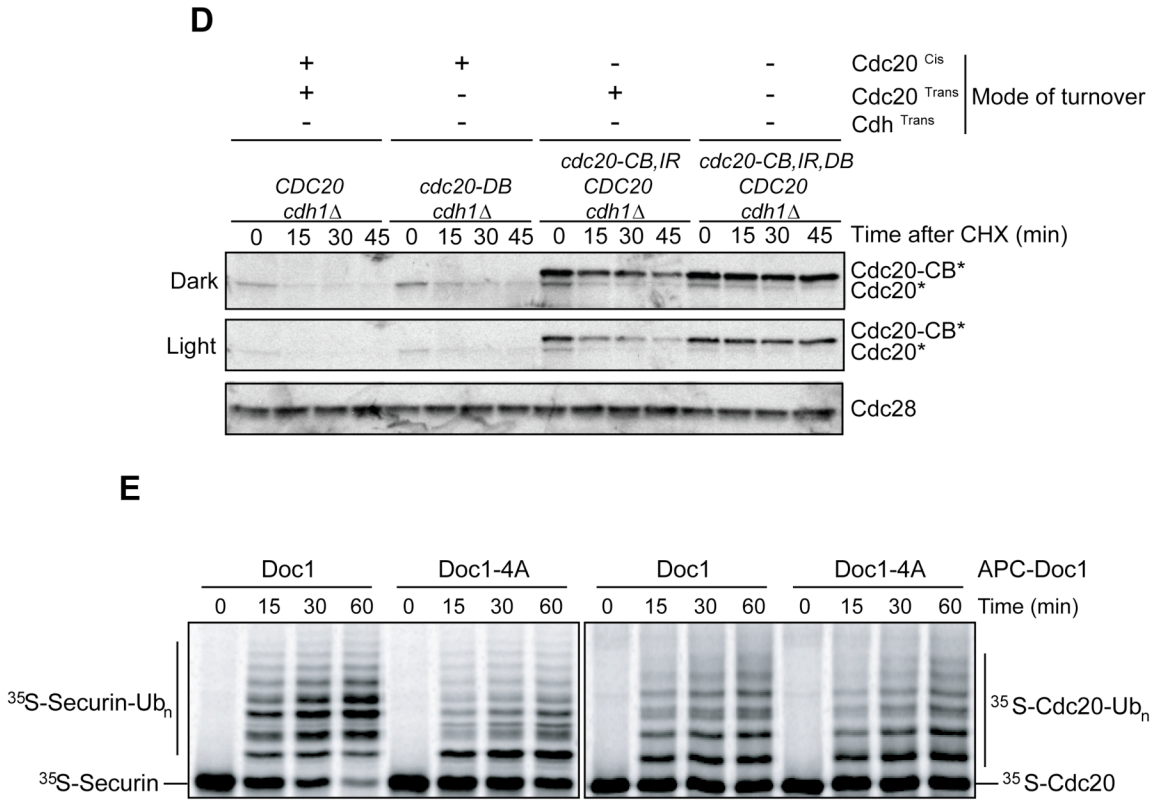

Figure 4. Cdc20 levels oscillate with the cell cycle in a Cdh1- and transcription-independent manner

(A) Asynchronous *cdc15-2* or *cdc15-2 cdh1Δ* cells were arrested at 37°C and released into 23°C media. Time points were taken every 20 min. A sample of each asynchronous (Asy) culture and a *cdc20*Δ mutant are shown for reference.

(B) *cdc15-2 TEF1p-CDC20* or *cdc15-2 TEF1p-CDC20 cdh1Δ* strains were arrested and released as in Figure 4A. Time points were taken every 10 min. Western blots were performed with the indicated antibody. See also Figure S2.

Figure 4

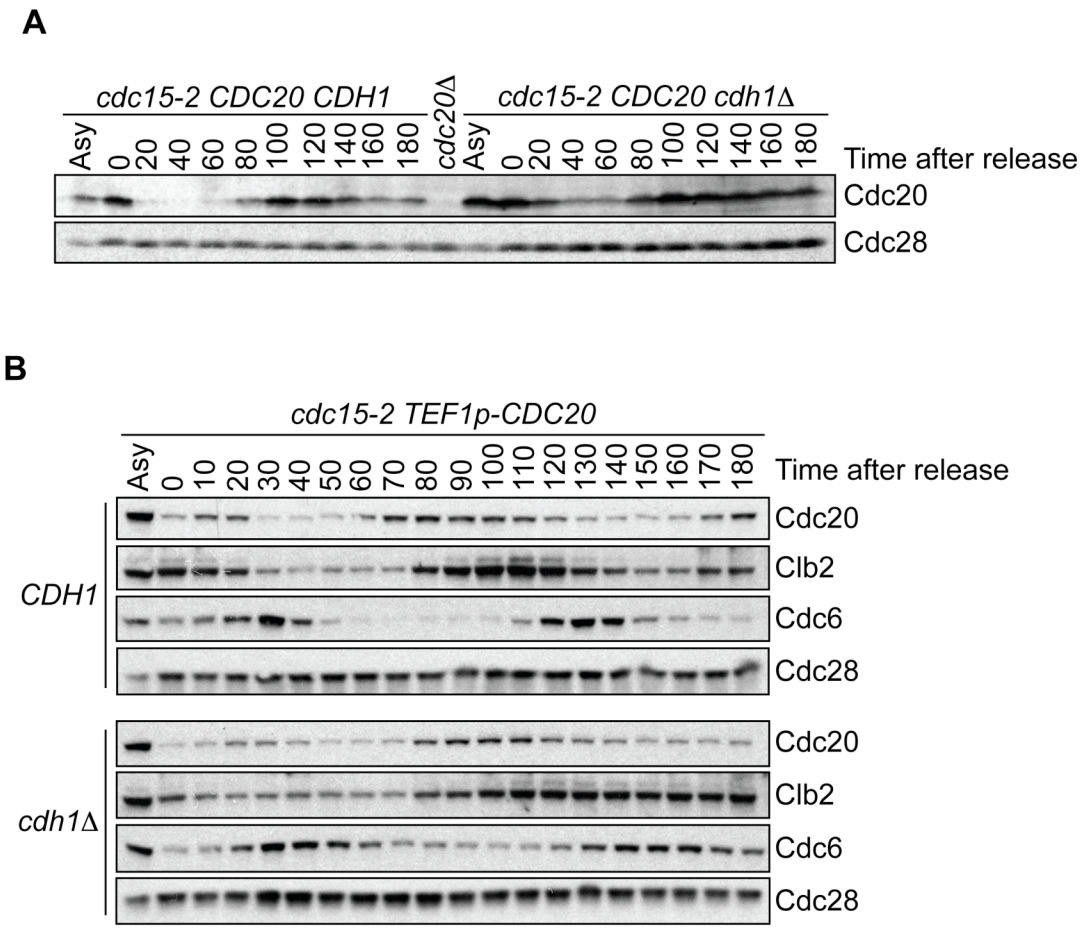
A
cdc15-2 CDC20 CDH1
cdc20Δ
cdc15-2 CDC20 cdh1Δ
Asy
0
20
40
60
80
100
120
140
160
180
Time after release
Cdc20
Cdc28
B
cdc15-2 TEF1p-CDC20
Asy
0
10
20
30
40
50
60
70
80
90
100
110
120
130
140
150
160
170
180
Time after release
CDH1
Cdc20
Clb2
Cdc6
Cdc28
cdh1Δ
Cdc20
Clb2
Cdc6
Cdc28

Figure 5. Cdc20^{cis} mechanism is inhibited by high substrate concentrations

(A) ZZ-tagged unlabeled Cdc20 generated by IVT was pre-incubated with APC (5 nM) and the specified concentration of the Securin/Pds1 fragment (referred to as Securin 1-110; values represent the final assay concentrations). After a 15 min preincubation, E1/E2(Ubc4)/Methyl-Ubiquitin mix and ZZ-tagged ^{35}S-Securin generated by IVT was added and ubiquitination reactions were performed for 10 min.

(B) ZZ-tagged unlabeled Cdc20 or ^{35}S-Cdc20 generated by IVT was pre-incubated for 15 min with APC (5 nM) and 10 μM Securin 1-110. For securin ubiquitination, E1/E2(Ubc4)/Methyl-Ubiquitin mix and ZZ-tagged ^{35}S-Securin generated by IVT was added for 10 min. For autoubiquitination, E1/E2(Ubc4)/Methyl-Ubiquitin mix was added for 10 min.

Figure 5

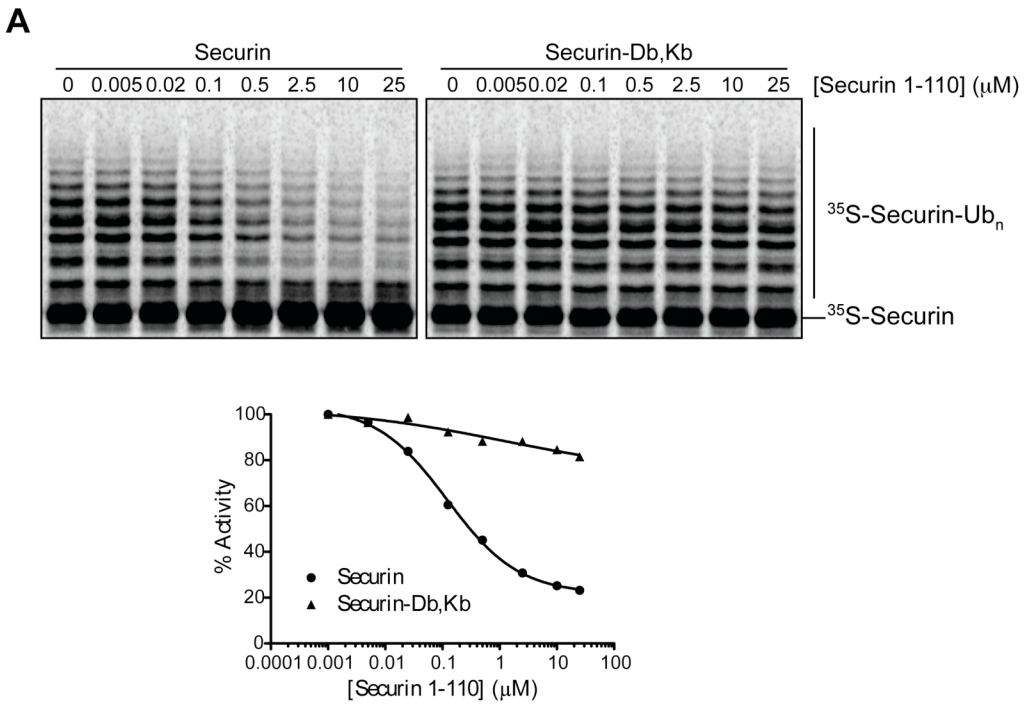
A
Securin
Securin-Db,Kb
0 0.005 0.02 0.1 0.5 2.5 10 25
[Securin 1-110] (μM)
35S-Securin-Ubn
35S-Securin
% Activity
Securin
Securin-Db,Kb
0.0001 0.001 0.01 0.1 1 10 100
[Securin 1-110] (μM)

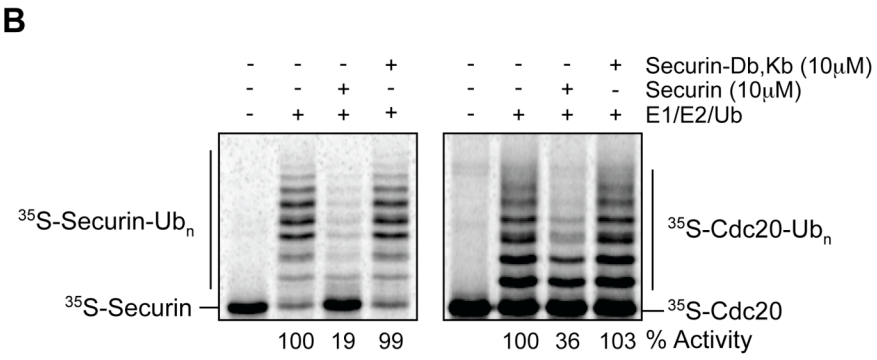
B
Securin-Db,Kb (10μM)
Securin (10μM)
E1/E2/Ub
35S-Securin-Ubn
35S-Securin
35S-Cdc20-Ubn
35S-Cdc20
100 19 99
100 36 103 % Activity

Figure 6. Model demonstrating how Cdc20^{cis} may be regulated by substrate

Red, purple, blue and green boxes represent the D-boxes, the C-box, the WD40, and the C-terminal IR of Cdc20, respectively (see Figure 1A).

Figure 6

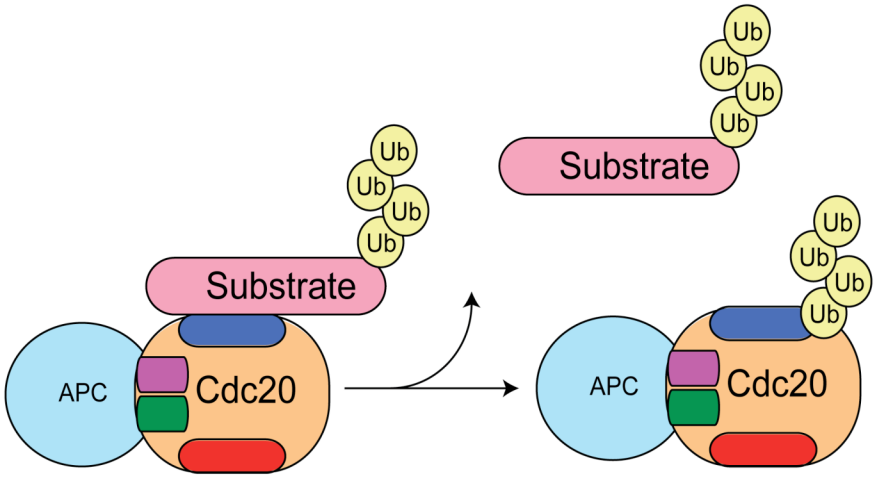
Ub
Ub
Ub
Ub
Substrate
APC
Cdc20
Ub
Ub
Ub
Ub
Substrate
APC
Cdc20

Figure S1. Characterization of Cdc20 IR and C box mutations

(A) *In vitro* Cdc20-IR and Cdc20-CB ubiquitination by Cdh1. ZZ-tagged ^{35}S-Cdc20 Wildtype, C-Box mutant (I147A, P148A; Cdc20-CB) or IR mutant (I609A, R610A; Cdc20-IR) was incubated with recombinant Cdh1 and APC (1 nM) for the indicated times.

(B) Cdc20-R145D turns over relatively fast. Asynchronous *pds1Δ clb5Δ SIC1^{10x}* cells were treated with cycloheximide, and analyzed as in Figure 2C. Cdc20-CB indicates the Cdc20-R145D allele.

(C) Cdc20-D144R, R145D turned over with similar kinetics to Cdc20-R145D. Cycloheximide was added to asynchronous *pds1Δ clb5Δ SIC1^{10x}* cells and samples were taken at indicated time points after addition. Cdc20-CB indicates the 3HA-Cdc20-R145D mutant or the 3HA-Cdc20-D144R, R145D mutant. Cdc28 is shown as a loading control. Two independent *cdc20-D144R, R145D* isolates are shown, blot was cropped to remove lanes between isolates.

Figure S1

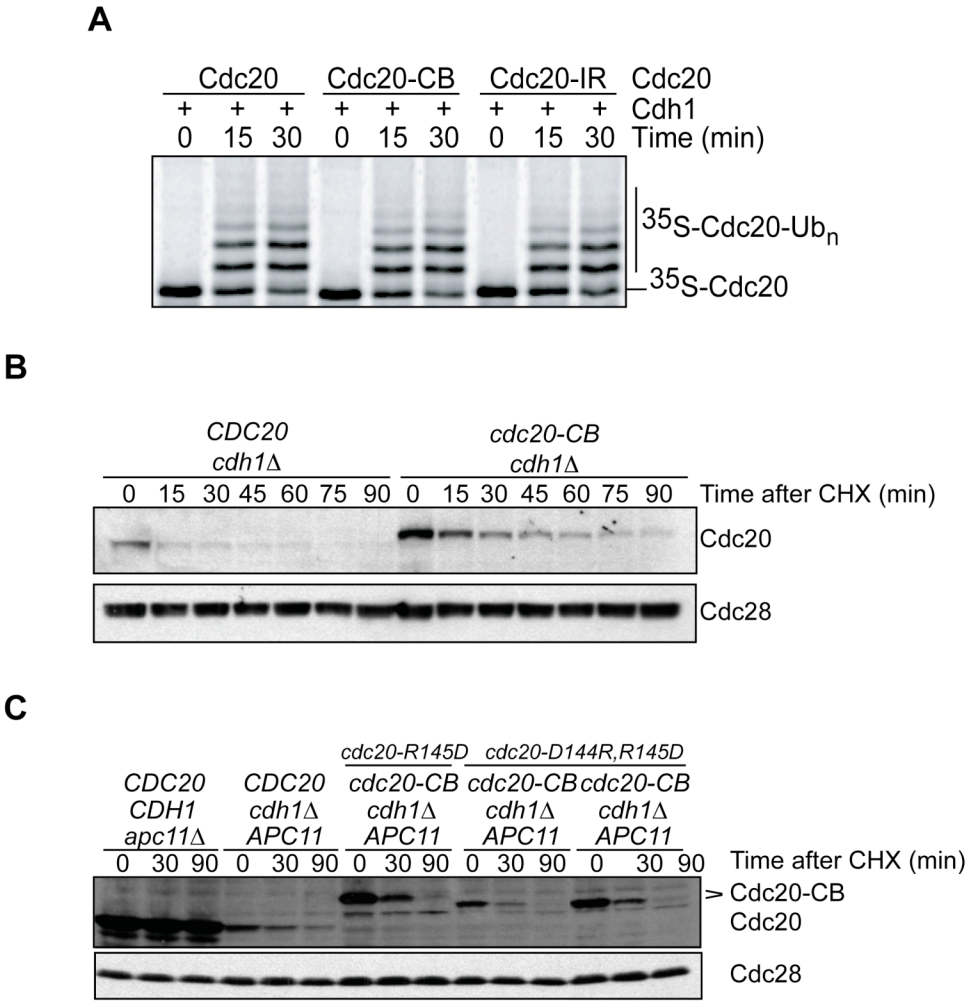
A
Cdc20
Cdc20-CB
Cdc20-IR
Cdc20
+ + + + + + + + +
Cdh1
0 15 30 0 15 30 0 15 30
Time (min)
35S-Cdc20-Ubn
35S-Cdc20
B
CDC20
cdh1Δ
cdc20-CB
cdh1Δ
0 15 30 45 60 75 90 0 15 30 45 60 75 90
Time after CHX (min)
Cdc20
Cdc28
C
cdc20-R145D
cdc20-D144R,R145D
CDC20
CDH1
apc11Δ
CDC20
cdh1Δ
APC11
cdc20-CB
cdh1Δ
APC11
cdc20-CB
cdh1Δ
APC11
cdc20-CB
cdh1Δ
APC11
0 30 90 0 30 90 0 30 90 0 30 90 0 30 90
Time after CHX (min)
Cdc20-CB
Cdc20
Cdc28

Figure S2. Flow cytometry profiles for the experiments in Figures 4A and 4B

(A) Samples were taken at the same time as the protein samples in Figure 4A (20 min time points).

(B) Samples were taken at the same time as the protein samples in Figure 4B (10 min time points).

Figure S2

A

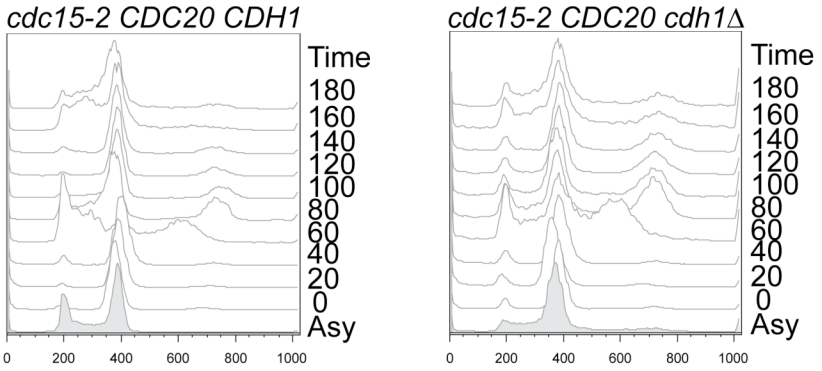
cdc15-2 CDC20 CDH1
Time
180
160
140
120
100
80
60
40
20
0
Asy
0
200
400
600
800
1000
cdc15-2 CDC20 cdh1Δ
Time
180
160
140
120
100
80
60
40
20
0
Asy
0
200
400
600
800
1000

B

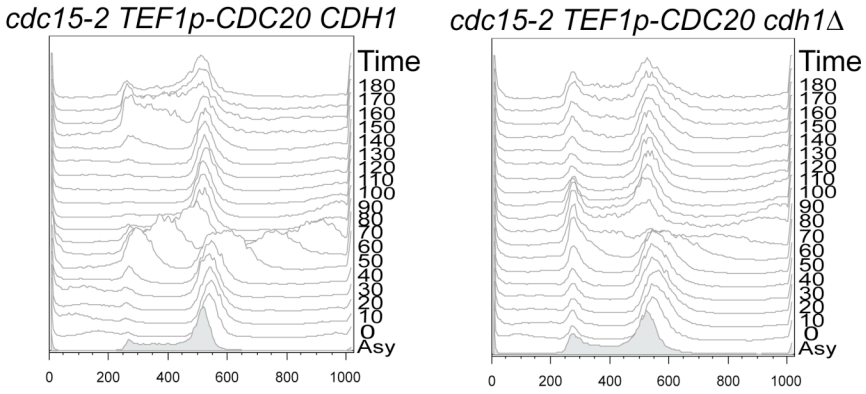
cdc15-2 TEF1p-CDC20 CDH1
Time
180
170
160
150
140
130
120
110
100
90
80
70
60
50
40
30
20
10
0
Asy
0
200
400
600
800
1000
cdc15-2 TEF1p-CDC20 cdh1Δ
Time
180
170
160
150
140
130
120
110
100
90
80
70
60
50
40
30
20
10
0
Asy
0
200
400
600
800
1000

ACKNOWLEDGEMENTS

We would like to thank C. Carroll, N. Lyons, M. Lopez, G. Yaakov, L. Holt, M. Rodrigo-Brenni, M. Matyskiela, E. Edenberg, M. Downey, T. Berens J. Lopez-Mosqueda, D. Simsek and J. Benanti for their input and advice during this project. Additionally, we would like to thank N. Lyons, E. Edenberg, and M. Downey for reading and commenting on the manuscript. This work was supported by funding from the National Institute of General Medical Sciences to D. P. T. (GM070539) and D.O.M. (GM053270).

REFERENCES

Amon, A., Irniger, S., and Nasmyth, K. (1994). Closing the cell cycle circle in yeast: G2 cyclin proteolysis initiated at mitosis persists until the activation of G1 cyclins in the next cycle. Cell *77*, 1037-1050.

Benanti, J.A., Cheung, S.K., Brady, M.C., and Toczyski, D.P. (2007). A proteomic screen reveals SCFGrr1 targets that regulate the glycolytic-gluconeogenic switch. Nat Cell Biol *9*, 1184-1191.

Burton, J.L., Tsakraklides, V., and Solomon, M.J. (2005). Assembly of an APC-Cdh1-substrate complex is stimulated by engagement of a destruction box. Mol Cell *18*, 533-542.

Carroll, C.W., Enquist-Newman, M., and Morgan, D.O. (2005). The APC subunit Doc1 promotes recognition of the substrate destruction box. Curr Biol *15*, 11-18.

Carroll, C.W., and Morgan, D.O. (2002). The Doc1 subunit is a processivity factor for the anaphase-promoting complex. Nat. Cell Biol. *4*, 880-887.

Carroll, C.W., and Morgan, D.O. (2005). Enzymology of the Anaphase-Promoting Complex. Meth. Enzymol. *398*, 219-230.

Cohen-Fix, O., Peters, J.-M., Kirschner, M.W., and Koshland, D. (1996). Anaphase initiation in *Saccharomyces cerevisiae* is controlled by the APC-dependent degradation of the anaphase inhibitor Pds1p. Genes Dev. *10*, 3081-3093.

da Fonseca, P.C., Kong, E.H., Zhang, Z., Schreiber, A., Williams, M.A., Morris, E.P., and Barford, D. (2011). Structures of APC/C(Cdh1) with substrates identify Cdh1 and Apc10 as the D-box co-receptor. Nature *470*, 274-278.

Dawson, I.A., Roth, S., and Artavanis-Tsakonas, S. (1995). The Drosophila cell cycle gene *fizzy* is required for normal degradation of cyclins A and B during mitosis and has homology to the *CDC20* gene of *Saccharomyces cerevisiae*. J. Cell Biol. *129*, 725-737.

Glotzer, M., Murray, A.W., and Kirschner, M.W. (1991). Cyclin is degraded by the ubiquitin pathway. Nature *349*, 132-138.

Goh, P., Lim, H.H., and Surana, U. (2000). Cdc20 protein contains a destruction-box but, unlike Clb2, its proteolysis is not acutely depdendent on the activity of the anaphase-promoting complex. European Journal of Biochemistry *267*, 434-449.

Hayes, M.J., Kimata, Y., Wattam, S.L., Lindon, C., Mao, G., Yamano, H., and Fry, A.M. (2006). Early mitotic degradation of Nek2A depends on Cdc20-independent interaction with the APC/C. Nat Cell Biol *8*, 607-614.

Kimata, Y., Baxter, J.E., Fry, A.M., and Yamano, H. (2008). A role for the Fizzy/Cdc20 family of proteins in activation of the APC/C distinct from substrate recruitment. Mol Cell *32*, 576-583.

King, R.W., Peters, J.-M., Tugendreich, S., Rolfe, M., Hieter, P., and Kirschner, M.W. (1995). A 20S complex containing CDC27 and CDC16 catalyzes the mitosis-specific conjugation of ubiquitin to cyclin B. Cell *81*, 279-288.

Koranda, M., Schleiffer, A., Endler, L., and Ammerer, G. (2000). Forkhead-like transcription factors recruit Ndd1 to the chromatin of G2/M-specific promoters. Nature *406*, 94-98.

Kraft, C., Vodermaier, H.C., Maurer-Stroh, S., Eisenhaber, F., and Peters, J.M. (2005). The WD40 propeller domain of Cdh1 functions as a destruction box receptor for APC/C substrates. Mol Cell *18*, 543-553.

Lim, H.H., and Surana, U. (1996). Cdc20, a ß-transducin homologue, links *RAD9*-mediated G2/M checkpoint control to mitosis in *Saccharomyces cerevisiae*. Mol. Gen. Genet. *253*, 138-148.

Lopez-Mosqueda, J., Maas, N.L., Jonsson, Z.O., Defazio-Eli, L.G., Wohlschlegel, J., and Toczyski, D.P. (2010). Damage-induced phosphorylation of Sld3 is important to block late origin firing. Nature *467*, 479-483.

Manchado, E., Eguren, M., and Malumbres, M. (2010). The anaphase-promoting complex/cyclosome (APC/C): cell-cycle-dependent and -independent functions. Biochemical Society transactions *38*, 65-71.

Matyskiela, M.E., and Morgan, D.O. (2009). Analysis of activator-binding sites on the APC/C supports a cooperative substrate-binding mechanism. Mol Cell *34*, 68-80.

Oliveira, R.A., and Nasmyth, K. (2010). Getting through anaphase: splitting the sisters and beyond. Biochemical Society transactions *38*, 1639-1644.

Pan, J., and Chen, R.H. (2004). Spindle checkpoint regulates Cdc20p stability in Saccharomyces cerevisiae. Genes Dev *18*, 1439-1451.

Passmore, L.A., McCormack, E.A., Au, S.W., Paul, A., Willison, K.R., Harper, J.W., and Barford, D. (2003). Doc1 mediates the activity of the anaphase-promoting complex by contributing to substrate recognition. Embo J *22*, 786-796.

Pesin, J.A., and Orr-Weaver, T.L. (2008). Regulation of APC/C activators in mitosis and meiosis. Annu Rev Cell Dev Biol *24*, 475-499.

Pfleger, C.M., and Kirschner, M.W. (2000). The KEN box: an APC recognition signal distinct from the D box targeted by Cdh1. Genes Dev *14*, 655-665.

Prinz, S., Hwang, E.S., Visintin, R., and Amon, A. (1998). The regulation of Cdc20 proteolysis reveals a role for the APC components Cdc23 and Cdc27 during S phase and early mitosis. Curr. Biol. *8*, 750-760.

Rape, M., and Kirschner, M.W. (2004). Autonomous regulation of the anaphase-promoting complex couples mitosis to S-phase entry. Nature *432*, 588-595.

Robbins, J.A., and Cross, F.R. (2011). Regulated degradation of the APC coactivator Cdc20. Cell division *5*, 23.

Rudner, A.D., and Murray, A.W. (2000). Phosphorylation by Cdc28 activates the Cdc20-dependent activity of the anaphase-promoting complex. J. Cell Biol. *149*, 1377-1390.

Schwab, M., Lutum, A.S., and Seufert, W. (1997). Yeast Hct1 is a regulator of Clb2 cyclin proteolysis. Cell *90*, 683-693.

Schwab, M., Neutzner, M., Mocker, D., and Seufert, W. (2001). Yeast Hct1 recognizes the mitotic cyclin Clb2 and other substrates of the ubiquitin ligase APC. Embo J *20*, 5165-5175.

Shirayama, M., Toth, A., Galova, M., and Nasmyth, K. (1999). APC-Cdc20 promotes exit from mitosis by destroying the anaphase inhibitor Pds1 and cyclin Clb5. Nature *402*, 203-207.

Shirayama, M., Zachariae, W., Ciosk, R., and Nasmyth, K. (1998). The Polo-like kinase Cdc5p and the WD-repeat protein Cdc20p/fizzy are regulators and substrates of the anaphase promoting complex in *Saccharomyces cerevisiae*. EMBO J. *17*, 1336-1349.

Spellman, P.T., Sherlock, G., Zhang, M.Q., Iyer, V.R., Anders, K., Eisen, M.B., Brown, P.O., Botstein, D., and Futcher, B. (1998). Comprehensive identification of cell cycle-regulated genes of the yeast Saccharomyces cerevisiae by microarray hybridization. Mol. Biol. Cell *9*, 3273-3297.

Sudakin, V., Ganoth, D., Dahan, A., Heller, H., Hershko, J., Luca, F.C., Ruderman, J.V., and Hershko, A. (1995). The cyclosome, a large complex containing cyclin-selective ubiquitin-ligase activity, targets cyclins for destruction at the end of mitosis. Mol. Biol. Cell *6*, 185-198.

Thornton, B.R., Ng, T.M., Matyskiela, M.E., Carroll, C.W., Morgan, D.O., and Toczyski, D.P. (2006). An architectural map of the anaphase-promoting complex. Genes Dev *20*, 449-460.

Thornton, B.R., and Toczyski, D.P. (2003). Securin and B-cyclin/CDK are the only essential targets of the APC. Nat Cell Biol *5*, 1090-1094.

Thornton, B.R., and Toczyski, D.P. (2006). Precise destruction: an emerging picture of the APC. Genes Dev *20*, 3069-3078.

Visintin, R., Prinz, S., and Amon, A. (1997). CDC20 and CDH1: a family of substrate-specific activators of APC-dependent proteolysis. Science *278*, 460-463.

Vodermaier, H.C., Gieffers, C., Maurer-Stroh, S., Eisenhaber, F., and Peters, J.M. (2003). TPR subunits of the anaphase-promoting complex mediate binding to the activator protein CDH1. Curr Biol *13*, 1459-1468.

Yoon, H.J., Feoktistova, A., Wolfe, B.A., Jennings, J.L., Link, A.J., and Gould, K.L. (2002). Proteomics analysis identifies new components of the fission and budding yeast anaphase-promoting complexes. Curr Biol *12*, 2048-2054.

Yu, H. (2007). Cdc20: a WD40 activator for a cell cycle degradation machine. Mol Cell *27*, 3-16.

Zachariae, W., Shevchenko, A., Andrews, P.D., Ciosk, R., Galova, M., Stark, M.J., Mann, M., and Nasmyth, K. (1998). Mass spectrometric analysis of the anaphase-promoting complex from yeast: identification of a subunit related to cullins. Science *279*, 1216-1219.

Zhu, G., Spellman, P.T., Volpe, T., Brown, P.O., Botstein, D., Davis, T.N., and Futcher, B. (2000). Two yeast forkhead genes regulate the cell cycle and pseudohyphal growth. Nature *406*, 90-94.

Chapter 3

The APC/C Subunit Mnd2/Apc15 Promotes Cdc20 Autoubiquitination and Spindle Assembly Checkpoint Inactivation

Scott A. Foster and David O. Morgan

Departments of Physiology and Biochemistry & Biophysics, University of California, San Francisco, San Francisco, CA.

Published: September 28, 2012 *Molecular Cell*, 47(6): 921-32.

SUMMARY

The fidelity of chromosome segregation depends on the spindle assembly checkpoint (SAC). In the presence of unattached kinetochores, anaphase is delayed when three SAC components (Mad2, Mad3/BubR1, and Bub3) inhibit Cdc20, the activating subunit of the Anaphase-Promoting Complex (APC/C). We analyzed the role of Cdc20 autoubiquitination in the SAC of budding yeast. Reconstitution with purified components revealed that a Mad3-Bub3 complex synergizes with Mad2 to lock Cdc20 on the APC/C and stimulate Cdc20 autoubiquitination, while inhibiting ubiquitination of substrates. SAC-dependent Cdc20 autoubiquitination required the Mnd2/Apc15 subunit of the APC/C. General inhibition of Cdc20 ubiquitination in vivo resulted in high Cdc20 levels and a failure to establish a SAC arrest, suggesting that SAC establishment depends on low Cdc20 levels. Specific inhibition of SAC-dependent ubiquitination, by deletion of Mnd2, allowed establishment of a SAC arrest but delayed release from the arrest, suggesting that Cdc20 ubiquitination is also required for SAC inactivation.

INTRODUCTION

The spindle assembly checkpoint (SAC) ensures accurate chromosome segregation by delaying the onset of anaphase until all sister chromatids are properly bioriented on the mitotic spindle (Musacchio and Salmon, 2007). The SAC is a signaling system that senses defects in sister chromatid attachments at the kinetochore and blocks anaphase by inhibiting a ubiquitin ligase called the Anaphase-Promoting Complex or Cyclosome (APC/C) (Barford, 2011).

The APC/C, together with its activator subunit Cdc20, normally initiates anaphase by targeting securin and mitotic cyclins for ubiquitination, leading to their destruction by the proteasome. Securin destruction unleashes separase, which cleaves cohesin to initiate sister chromatid separation; cyclin destruction inactivates cyclin-dependent kinases, allowing dephosphorylation of their substrates and thus the completion of mitosis. In late mitosis, Cdc20 is replaced by a related activator subunit called Cdh1, which maintains APC/C activity in G1.

Cdc20 and Cdh1 are substrate adaptor subunits that recruit substrates to the APC/C core for ubiquitination (Barford, 2011). These substrates generally contain 'Destruction-box (D-box)' or 'KEN-box' sequence motifs that bind a WD40 domain in the activator. Cdc20 and Cdh1 also contain multiple binding motifs, including an N-terminal 'C-box' motif and a C-terminal Isoleucine-Arginine 'IR' motif, which mediate a very high affinity interaction with the APC/C (Figure S1A).

Cdc20 levels decrease rapidly in late mitosis during a normal cell cycle, and various lines of evidence suggest that this decrease is due to a combination of two

mechanisms. First, Cdc20 turnover in late mitosis and G1 is mediated in part by the alternate activator Cdh1, which interacts with a D-box at the N-terminus of Cdc20 and thereby targets Cdc20 for ubiquitination (Prinz et al., 1998). However, Cdc20 levels decrease in late mitosis even when its D-box is mutated or in cells lacking Cdh1 (Foe et al., 2011; Robbins and Cross, 2011). Mutation of the IR motif of Cdc20 leads to stabilization of the protein in yeast cells (Thornton et al., 2006), and recent studies indicate that Cdc20 autoubiquitinates at significant rates while bound as an activator (Foe et al., 2011). Cdc20 autoubiquitination is also likely an important mechanism for promoting rapid Cdc20 turnover during a SAC arrest (Ge et al., 2009; Mansfeld et al., 2011; Nilsson et al., 2008; Pan and Chen, 2004; Varetti et al., 2011).

The key components of the SAC include the proteins Mad1, Mad2, Mad3 (BubR1 in vertebrates), and Bub3 (Musacchio and Salmon, 2007). The SAC signal is initiated by formation of a stable Mad1-Mad2 complex at unattached kinetochores (Kulukian et al., 2009; Shah et al., 2004). Mad2 within this complex interacts with soluble Mad2 molecules, thereby catalyzing the formation of a complex between soluble Mad2 and Cdc20 (De Antoni et al., 2005; Hewitt et al., 2010; Maldonado and Kapoor, 2011; Simonetta et al., 2009). Cdc20 also interacts with Mad3 and its tightly bound partner Bub3 (Hardwick et al., 2000). The interdependencies of these binding events are not well understood, but the final output is an inhibitory complex known as the mitotic checkpoint complex (MCC), which contains Cdc20, Mad2, Mad3/BubR1, and Bub3 (Sudakin et al., 2001).

The mechanism of APC/C inhibition by these proteins remains unclear. While Mad2 and Mad3-Bub3 can each inhibit APC/C activity in vitro, together these proteins

are much more potent inhibitors (Fang, 2002; Fang et al., 1998; Kulukian et al., 2009; Tang et al., 2001). Early evidence suggested that the MCC sequesters Cdc20, preventing its binding to the APC/C. However, in subsequent work all proteins of the MCC were found to associate with the APC/C and block its activity, probably by inhibiting substrate binding (Braunstein et al., 2007; Chao et al., 2012; Herzog et al., 2009). The contribution of different MCC components is unclear, although Mad3/BubR1 acts in part as a pseudosubstrate inhibitor of Cdc20 (Burton and Solomon, 2007; Chao et al., 2012; Lara-Gonzalez et al., 2011; Malureanu et al., 2009).

APC/C inhibition during a SAC arrest might also depend on Cdc20 autoubiquitination. In budding yeast, the instability of Cdc20 during a SAC arrest requires Mad2 and Mad3 (King et al., 2007; Pan and Chen, 2004). Cdc20 is also degraded rapidly in human cells during a SAC arrest, and stabilization of Cdc20 (by mutation of all lysines in the protein) causes cells to bypass the arrest (Ge et al., 2009; Nilsson et al., 2008). These studies led to the suggestion that destruction of Cdc20 is required for inhibition of APC/C function during a SAC arrest, perhaps because it reduces Cdc20 levels below some threshold required for APC/C activation.

On the other hand, evidence from studies in human mitotic extracts led to speculation that Cdc20 ubiquitination promotes disassembly of the MCC and thus checkpoint inactivation (Reddy et al., 2007; Stegmeier et al., 2007). Consistent with this idea, numerous recent studies in human cells and cell lysates suggest that MCC disassembly and checkpoint inactivation depend on APC/C-dependent ubiquitination, ATP hydrolysis, and proteasomal function (Braunstein et al., 2007; Garnett et al., 2009; Jia et al., 2011; Ma and Poon, 2011; Miniowitz-Shemtov et al., 2010; Teichner et al.,

2011; Varetti et al., 2011; Visconti et al., 2010; Williamson et al., 2009; Zeng et al., 2010). In vertebrates, MCC disassembly is also promoted by the Mad2-binding protein $p31^{comet}$ (Fava et al., 2011; Habu et al., 2002; Hagan et al., 2011; Jia et al., 2011; Mapelli et al., 2006; Reddy et al., 2007; Teichner et al., 2011; Varetti et al., 2011; Westhorpe et al., 2011; Xia et al., 2004; Yang et al., 2007). Recent studies also suggest that the human APC/C subunit, Apc15, is required for efficient MCC turnover on the APC/C (Mansfeld et al., 2011). However, the biochemical mechanisms underlying MCC disassembly remain poorly understood, and the contributions of Cdc20 autoubiquitination to APC/C function in the SAC are not clear.

Here we explored the mechanism and function of Cdc20 ubiquitination in the SAC of budding yeast. Studies with purified proteins revealed that Mad2 and Mad3-Bub3 synergize to effectively inhibit securin ubiquitination, while at the same time promoting Cdc20 autoubiquitination. This activity required the APC/C subunit Mnd2/Apc15. To test the role of Cdc20 ubiquitination in SAC function, we analyzed mutants that reduce Cdc20 ubiquitination. Using a Cdc20 mutant that is poorly ubiquitinated throughout the cell cycle, we found that Cdc20 turnover is required for establishment of a SAC arrest. On the other hand, specific inhibition of MCC-dependent Cdc20 autoubiquitination, achieved by deletion of Mnd2, allowed a checkpoint arrest but delayed release from the arrest. Our results argue that Cdc20 ubiquitination has multiple functions: it suppresses Cdc20 levels to allow establishment of the SAC arrest and is also required for efficient release from the arrest.

RESULTS

Mad2 and Mad3 have opposing effects on autoubiquitination

Cdc20 is a highly unstable protein throughout the cell cycle. We showed previously that Cdc20 turnover in a normal cell cycle depends primarily on APC/C-dependent ubiquitination that is distinct from that of a canonical substrate (Foe et al., 2011). We dissected Cdc20 ubiquitination by reconstituting the reaction with purified proteins. By incubating radiolabeled Cdc20 with purified APC/C and other ubiquitination components, we found that Cdc20 is rapidly ubiquitinated while bound in its activator position on the APC/C. Autoubiquitination was not greatly affected by mutation of the D-box or by addition of unlabeled Cdc20, but was inhibited by mutation of the IR or C-box sequence motifs (Figure S1B, bottom panel) (Foe et al., 2011). We also performed Cdh1-mediated Cdc20 ubiquitination reactions in parallel and the resulting Cdc20 ubiquitination depended only on its D-box (Figure S1B, middle panel). For clarity and ease of quantitation, we prevented polyubiquitin chain formation on Cdc20 by using methylated ubiquitin and the E2 Ubc4, which is a poor catalyst of polyubiquitin assembly (Figure S1C) (Rodrigo-Brenni and Morgan, 2007).

Cdc20 is turned over rapidly during a SAC arrest, and there is evidence that this turnover depends on Cdc20 autoubiquitination (Nilsson et al., 2008; Pan and Chen, 2004). Consistent with these results, we found that Cdc20 instability during a checkpoint arrest requires a functional APC/C and proteasome activity (Figure S2A), but is independent of the APC/C activator Cdh1 (Figure S2B) (Pan and Chen, 2004). In

addition, checkpoint components are required for Cdc20 turnover (Figure S2C) (King et al., 2007; Pan and Chen, 2004).

To explore the mechanisms underlying Cdc20 autoubiquitination in a SAC arrest, we used purified components to test the effects of checkpoint proteins on Cdc20 function and autoubiquitination. We first analyzed the role of Mad2 using recombinant protein purified from *E. coli* (Figure S3). As expected from previous studies, purified Mad2 inhibited Cdc20 activity toward securin (Figure 1A). Surprisingly, Mad2 had the same inhibitory effect on Cdc20 autoubiquitination (IC_{50} for both reactions was ~0.5 μM).

Unlike Mad2, Mad3 expressed in *E. coli* was largely insoluble (Larsen et al., 2007). However, co-expression of Mad3 with Bub3 yielded a well-behaved complex (Figure S3). We found that this complex inhibited Cdc20-dependent securin ubiquitination (IC_{50} ~1 μM), but had little effect on autoubiquitination except at very high concentrations (Figure 1B).

To better characterize the Mad3-Bub3 effect on autoubiquitination, we used a sensitized Cdc20 mutant carrying a C-terminal IR motif mutation (Cdc20-IR) that reduces the affinity of Cdc20 for the APC/C and thereby reduces autoubiquitination (Figure S1B, bottom panel). The low level of Cdc20-IR autoubiquitination was stimulated by the Mad3-Bub3 complex (Figure 1C). Autoubiquitination was inhibited at the highest concentrations of Mad3-Bub3.

Checkpoint proteins regulate Cdc20 binding to the APC/C

The results in Figure 1 led us to hypothesize that the checkpoint proteins act, at least in part, by controlling the binding of Cdc20 to the APC/C. To test this possibility,

we developed a quantitative Cdc20-APC/C binding assay, similar to a Cdh1-APC/C binding assay we described previously (Matyskiela and Morgan, 2009). In this assay, yeast APC/C is immunopurified on magnetic beads and incubated with radiolabeled Cdc20 prepared by translation in vitro, followed by washing to remove unbound Cdc20.

First, we tested the effect of Mad2 by pre-incubating Cdc20 with increasing concentrations of Mad2 or a Mad2 C-terminal deletion mutant (Mad2-CΔ) that is known to be defective in binding Cdc20 (Luo et al., 2000). Mad2 reduced Cdc20 binding to the APC/C, while Mad2-CΔ had no effect (Figure 2A). These results are likely to explain the ability of Mad2 to inhibit both securin ubiquitination and Cdc20 autoubiquitination (see Figure 1A).

Our observation that Mad3-Bub3 stimulated autoubiquitination (Figure 1B, C) suggested that Mad3 might promote the association of Cdc20 with the APC/C. Indeed, addition of 1 μM Mad3-Bub3 induced a small (~2-fold) but reproducible stimulation of binding (Figure 2B). This small effect is perhaps not surprising because the affinity of Cdc20 for the APC/C is likely to be very high. To sensitize this assay, we used the Cdc20-IR mutation to reduce Cdc20 affinity for the APC/C. Mad3-Bub3 dramatically stimulated Cdc20-IR binding to the APC/C (Figure 2B), consistent with its ability to promote autoubiquitination of this mutant (Figure 1C).

In previous work, we showed that APC/C substrates stimulate the association of Cdh1 with the APC/C through a bivalent interaction between the activator and the APC/C core (Matyskiela and Morgan, 2009). This stimulation requires the core subunit Doc1/Apc10, which may interact directly with substrate (Buschhorn et al., 2011; Carroll and Morgan, 2002; da Fonseca et al., 2011; Passmore et al., 2003). Mutation of four

residues within Doc1 (Doc1-4A) inhibits substrate binding and blocks the ability of substrate to stimulate Cdh1 binding to the APC/C (Carroll et al., 2005; Matyskiela and Morgan, 2009). Similar stimulation and Doc1-dependence was observed for Cdc20 binding to the APC/C using a fragment of securin (Figure 2C, left panel) (Matyskiela and Morgan, 2009). To determine if Mad3-Bub3 promotes activator binding by a similar mechanism, we tested whether Doc1 was required for the stimulation of Cdc20 binding by Mad3-Bub3. Mad3-Bub3 had the same effect on Cdc20-IR binding to Doc1 and Doc1-4A APC/C (Figure 2C, right panel), suggesting that Mad3-Bub3 associates with the APC/C-Cdc20 complex through contacts not involving the substrate-binding site on Doc1.

Mad2 and Mad3-Bub3 synergize to inhibit securin ubiquitination and promote Cdc20 autoubiquitination

Mad2 and BubR1 (Mad3) are known to be poor inhibitors of vertebrate APC/C activity when tested individually, but inhibit at lower concentrations when added together (Fang, 2002). We tested this synergy using combinations of 0.5 μM Mad2 and increasing concentrations of the Mad3-Bub3 complex. The presence of Mad2 dramatically increased the potency of the Mad3-Bub3 complex, shifting the IC_{50} from ~1 μM to 6 nM (Figure 3A, C).

Next we tested the combined effects of Mad2 and Mad3-Bub3 on Cdc20 autoubiquitination. Since we observed opposite effects of Mad2 and Mad3-Bub3 when they were tested individually (Figure 1), we were particularly interested in the possibility that Mad3-Bub3 might reverse the effect of Mad2. We used 5 μM Mad2, a concentration

at which we observed clear inhibition of binding and autoubiquitination (Figure 1A and 2A). Strikingly, we found that Mad3-Bub3 reversed the inhibitory effect of Mad2 on Cdc20 autoubiquitination, and the dose response curve was the mirror image of the securin inhibition curve (Figure 3B, C): the IC_{50} of securin inhibition was similar to the EC_{50} for autoubiquitination (6 and 12 nM, respectively). We thus reconstituted the two major effects of the SAC – inhibition of securin ubiquitination and stimulation of Cdc20 autoubiquitination – at low concentrations of Mad3-Bub3. While Mad2 concentrations were higher, we suspect that the specific activity of our purified Mad2 preparations is low, and Mad2 is likely to be more active in vivo due to stimulation by the kinetochore-associated Mad1-Mad2 complex (De Antoni et al., 2005).

MCC-dependent Cdc20 autoubiquitination depends on the Mnd2 subunit of the APC/C

Recent studies in human cells suggest that Cdc20-MCC turnover during a SAC arrest depends on the nonessential APC/C subunit Apc15 (Mansfeld et al., 2011), but the effects of this subunit on Cdc20 autoubiquitination are not clear. The budding yeast homolog of Apc15 was suggested to be Mnd2 (Mansfeld et al., 2011). Mnd2 is known to be required for meiotic progression (Oelschlaegel et al., 2005; Penkner et al., 2005; Rabitsch et al., 2001) but is thought to have little, if any, effect in mitosis (Hall et al., 2003). To explore the roles of Mnd2 in yeast APC/C function and the SAC, we purified APC/C from an *mnd2Δ* strain. As previously shown, deletion of Mnd2 did not significantly affect the subunit composition of purified APC/C (Hall et al., 2003; Oelschlaegel et al., 2005). Also consistent with previous results, Mnd2Δ APC/C was

similar to wild-type APC/C in its ability to target securin for ubiquitination in vitro, using Cdc20 as activator (Figure 4A) (Oelschlaegel et al., 2005). Mnd2Δ APC/C also displayed wild-type activity with the activator Cdh1 and with the E2 Ubc1 (J. Girard, unpublished results) (Oelschlaegel et al., 2005). Importantly, we found that Mnd2Δ APC/C also catalyzed Cdc20 autoubiquitination at wild-type rates in the absence of checkpoint components (Figure 4B).

We also analyzed Cdc20 autoubiquitination in the presence of checkpoint proteins. We observed a striking defect in Cdc20 autoubiquitination with Mnd2Δ APC/C (Figure 4C), suggesting that the Mnd2 subunit is required for Cdc20 autoubiquitination in the context of the MCC, but not in its absence.

We next tested if the defect in Cdc20 autoubiquitination was due to a defect in Cdc20 binding to the APC/C in the context of the checkpoint proteins. Loss of the Mnd2 subunit had no detectable effect on the ability of Mad3-Bub3 to stimulate Cdc20 binding to the APC/C (Figure 4D), suggesting that MCC binding does not depend on Mnd2. Thus, reduced MCC-dependent Cdc20 autoubiquitination in the absence of Mnd2 does not result from poor Cdc20 binding but might instead result from a defect in the positioning of Cdc20 for autoubiquitination.

Stabilized Cdc20 allows bypass of the spindle assembly checkpoint

We next sought to explore the role of Cdc20 ubiquitination in vivo by creating mutations that prevent Cdc20 ubiquitination without affecting its activator function or interaction with checkpoint proteins. First, we generated a *CDC20* mutant encoding a protein with all 39 lysines mutated to arginines (*cdc20-0K* mutant) (Figure S4A).

Surprisingly, we found that this mutant rescued *CDC20* function nearly as well as the wild-type gene at 25°C, implying that ubiquitination of Cdc20 is dispensable for viability (Figure S4B). However, the *cdc20-0K* mutant was temperature-sensitive and inviable at 37°C. Consistent with this sensitivity, we found that the Cdc20-0K protein was significantly less active toward securin in vitro (Figure 5A).

We hypothesized that specific lysines might be required for Cdc20 activity but not for ubiquitination. To identify these lysines, we carried out the analyses shown in Figure S4C and D. First, we generated three Cdc20 mutants, each with the lysines in one region (either N-terminal (N), middle (M), or C-terminal (C)) mutated to arginines (with the other regions remaining wild-type) (Figure S4A). Mutation of the nineteen C-terminal lysines (Cdc20-C mutant), but not mutation of lysines elsewhere in the protein, resulted in loss of activity towards securin in vitro (Figure S4C, left panel), suggesting that Cdc20 activity depends on lysines in the C-terminal region.

To identify specific C-terminal lysines required for activity, we analyzed Cdc20 proteins with single lysine-to-arginine mutations. Mutations at four lysines (K320, K431, K516, K550) each reduced Cdc20 activity toward securin over two-fold (Figure S4D). The K514R mutant also had a significant defect that became more pronounced when combined with the K516R mutation. These five residues fall within the predicted WD40 domain, and we suspect that these mutations affect the stability of this domain. To determine whether these five mutations caused the loss of function of the Cdc20-0K mutant, we generated a Cdc20-5K mutant in which these lysines were added back to the Cdc20-0K mutant. The Cdc20-5K protein exhibited near wild-type activity towards

securin and other APC/C^{Cdc20} substrates (Figure 5A, S4E), and the *CDC20-5K* mutant supported normal viability at all temperatures (Figure S4B).

We also analyzed ubiquitination of the Cdc20-N, M, and C mutants (Figure S4C, middle and right panels). Mutation of the 12 lysines in the N-terminal region (Cdc20-N mutant) resulted in significant loss of autoubiquitination, while only partially removing sites targeted by Cdh1. Autoubiquitination of human Cdc20 has also been mapped primarily to N-terminal lysines (Zeng and King, 2012). Autoubiquitination was also reduced in the Cdc20-C mutant, perhaps as a result of its general loss of stability (Figure S4C). Analysis of C-terminal lysine point mutants revealed that one mutation (K374R) reduced autoubiquitination despite having no apparent effect on activity (data not shown). Mutation of K374 reduced autoubiquitination in the Cdc20-N mutant, but two ubiquitination sites remained (Figure S4F).

Most importantly, we found that the Cdc20-5K protein was not detectably modified by either autoubiquitination or Cdh1-dependent ubiquitination in vitro (Figure 5B), indicating that this mutant lacks all major ubiquitination sites while retaining function as an APC/C activator (Figures 5A, S4B, S4E).

We constructed a strain in which the endogenous *CDC20* was replaced with the *CDC20-5K* mutant. *CDC20* and *CDC20-5K* strains were released from a G1 arrest into a single cell cycle. The Cdc20-5K protein was significantly stabilized, resulting in dampened oscillations with a peak mitotic level greater than that of the wild-type protein (Figure 5C). Oscillations in Cdc20-5K protein levels might be due to a low rate of ubiquitination in vivo on one or more of the five remaining lysines, which was not detectable in our ubiquitination studies in vitro. In addition, *CDC20* transcription is

known to peak in mitosis (Prinz et al., 1998). Despite the stabilization of the Cdc20-5K mutant protein, *CDC20-5K* cells progressed at wild-type rates through the cell cycle, undergoing DNA replication and mitosis at normal times (data not shown). Oscillations in securin levels appeared identical in the *CDC20* and *CDC20-5K* strains (Figure 5C). Cdc20 ubiquitination and rapid turnover are therefore not required for normal cell-cycle progression.

We next tested the spindle checkpoint function of the *CDC20-5K* mutant by measuring sensitivity to the spindle poison benomyl. The *CDC20-5K* mutant showed a clear benomyl sensitivity that was similar to that of *mad3Δ* cells, but not as severe as that in the *mad2Δ* mutant (Figure S5).

We also arrested *CDC20*, *CDC20-5K*, *mad2Δ*, or *mad3Δ* strains in G1 and released the cells into high benomyl concentrations. In wild-type cells, the checkpoint arrest was accompanied by high levels of Cdc20 and securin (Figure 5D). However, the *CDC20-5K*, *mad2Δ*, and *mad3Δ* strains all failed to establish the SAC arrest, leading to destruction of securin with relatively normal timing (Figure 5D; *mad3Δ* data not shown). As in the normal cell cycle (Figure 5C), the Cdc20-5K protein was present at high levels in benomyl-treated mitotic cells. Consistent with this observation, Cdc20-5K was significantly stabilized in cells in which benomyl was added to cells arrested in metaphase by overexpression of a stabilized securin mutant (Figure 5E).

Studies with purified components revealed that the Cdc20-5K protein displayed wild-type sensitivity to Mad2 (Figure 5F). Mad3-Bub3 was also an effective inhibitor of securin ubiquitination by the mutant Cdc20-5K protein (Figure 5G). Thus, the checkpoint defect in *CDC20-5K* cells is not caused by a defect in the interaction of Cdc20-5K with

checkpoint proteins. Instead, our results suggest that the stabilization of Cdc20 results in a defective spindle checkpoint, although they do not allow us to conclude whether this defect is in the establishment or maintenance of the checkpoint.

Mnd2 is required for efficient checkpoint release

To further characterize the role of Cdc20 ubiquitination in SAC signaling, we sought a mutant that was specifically defective in Cdc20 ubiquitination during a checkpoint arrest, which would allow us to determine the importance of ubiquitination in maintenance of the arrest. The *mnd2*Δ strain seemed an ideal candidate for such a mutant, as our studies in Figure 4 had shown that Mnd2Δ APC/C is defective in Cdc20 autoubiquitination in the presence of checkpoint proteins but not in their absence.

Consistent with our evidence that removal of Mnd2 has no effect on APC/C activity in vitro (Figure 4A, B), we found that *mnd2Δ* cells released from G1 display no significant defects in progression through an unperturbed mitosis, with securin destruction occurring with normal timing (Figure 6A). Peak mitotic levels of Cdc20 were slightly elevated in *mnd2*Δ cells, suggesting that the nonessential SAC of budding yeast may be controlling Cdc20 levels in mitosis even in unperturbed cells. Importantly, the drop in Cdc20 levels after securin destruction was similar to that in wild-type cells, suggesting that Cdc20 turnover outside of the checkpoint was unaffected.

Interestingly, *mnd2*Δ cells displayed a normal SAC arrest when released from G1 into high benomyl concentrations (Figure 6B). In agreement with our studies showing that Mnd2 promotes SAC-dependent Cdc20 ubiquitination (Figure 4C), Cdc20 was stabilized in checkpoint-arrested *mnd2Δ* cells (Figure 6C), in contrast to the normal

instability of Cdc20 in unperturbed cells (Figure 6A). We conclude that once the checkpoint is established, rapid Cdc20 turnover is not required to maintain the mitotic arrest.

The *mnd2*Δ mutant allowed us to test the possibility that Cdc20 ubiquitination promotes release from the arrest in budding yeast, as suggested by previous studies in human cells and cell lysates (Jia et al., 2011; Mansfeld et al., 2011; Reddy et al., 2007; Stegmeier et al., 2007; Varetti et al., 2011). Benomyl-arrested wild-type and *mnd2Δ* cells were released from the arrest by removal of benomyl, and then held in the following G1 to prevent progression into the next cell cycle. Securin destruction and chromosome segregation were delayed by approximately ten minutes, and were less abrupt, in *mnd2Δ* cells relative to wild-type control cells (Figure 6D, E). These results are consistent with the notion that Mnd2-dependent Cdc20 autoubiquitination is required for efficient inactivation of the spindle checkpoint.

DISCUSSION

The regulation of Cdc20, like that of most key regulatory proteins, depends on its short lifetime in the cell. This instability arises primarily from self-inhibition by autoubiquitination, which targets the protein for destruction in the proteasome. In a normal cell cycle, autoubiquitination is the primary mechanism underlying the drop in Cdc20 levels that occurs in late mitosis (Foe et al., 2011). Surprisingly, however, we found that cells expressing the poorly ubiquitinated Cdc20-5K mutant are viable and display no significant cell cycle defects, despite the presence in these cells of high Cdc20 levels that decline only slightly outside of mitosis. Thus, rapid Cdc20 turnover is not essential in a normal cell cycle. The same is not true in a spindle checkpoint, however. The *CDC20-5K* strain failed to establish a spindle checkpoint arrest, to a similar extent as mutants lacking the checkpoint genes *MAD2* or *MAD3*.

A lysine-free form of human Cdc20 also bypasses the SAC (Nilsson et al., 2008), but it has been suggested that this bypass might be due to a slight decrease in Mad2 affinity caused by mutation of two lysines in the Mad2-binding region (Varetti et al., 2011). However, budding yeast Cdc20 does not contain these lysines and instead contains one lysine N-terminal of the conserved interaction motif (Luo et al., 2002). Furthermore, we found that wild-type Cdc20 and Cdc20-5K interact equally well with checkpoint proteins in vitro (Figures 5F, G). We therefore conclude that the yeast Cdc20-5K mutant is not defective in its interaction with checkpoint proteins.

How, then, does the Cdc20-5K mutant allow progression through mitosis despite activation of the checkpoint? The most likely possibility, which is consistent with

previous evidence that moderate *CDC20* overexpression drives yeast cells through a checkpoint arrest (Pan and Chen, 2004), is that the higher levels of Cdc20-5K protein somehow provide resistance to activated checkpoint proteins. One simple possibility is that checkpoint proteins are limiting, allowing high levels of Cdc20 to outnumber Mad2 to allow formation of active APC/C-Cdc20 complexes despite the checkpoint activation. This seems unlikely, however, given the ability of *mnd2*Δ cells to arrest normally despite accumulating higher Cdc20 levels within the arrest (Figure 6C). A more appealing possibility stems from our observation that Mad2 does not inhibit the activity of preformed APC/C-Cdc20 complexes in vitro (data not shown), presumably because the binding affinity of Cdc20 is so high that Mad2 cannot gain access to its binding site on Cdc20. Thus, the downregulation of Cdc20 from late mitosis through S phase may be required to keep Cdc20 levels at a low level that prevents the premature formation of checkpoint-resistant APC/C-Cdc20 complexes. Thus, our results argue that the degradation of Cdc20 outside mitosis is required for efficient establishment of a checkpoint arrest.

Checkpoint proteins are required for rapid Cdc20 turnover during a checkpoint arrest (King et al., 2007; Pan and Chen, 2004) (Figure S2C). To explore the underlying mechanism, we reconstituted the effects of Mad2 and the Mad3-Bub3 complex with purified components. We found that Mad2 alone inhibited Cdc20 binding and autoubiquitination. The incomplete effect of Mad2, even at apparently saturating concentrations, suggests that the target of Mad2 may be just one of the multiple contact points that mediate Cdc20 binding to the APC/C. Given that the Mad2 binding motif in

Cdc20 lies in the amino-terminal region near the C-box, a likely possibility is that Mad2 somehow interferes with C-box function.

Checkpoint proteins clearly synergize in forming the Cdc20-Mad2-Mad3-Bub3 complex (MCC). Although Mad2 inhibits Cdc20 binding to the APC/C, the Mad3-Bub3 complex reverses this effect and stimulates Cdc20 binding and autoubiquitination. We find that the three budding yeast checkpoint proteins are sufficient to promote robust Cdc20 autoubiquitination in the absence of additional components, in contrast to the dependence on $p31^{comet}$ in human cells and lysates (Reddy et al., 2007; Varetti et al., 2011). Yeast do not contain a clear homolog of $p31^{comet}$, and so vertebrate cells may have evolved additional control mechanisms. The synergistic actions of checkpoint proteins are likely to depend on interactions between Mad2 and Mad3, as suggested by recent studies supporting a direct interaction between purified human Mad2 and BubR1 (Tipton et al., 2011). Recent structural analysis of fission yeast MCC components (Mad3, Mad2, and Cdc20) also revealed Mad2-Mad3 interactions that would explain the synergistic effect (Chao et al., 2012).

Interestingly, the full set of checkpoint proteins has opposite effects on two APC/C-dependent activities: inhibition of securin ubiquitination and stimulation of Cdc20 autoubiquitination. Thus, the MCC is not a global inhibitor of the APC/C, but inhibits only its substrate-targeting function. How is this possible? KEN boxes in Mad3 were proposed to function as pseudosubstrate inhibitor motifs that interfere with substrate binding to Cdc20 (Burton and Solomon, 2007), and recent structural data provides evidence for engagement of a Mad3 KEN box by the WD40 domain of Cdc20 (Chao et al., 2012). Interestingly, other studies suggest that the MCC causes a shift in the position

of Cdc20 on the APC/C, away from the Doc1/Apc10 subunit that contributes to substrate binding (Herzog et al., 2009; Izawa and Pines, 2011); thus, the MCC might reduce substrate binding in part by separating Cdc20 from Doc1. We found that the majority of autoubiquitination sites lie within the Cdc20 N-terminal region, which is predicted to be unstructured and also contains the C-box motif, which recent studies suggest could interact with the Apc2 subunit at a location that is close to the site of E2 binding – and thus in a good position to attack the E2-ubiquitin conjugate (da Fonseca et al., 2011), as also suggested recently for human Cdc20 (Zeng and King, 2012). Perhaps MCC binding shifts Cdc20 to a position that reduces substrate interactions while favoring autoubiquitination.

The stimulation of Cdc20-APC/C binding by Mad3-Bub3 suggests that Mad3 (and/or Bub3) interacts with the APC/C core. Structural analysis of the APC/C-MCC complex suggests that the MCC could contact multiple subunits (Herzog et al., 2009). We found that Doc1/Apc10 is not required for the stimulation of Cdc20 binding by Mad3, suggesting that this subunit does not contribute to MCC binding – and consistent with the notion, mentioned above, that the MCC shifts Cdc20 away from Doc1. We also tested another nonessential subunit, Mnd2, based on recent evidence that a related human subunit, Apc15, is required for Cdc20-MCC turnover in the checkpoint (Mansfeld et al., 2011). Mnd2 has been suggested to interact with Apc1, Apc5, and Cdc23 (Hall et al., 2003), three subunits in the APC/C region where the MCC appears to bind (Chao et al., 2012; Herzog et al., 2009; Schreiber et al., 2011). Furthermore, Cdc23/Apc8 is particularly important in Cdc20 binding in the checkpoint (Izawa and Pines, 2011). Deletion of Mnd2 had a striking and specific effect: autoubiquitination and activity

toward securin were largely unaffected in the absence of checkpoint proteins, but the loss of Mnd2 blocked the ability of Mad3-Bub3 to stimulate autoubiquitination in the presence of Mad2. Interestingly, we found that the loss of Mnd2 did not prevent the stimulation of Cdc20 binding to the APC by Mad3-Bub3. These results argue strongly that Mnd2 (and perhaps Apc15 in the human APC/C) is required for the MCC to shift the position of Cdc20 for checkpoint-induced autoubiquitination.

Surprisingly, despite the rapid turnover of Cdc20 that occurs in checkpoint-arrested cells, steady-state levels of Cdc20 appear constant (Figure 5D). Thus, a high rate of mitotic Cdc20 synthesis balances increased destruction. As recently proposed (Varetti et al., 2011), this constant flux of Cdc20 is likely to be important for reversing the effects of the checkpoint when all sister-chromatid pairs achieve correct spindle attachment. Cells lacking *MND2* provided us with an effective approach to explore this possibility. In these cells, the lack of Mnd2 did not greatly affect Cdc20 oscillations in a normal cell cycle, and thus these cells do not have the general increase in Cdc20 levels that we observed in the *CDC20-5K* cells. Instead, *mnd2*Δ cells displayed a more specific defect in autoubiquitination and Cdc20 turnover in the presence of checkpoint proteins. These cells establish and maintain a checkpoint arrest, indicating that MCC-dependent autoubiquitination and rapid Cdc20 degradation are not required for the arrest. These results also support the notion, discussed above, that the Cdc20-5K mutant bypasses the arrest because of its high levels throughout the cell cycle.

Although *mnd2*Δ cells arrest in the checkpoint, they are less efficient than wild-type cells in inactivation of the checkpoint when spindle poisons are removed, as observed in human cells depleted of Apc15 (Mansfeld et al., 2011). Thus, inactivation of

the checkpoint might depend, at least in part, on MCC-dependent Cdc20 autoubiquitination. How does ubiquitination promote checkpoint inactivation? In purified reactions, we have not seen evidence that polyubiquitination causes dissociation of Cdc20 from the checkpoint complex and APC/C (Figure S6). Instead, we suspect that MCC removal is an active process mediated in part by the proteasome and other factors, as suggested by recent evidence for the involvement of ATP hydrolysis and proteolysis (Ma and Poon, 2011; Miniowitz-Shemtov et al., 2010; Teichner et al., 2011; Visconti et al., 2010; Zeng et al., 2010). In vertebrates, checkpoint inactivation also depends on the protein $p31^{comet}$, which has been proposed to provide a functionally redundant mechanism for driving MCC disassembly (Jia et al., 2011). We speculate that when the SAC signal is extinguished, the ATP-dependent removal of polyubiquitinated Cdc20, together with its checkpoint partners, helps allow newly synthesized Cdc20 to reactivate the APC/C. In this way, the dynamic features of the checkpoint – balanced high rates of Cdc20 synthesis and destruction – allow cells to rapidly initiate anaphase upon checkpoint inactivation.

EXPERIMENTAL PROCEDURES

Yeast Methods

See Table S1 for yeast strains. All strains were derivatives of W303. Synchronization and analysis of yeast cultures is described in Supplemental Experimental Procedures.

APC/C Assays

APC/C was purified from a *TAP-CDC16 cdh1Δ* strain. E1, E2 (Ubc4 or Ubc1), APC/C, and Cdh1 were expressed and purified as previously described (Carroll and Morgan, 2005; Rodrigo-Brenni and Morgan, 2007). Cdc20, securin, Acm1, Dbf4 (amino acids 1-236), and Clb5 (with a C-terminal 3HA-tag) were cloned into plasmids containing a T7 promoter and an N-terminal or C-terminal ZZ tag. ZZ-tagged proteins were generated in vitro with TnT T7 Quick Coupled Transcription/Translation Systems (Promega) either in the presence of ^{35}S-methionine or unlabeled methionine. ZZ-tagged proteins were purified from the reticulocyte lysate using IgG-coupled Dynabeads (Invitrogen) and cleaved using TEV protease. E2 charging was performed in the presence of E1 (Uba1, 300 nM), E2 (Ubc4 or Ubc1, 50 μM), ubiquitin (wild-type, K48R, or methyl-ubiquitin; Boston Biochem, 150 μM), and ATP (1 mM) for 20 min. Reactions were initiated by the addition of charged E2, APC/C (1-5 nM), purified Cdc20, and purified securin. Reactions were performed at 23°C for the indicated time. For reactions containing Mad2, Cdc20 was pre-incubated with the indicated final concentration of Mad2 before addition of other components. For Mad3 reactions, Cdc20 was pre-incubated with the APC/C and the indicated final concentration of Mad3-Bub3 before addition of other components. All

reactions were stopped by the addition of SDS sample buffer, separated by SDS-PAGE, and visualized and quantified with a Molecular Dynamics PhosphorImager and ImageQuant (Amersham Biosciences/GE Healthcare).

Cdc20-APC/C binding assays

APC/C was immunopurified from *TAP-CDC16 cdh1Δ* strains using IgG beads. APC/C-bound beads or beads incubated with untagged lysate were incubated with in vitro translated ^{35}S-Cdc20. Immunoprecipitates were washed two times to remove unbound proteins and bound proteins were eluted with SDS sample buffer. For Mad2 experiments, Cdc20 was pre-incubated with the indicated final concentration of Mad2 or Mad2-CΔ before addition of beads. The securin fragment was generated as previously described (Matyskiela and Morgan, 2009).

SUPPLEMENTAL EXPERIMENTAL PROCEDURES

Yeast Cell Cycle Methods and Western Blotting

For the *CDC20* shutoff experiments, strains were generated with P_{GALL}-*CDC20* on a plasmid covering Cdc20 function, allowing manipulation of the endogenous *CDC20* locus. Cells were grown in minimal media containing galactose to select for the plasmid and to cover loss of function alleles. Cell cycle arrests were done with 1 μg/ml alpha factor or 60 μg/ml benomyl for 3 h at 30˚C unless otherwise stated. All arrests were confirmed by flow cytometry analysis of DNA content. Benomyl-sensitivity experiments were performed by serially diluting cells onto YPD plates containing the specified final concentration of benomyl. Half-life assays were performed in benomyl by the addition of 100 mg/ml cycloheximide. To inhibit proteasome activity, 200 μM MG132 was added to cells containing *pdr5*Δ to increase retention of the drug. For the turnover experiments in the *mad3Δ* and *CDC20-5K* strains, a metaphase-arrest was maintained by the expression of P_{GAL1}-*PDS1*-Δ*db*. Asynchronous cells were grow in YEP media containing 2% raffinose and arrested simultaneously in both 2% galactose and benomyl. For the spindle checkpoint release experiments, cells were shifted to 25˚C prior to removing benomyl-containing media. Antibodies were α-myc (1:1000, 9E10, Covance), α-Cdk1 (1:1000, sc-53, Santa Cruz), and α-Cdc20 (1:1000, yC-20, Santa Cruz).

Figure 1. Mad2 and Mad3 have opposite effects on autoubiquitination

(A) APC/C was immunopurified from lysates of *CDC16-TAP cdh1Δ* cells and used in ubiquitination reactions. Unlabeled Cdc20 (left) or ^{35}S-Cdc20 (right), translated in and purified from rabbit reticulocyte lysates as ZZ-tagged proteins, was pre-incubated with the indicated Mad2 concentration before addition of APC/C (5 nM), E1/E2(Ubc4)/methyl-ubiquitin, and purified ZZ-tagged ^{35}S-securin (left) or APC/C (5 nM) and E1/E2(Ubc4)/methyl-ubiquitin (right). Data were analyzed using Prism, with the zero concentration plotted on a log scale as 0.01 μM. Results are representative of two independent experiments.

(B) Purified unlabeled Cdc20 (left) or ^{35}S-Cdc20 (right) was pre-incubated with the indicated Mad3-Bub3 concentration and APC/C (5 nM), as well as purified ^{35}S-securin for the reactions at left. Reactions were started by the addition of E1/E2(Ubc4)/methyl-ubiquitin. The zero concentration was plotted on a log scale as 0.05 μM. Results are representative of two independent experiments.

(C) Purified ^{35}S-Cdc20-IR (I609A, R610A) was pre-incubated with the indicated Mad3-Bub3 concentration and APC/C (5 nM). Reactions were started by the addition of E1/E2(Ubc4)/methyl-ubiquitin. Results are representative of two independent experiments.

Figure 1

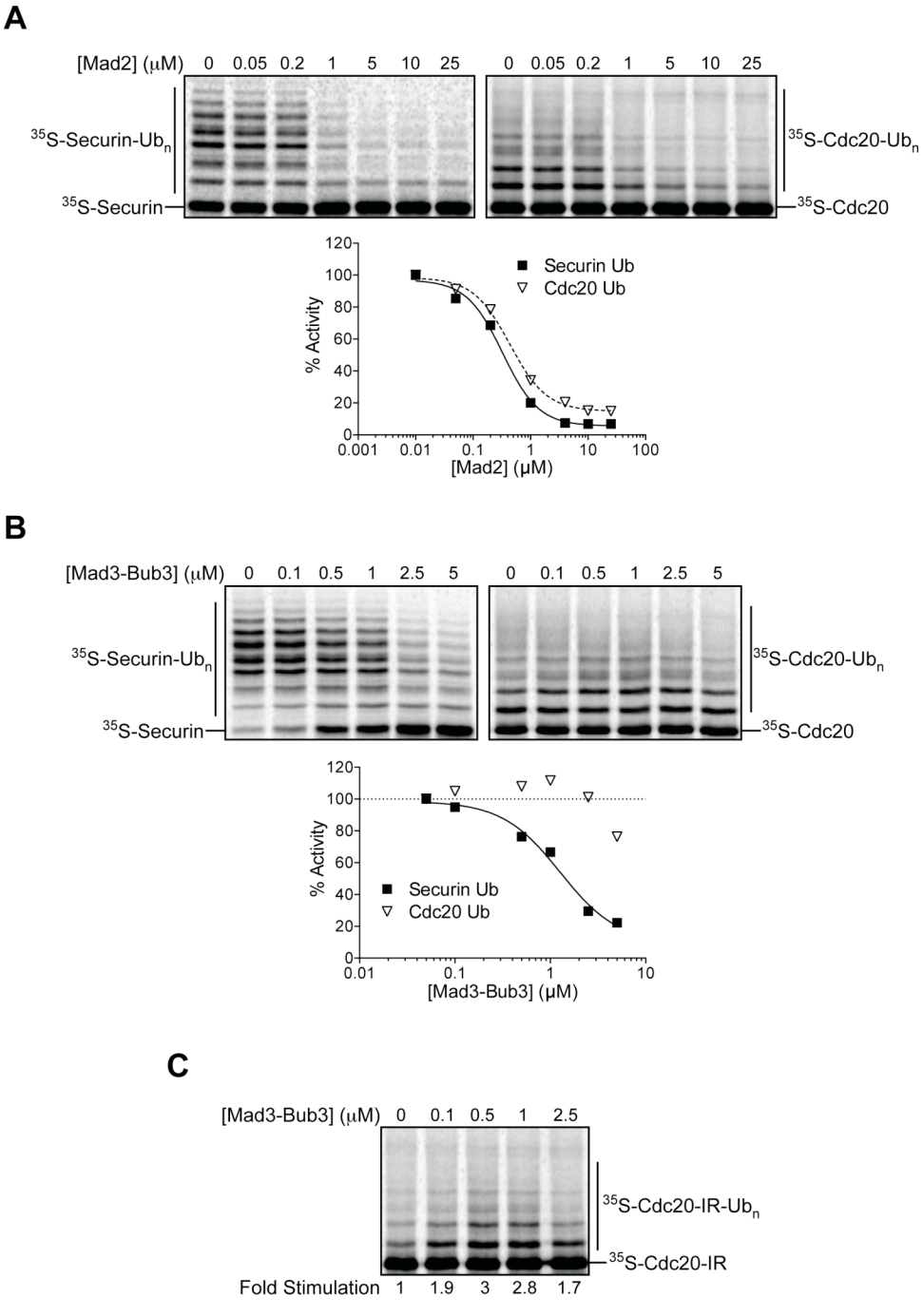
A
[Mad2] (μM) 0 0.05 0.2 1 5 10 25 0 0.05 0.2 1 5 10 25
35S-Securin-Ubn
35S-Securin
35S-Cdc20-Ubn
35S-Cdc20
Securin Ub
Cdc20 Ub
% Activity
[Mad2] (μM)
B
[Mad3-Bub3] (μM) 0 0.1 0.5 1 2.5 5 0 0.1 0.5 1 2.5 5
35S-Securin-Ubn
35S-Securin
35S-Cdc20-Ubn
35S-Cdc20
Securin Ub
Cdc20 Ub
% Activity
[Mad3-Bub3] (μM)
C
[Mad3-Bub3] (μM) 0 0.1 0.5 1 2.5
35S-Cdc20-IR-Ubn
35S-Cdc20-IR
Fold Stimulation 1 1.9 3 2.8 1.7

Figure 2. Checkpoint proteins regulate Cdc20 binding to the APC/C

(A) ^{35}S-Cdc20 in reticulocyte lysate was pre-incubated with the indicated Mad2 or Mad2-CΔ concentration and added to TAP-APC/C beads. Following a 30 min incubation, beads were washed and the bound Cdc20 was analyzed by SDS-PAGE and autoradiography. Results are representative of two independent experiments.

(B) ^{35}S-Cdc20 or ^{35}S-Cdc20-IR in reticulocyte lysate was incubated with the indicated Mad3-Bub3 concentration and TAP-APC/C beads, and analyzed as in panel (A). Similar results were obtained in three independent experiments.

(C) ^{35}S-Cdc20-IR in reticulocyte lysate was incubated with the indicated concentration of securin fragment (aa 1-110) or Mad3-Bub3 and TAP-APC/C beads immunopurified from *DOC1* or *doc1-4A* strains. Results are representative of two independent experiments.

Figure 2

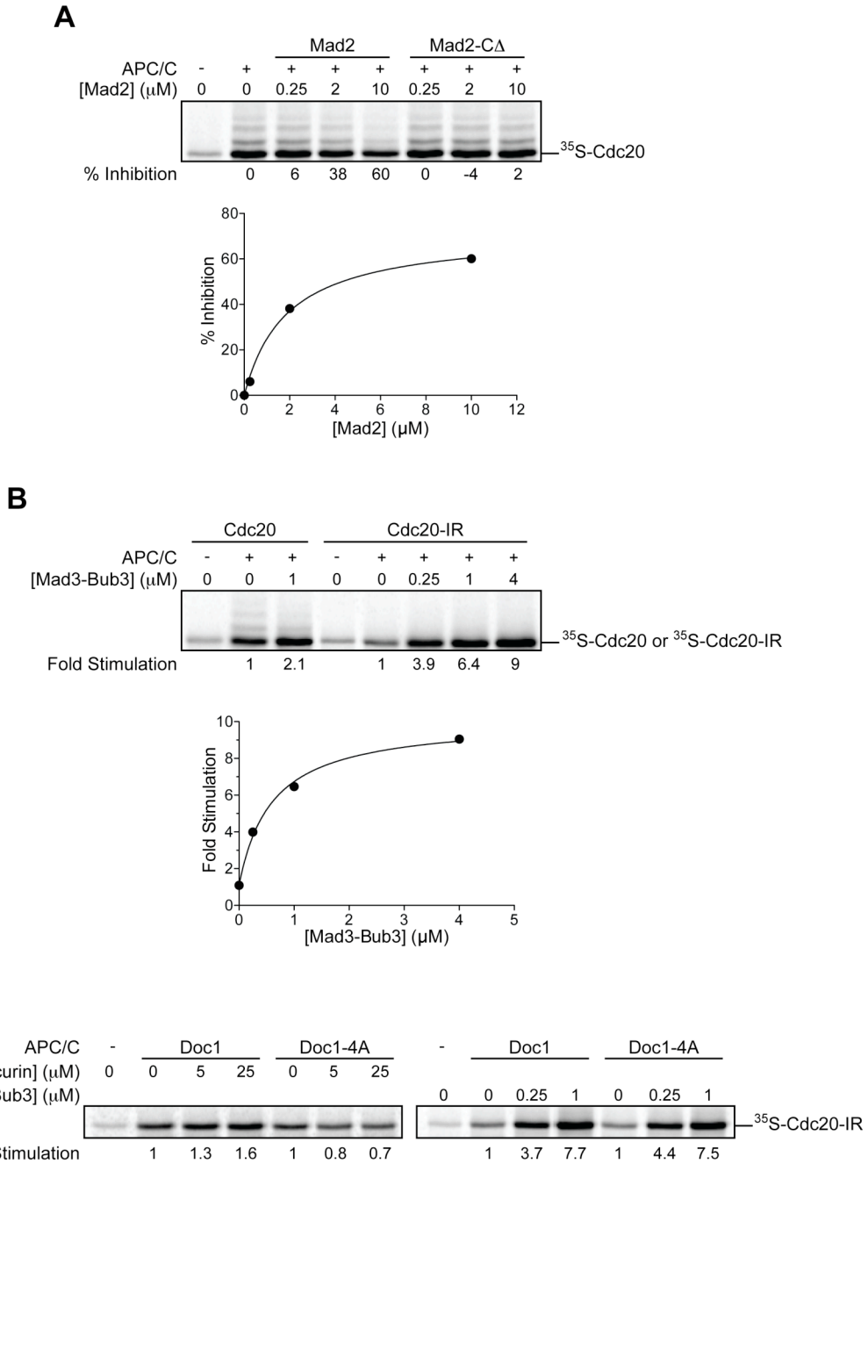
A
Mad2
Mad2-CΔ
APC/C - + + + + + +
[Mad2] (μM) 0 0 0.25 2 10 0.25 2 10
35S-Cdc20
% Inhibition 0 6 38 60 0 -4 2
% Inhibition
[Mad2] (μM)
B
Cdc20
Cdc20-IR
APC/C - + + - + + + +
[Mad3-Bub3] (μM) 0 0 1 0 0 0.25 1 4
35S-Cdc20 or 35S-Cdc20-IR
Fold Stimulation 1 2.1 1 3.9 6.4 9
Fold Stimulation
[Mad3-Bub3] (μM)
C
APC/C - Doc1 Doc1-4A - Doc1 Doc1-4A
[Securin] (μM) 0 0 5 25 0 5 25
[Mad3-Bub3] (μM) 0 0 0.25 1 0 0.25 1
35S-Cdc20-IR
Fold Stimulation 1 1.3 1.6 1 0.8 0.7 1 3.7 7.7 1 4.4 7.5

Figure 3. Mad2 and Mad3-Bub3 synergize to inhibit securin ubiquitination and allow autoubiquitination

(A) Purified unlabeled Cdc20 was pre-incubated with 0.5 μM Mad2 and the indicated Mad3-Bub3 concentration. Reactions were started by the addition of purified ^{35}S-securin, APC/C (5 nM), and E1/E2(Ubc4)/methyl-ubiquitin mix. Similar results were obtained in three independent experiments.

(B) Purified ^{35}S-Cdc20 was pre-incubated with 5 μM Mad2 and the indicated Mad3-Bub3 concentration. Reactions were started by the addition of APC/C (5 nM) and E1/E2(Ubc4)/methyl-ubiquitin mix. Similar results were obtained in two independent experiments.

(C) The data from (A) and (B) were analyzed using Prism, and the zero concentration was plotted on a log scale as 0.01 nM.

Figure 3

A

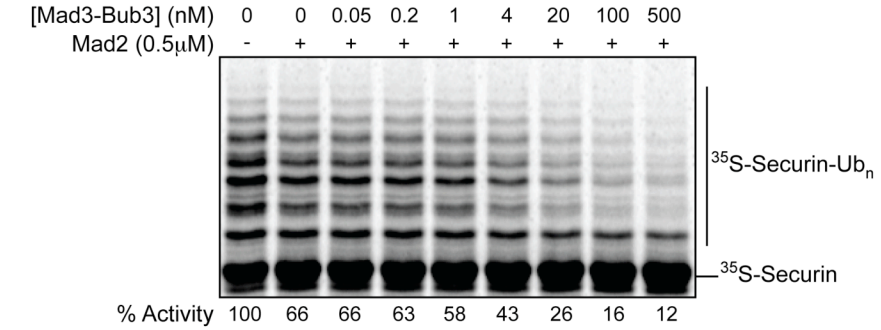
[Mad3-Bub3] (nM) 0 0 0.05 0.2 1 4 20 100 500
Mad2 (0.5μM) - + + + + + + + +
35S-Securin-Ubn
35S-Securin
% Activity 100 66 66 63 58 43 26 16 12

B

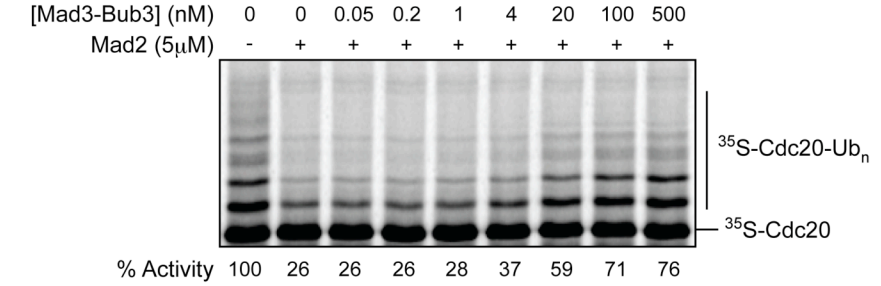
[Mad3-Bub3] (nM) 0 0 0.05 0.2 1 4 20 100 500
Mad2 (5μM) - + + + + + + + +
35S-Cdc20-Ubn
35S-Cdc20
% Activity 100 26 26 26 28 37 59 71 76

C

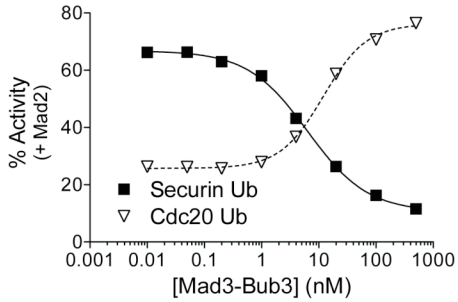
% Activity (+ Mad2)
80
60
40
20
0
Securin Ub
Cdc20 Ub
0.001 0.01 0.1 1 10 100 1000
[Mad3-Bub3] (nM)

Figure 4. MCC-dependent Cdc20 autoubiquitination depends on the Mnd2 subunit of the APC/C

(A) APC/C was immunopurified from lysates of *CDC16-TAP cdh1Δ* (WT) or *CDC16-TAP cdh1Δ mnd2Δ* cells and used in ubiquitination reactions with purified ^{35}S-securin, APC/C (1 nM [+] or 5 nM [++]) or APC/C buffer (-) as a control, and E1/E2(Ubc4)/methyl-ubiquitin mix. Similar results were obtained in three independent experiments.

(B) Purified ^{35}S-Cdc20 was incubated with wild-type (WT) or Mnd2Δ APC/C (5 nM) and E1/E2(Ubc4)/methyl-ubiquitin mix. Similar results were obtained in three independent experiments.

(C) Purified ^{35}S-Cdc20 was pre-incubated with 5 μM Mad2 and the indicated Mad3-Bub3 concentration. Reactions were started by the addition of wild-type (WT) or Mnd2Δ APC/C (5 nM) and E1/E2(Ubc4)/methyl-ubiquitin mix. Data were analyzed using Prism, and the zero concentration was plotted on a log scale as 0.01 nM. Similar results were obtained in two independent experiments.

(D) ^{35}S-Cdc20-IR in reticulocyte lysate was incubated with the indicated concentration of Mad3-Bub3 and TAP-APC/C immunopurified from *MND2* or *mnd2Δ* strains. Similar results were obtained in two independent experiments.

Figure 4

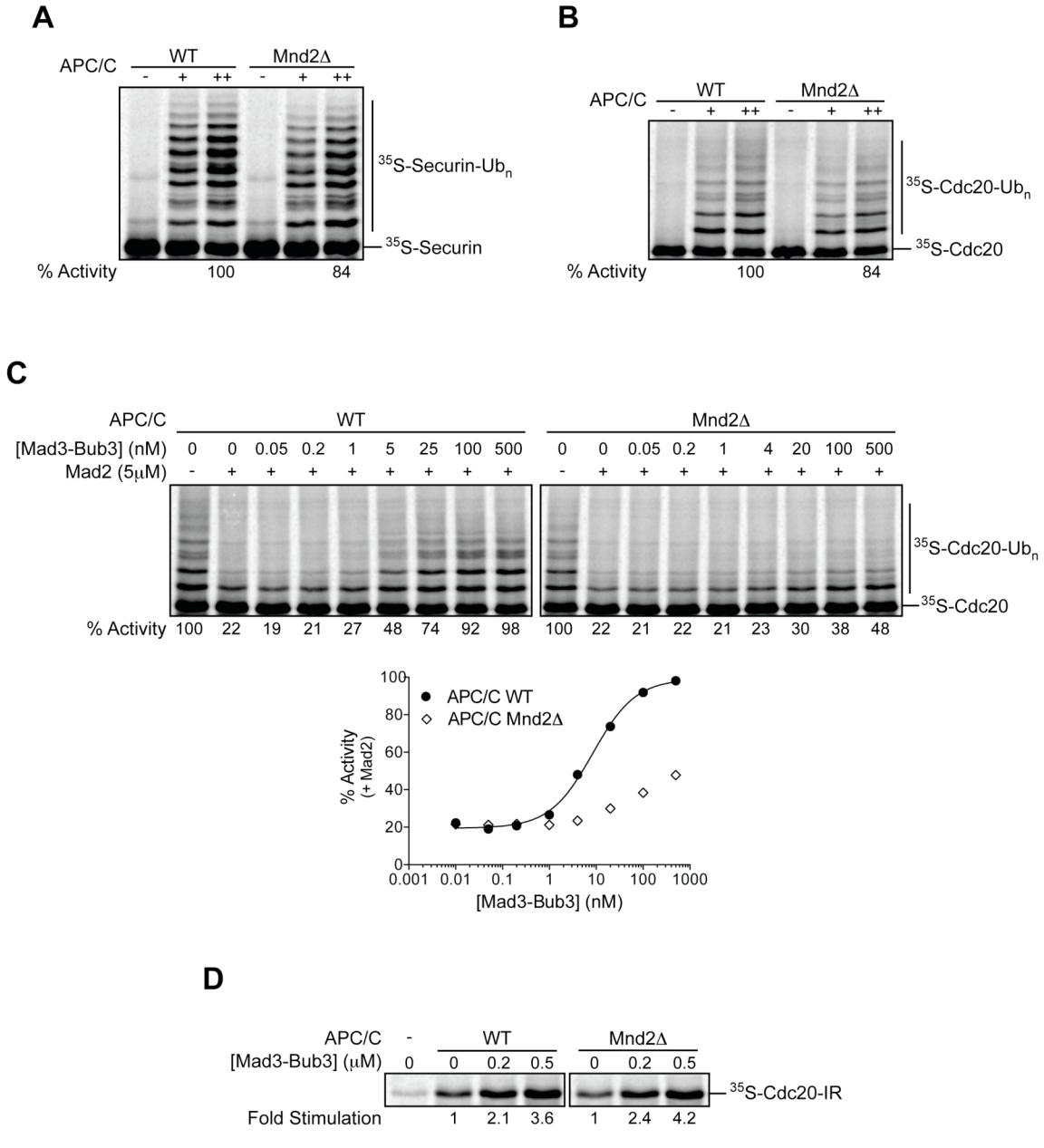
A
APC/C
WT
Mnd2Δ
- + ++ - + ++
35S-Securin-Ubn
35S-Securin
% Activity 100 84
B
APC/C
WT
Mnd2Δ
- + ++ - + ++
35S-Cdc20-Ubn
35S-Cdc20
% Activity 100 84
C
APC/C
WT
Mnd2Δ
[Mad3-Bub3] (nM) 0 0 0.05 0.2 1 5 25 100 500 0 0 0.05 0.2 1 4 20 100 500
Mad2 (5μM) - + + + + + + + + - + + + + + + + +
35S-Cdc20-Ubn
35S-Cdc20
% Activity 100 22 19 21 27 48 74 92 98 100 22 21 22 21 23 30 38 48
APC/C WT
APC/C Mnd2Δ
% Activity (+ Mad2)
0 20 40 60 80 100
0.001 0.01 0.1 1 10 100 1000
[Mad3-Bub3] (nM)
D
APC/C - WT Mnd2Δ
[Mad3-Bub3] (μM) 0 0 0.2 0.5 0 0.2 0.5
35S-Cdc20-IR
Fold Stimulation 1 2.1 3.6 1 2.4 4.2

Figure 5. Stabilized Cdc20 allows bypass of the spindle assembly checkpoint

(A) APC/C reactions were performed using purified unlabeled Cdc20 (WT), Cdc20-0K, Cdc20-5K, or a mock translation (-) incubated with APC/C (5 nM), ^{35}S-securin and E1/E2(Ubc4)/methyl-ubiquitin.

(B) Reactions were performed using purified ^{35}S-Cdc20 or ^{35}S-Cdc20-5K, plus APC/C (1 nM [+] or 5 nM [++]). Recombinant His_6-Cdh1 was purified from baculovirus-infected insect cells.

(C) Asynchronous log-phase cultures of strains carrying *CDC20* or *CDC20-5K* at the endogenous locus were arrested in G1 with 1 μg/ml α-factor (αF) for 3 h. α-factor was washed out and cells were harvested at the indicated times. α-factor was re-added when a majority of the cells had budded. Samples were analyzed by western blotting with anti-Cdc20, anti-Myc (securin), and anti-Cdk1 (as a loading control). Similar results were observed by flow cytometry analysis of DNA content (data not shown).

(D) Asynchronous log-phase cultures of *CDC20*, *CDC20-5K*, or *mad2Δ* cells were arrested with α-factor and released into media containing 60 μg/ml benomyl. Cells were harvested at the indicated times and α-factor was re-added when a majority of the cells had budded. Samples were analyzed by western blotting.

(E) *CDC20* or *CDC20-5K* strains, carrying a non-destructible securin mutant, *PDS1*-Δ*db*, under the control of the *GAL* promoter, were arrested in benomyl in galactose-containing media to induce a metaphase arrest. 100 μg/ml Cycloheximide (CHX) was added and samples were analyzed by western blotting.

(F) Purified unlabeled Cdc20 (left) or Cdc20-5K (right) was pre-incubated with the indicated Mad2 concentration before addition of APC/C (5 nM), E1/E2(Ubc4)/methyl-

ubiquitin, and purified ^{35}S-securin. The (-) control represents background activity and was subtracted from activity in the presence of exogenous activator. The zero concentration was plotted on a log scale as 0.01 μM. Similar results were obtained in three independent experiments.

(G) Purified unlabeled Cdc20 (left) or Cdc20-5K (right) was pre-incubated with the indicated Mad3-Bub3 concentration and APC/C (5 nM). Reactions were started by the addition of ^{35}S-securin and E1/E2(Ubc4)/methyl-ubiquitin. Results are representative of two independent experiments.

Figure 5

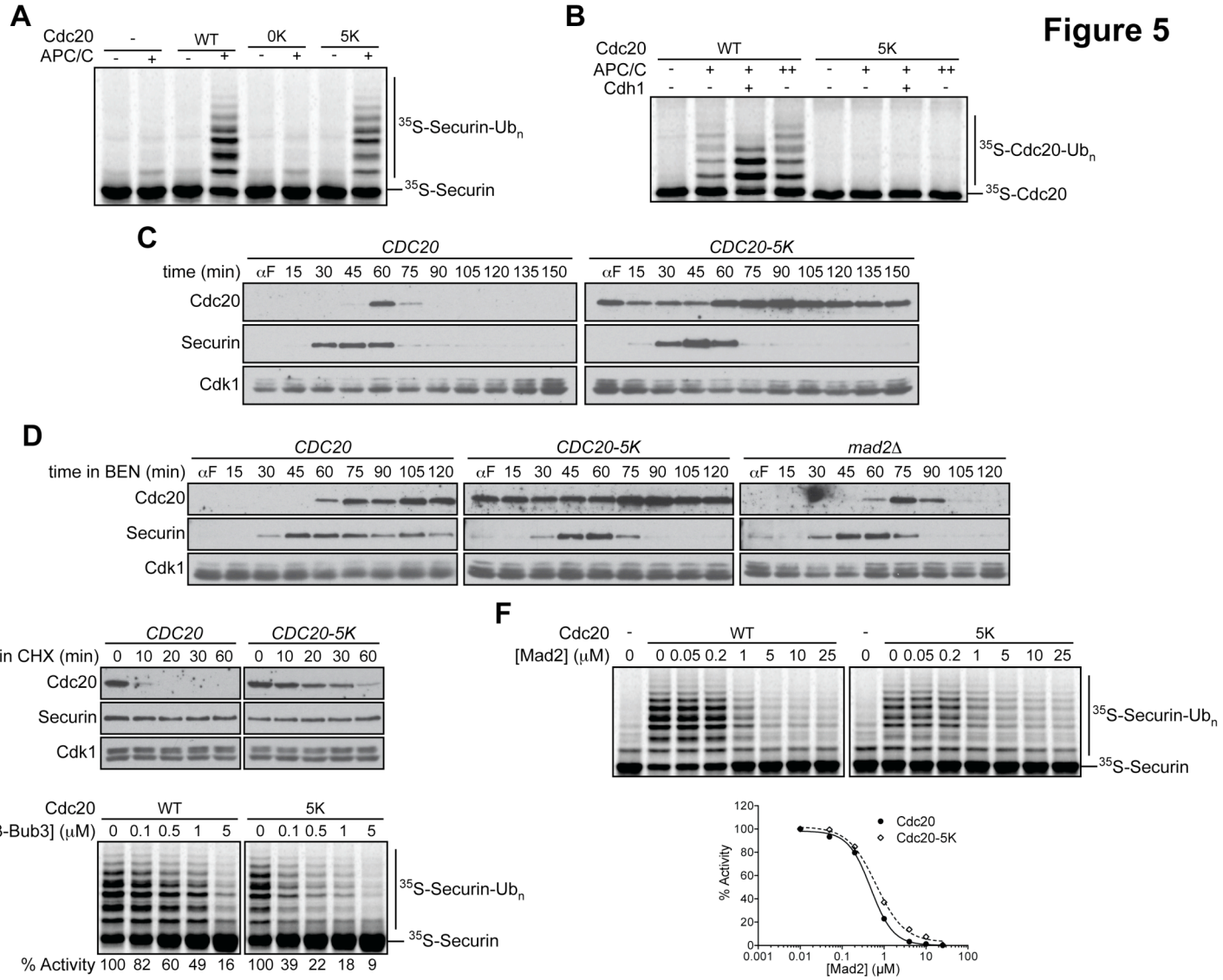
A
Cdc20
APC/C
WT
0K
5K
^{35}S-Securin-Ub$_n$
^{35}S-Securin
B
Cdc20
APC/C
Cdh1
WT
5K
^{35}S-Cdc20-Ub$_n$
^{35}S-Cdc20
C
CDC20
CDC20-5K
time (min)
αF 15 30 45 60 75 90 105 120 135 150
Cdc20
Securin
Cdk1
D
CDC20
CDC20-5K
mad2Δ
time in BEN (min)
αF 15 30 45 60 75 90 105 120
Cdc20
Securin
Cdk1
E
CDC20
CDC20-5K
time in CHX (min)
0 10 20 30 60
Cdc20
Securin
Cdk1
F
Cdc20
WT
5K
[Mad2] (μM)
0 0 0.05 0.2 1 5 10 25
^{35}S-Securin-Ub$_n$
^{35}S-Securin
% Activity
Cdc20
Cdc20-5K
[Mad2] (μM)
G
Cdc20
WT
5K
[Mad3-Bub3] (μM)
0 0.1 0.5 1 5
^{35}S-Securin-Ub$_n$
^{35}S-Securin
% Activity 100 82 60 49 16 100 39 22 18 9

Figure 6. Mnd2 is required for efficient checkpoint release

(A) Asynchronous log-phase cultures of *MND2* or *mnd2Δ* cells were arrested in G1 with α-factor. α-factor was washed out and cells were harvested at the indicated times. α-factor was re-added when a majority of the cells had budded. Samples were analyzed by western blotting. Similar results were obtained by flow cytometry analysis of DNA content (data not shown).

(B) Asynchronous log-phase cultures of *MND2*, *mnd2Δ*, or *CDC20-5K* cells were arrested with α-factor and released into media containing 60 μg/ml benomyl. Cells were harvested at the indicated times and α-factor was re-added when a majority of the cells had budded. Samples were analyzed by western blotting.

(C) *MND2* or *mnd2Δ* strains were arrested in benomyl before addition of cycloheximide. Samples were analyzed by western blotting.

(D) Asynchronous log-phase cultures of *MND2* or *mnd2Δ* cells were arrested with α-factor and released into media containing 60 μg/ml benomyl. Cells were released from benomyl into α-factor and harvested at the indicated times. Samples were analyzed by western blotting.

(E) Cells from an experiment like that in panel (D) were analyzed for separation of DNA masses by DAPI staining. Two hundred cells were counted per time point. A similar delay was obtained by counting the percent of large budded cells and by flow cytometry analysis of DNA content (data not shown).

Figure 6

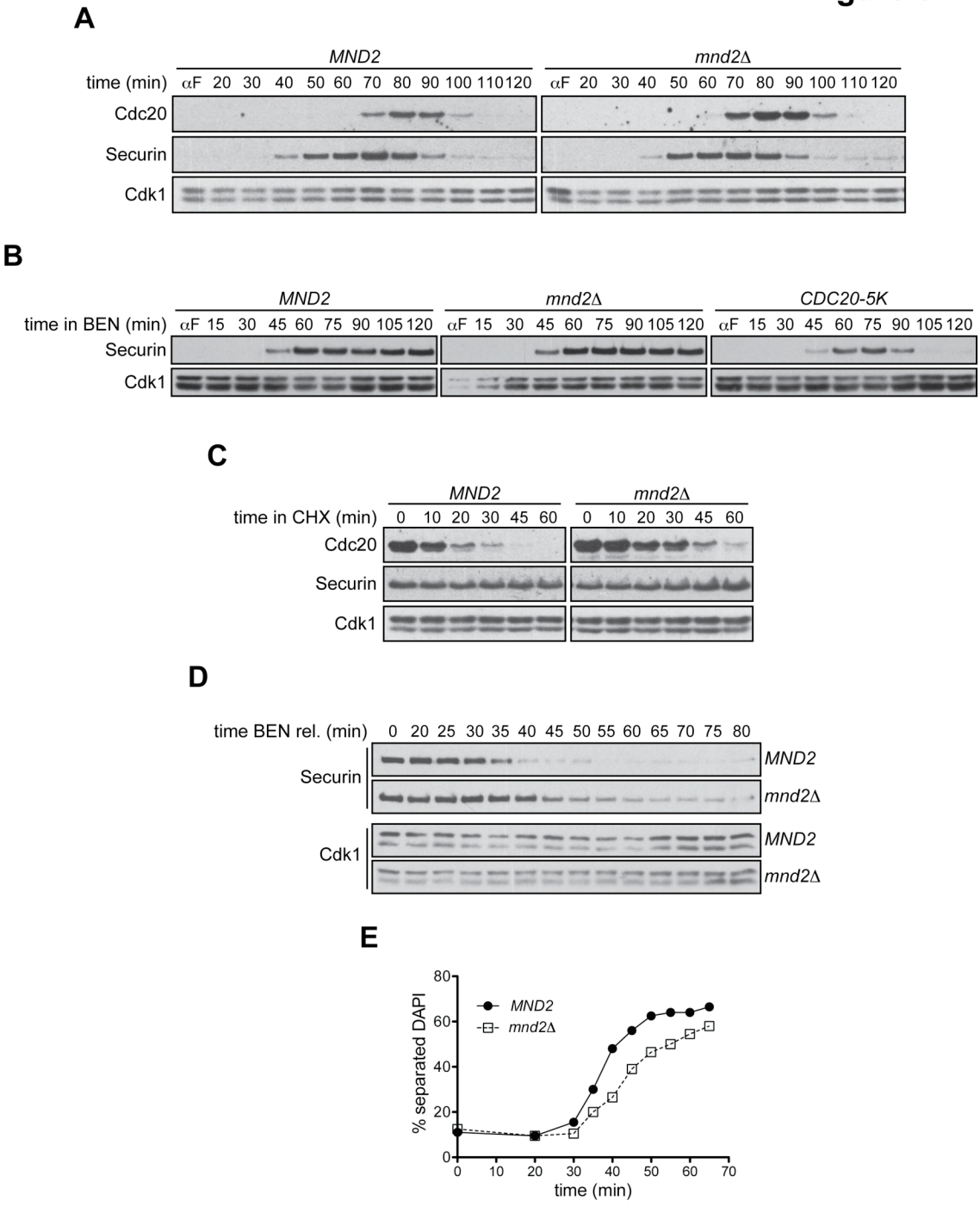
A
MND2
mnd2Δ
time (min)
αF 20 30 40 50 60 70 80 90 100 110 120
Cdc20
Securin
Cdk1
B
MND2
mnd2Δ
CDC20-5K
time in BEN (min)
αF 15 30 45 60 75 90 105 120
Securin
Cdk1
C
MND2
mnd2Δ
time in CHX (min)
0 10 20 30 45 60
Cdc20
Securin
Cdk1
D
time BEN rel. (min)
0 20 25 30 35 40 45 50 55 60 65 70 75 80
Securin
MND2
mnd2Δ
Cdk1
MND2
mnd2Δ
E
% separated DAPI
MND2
mnd2Δ
0 20 40 60 80
0 10 20 30 40 50 60 70
time (min)

Figure S1. Characterization of Cdc20 autoubiquitination

(A) Schematic diagram of budding yeast Cdc20, showing the relative positions of D-box, C-box, Mad2-binding motif, and WD40 domain.

(B) For securin ubiquitination (top panel), purified unlabeled wild-type or mutant Cdc20 was incubated with APC/C (5 nM), E1/E2(Ubc4)/methyl-ubiquitin, and purified ^{35}S-securin. For Cdc20 ubiquitination by Cdh1 (middle panel), purified ^{35}S-Cdc20 (wild-type or mutant) was incubated with APC/C (1 nM), E1/E2(Ubc4)/methyl-ubiquitin, and Cdh1. For Cdc20 autoubiquitination (bottom panel), purified ^{35}S-Cdc20 (wild-type or mutant) was incubated with APC/C (5 nM), purified unlabeled wild-type Cdc20, and E1/E2(Ubc4)/methyl-ubiquitin (bottom). The unlabeled wild-type Cdc20 was not required for ^{35}S-Cdc20 ubiquitination and was omitted in other experiments.

(C) Autoubiquitination reactions with ^{35}S-Cdc20 incubated with APC/C (5 nM) and indicated E1/E2/ubiquitin mix (either Ubc4/ubiquitin, Ubc1/ubiquitin, Ubc4+Ubc1/ubiquitin, or Ubc4/methyl-ubiquitin, left to right).

Figure S1

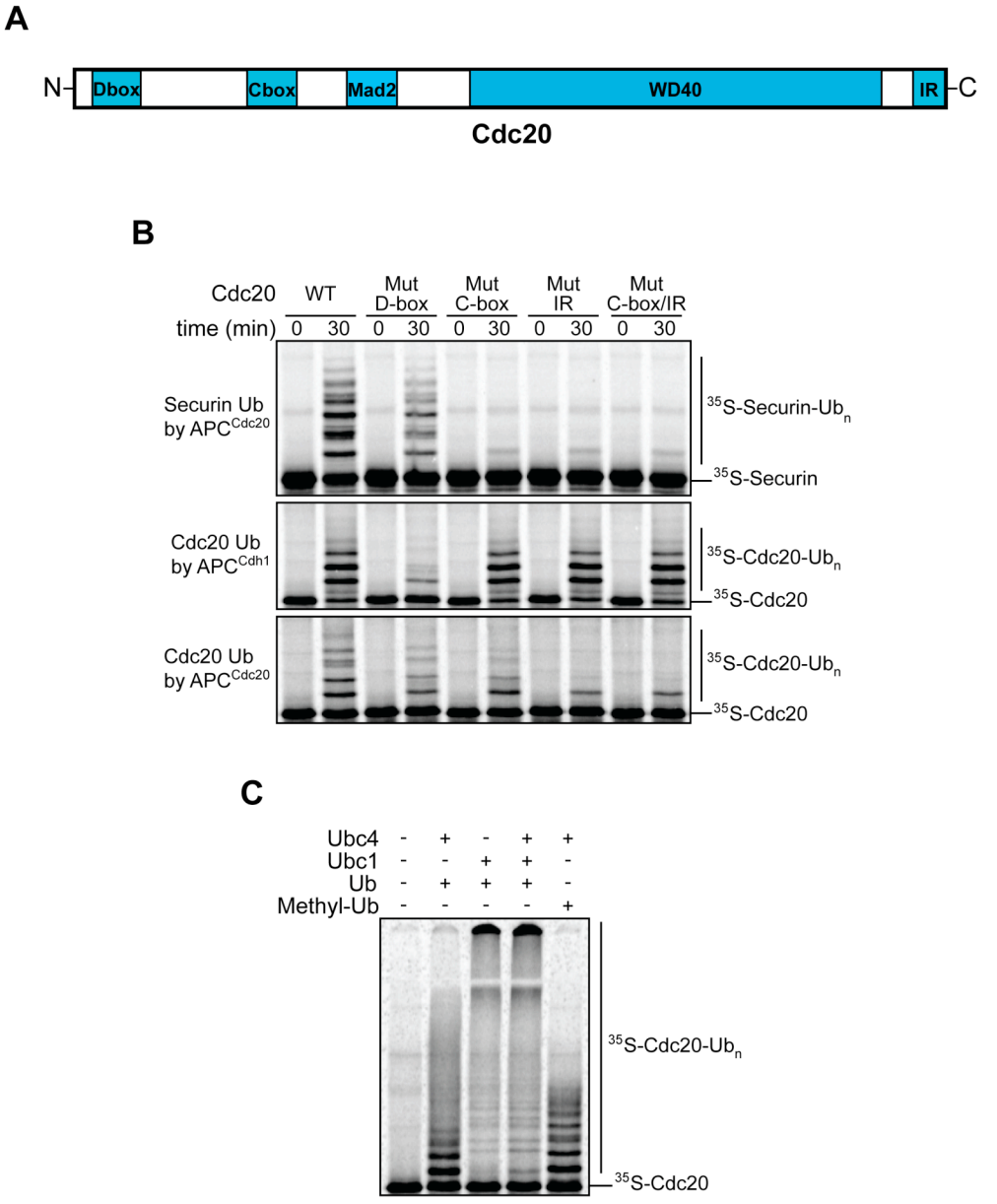
A
N
Dbox
Cbox
Mad2
WD40
IR
C
Cdc20
B
Cdc20
WT
Mut D-box
Mut C-box
Mut IR
Mut C-box/IR
time (min)
0 30 0 30 0 30 0 30 0 30
Securin Ub by APC^Cdc20
35S-Securin-Ubn
35S-Securin
Cdc20 Ub by APC^Cdh1
35S-Cdc20-Ubn
35S-Cdc20
Cdc20 Ub by APC^Cdc20
35S-Cdc20-Ubn
35S-Cdc20
C
Ubc4 - + - + +
Ubc1 - - + + -
Ub - + + + -
Methyl-Ub - - - - +
35S-Cdc20-Ubn
35S-Cdc20

Figure S2. Cdc20 instability in a checkpoint arrest

(A) A *pdr5*Δ strain was arrested in benomyl for 3 h and treated with 200 μM MG132 or DMSO for 1 h before addition of 100 μg/ml cycloheximide (CHX). Samples were analyzed by western blotting.

(B) *CDH1* or *cdh1Δ* strains were arrested in benomyl before addition of cycloheximide. Samples were analyzed by western blotting.

(C) *MAD3* or *mad3Δ* strains, carrying a non-destructible securin mutant, *PDS1*-Δ*db*, under the control of the *GAL* promoter, were arrested in benomyl in galactose-containing media to induce a metaphase arrest. Cycloheximide was added and samples were analyzed by western blotting.

Figure S2

A

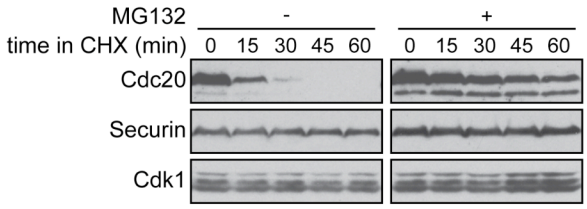

B

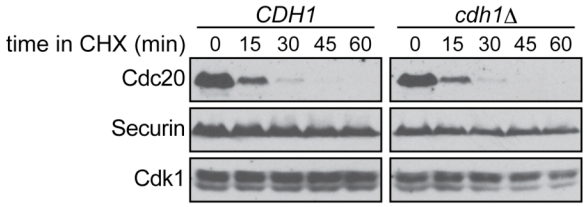

C

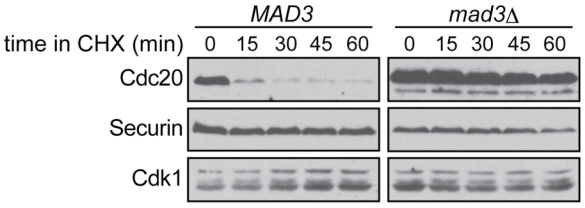

Figure S3. In vitro assay components

Coomassie Blue-stained gel showing the purified components used in the experiments in Figures 1-4. Expression was performed in the *E. coli* strain BL21-RIL. Mad2 was expressed with a His6-tag, while His6-gB1-tagged Mad3 was co-expressed with Bub3. Both were purified using Ni-NTA agarose followed by TEV protease cleavage to remove the tag. The Mad2 dimer was isolated using size exclusion chromatography. The Mad2 C-terminal 6 amino acid deletion (Mad2-CΔ) was purified similarly, except that it behaved entirely as a monomer. The Mad3-Bub3 complex was further purified using anion exchange chromatography and size exclusion chromatography.

Figure S3

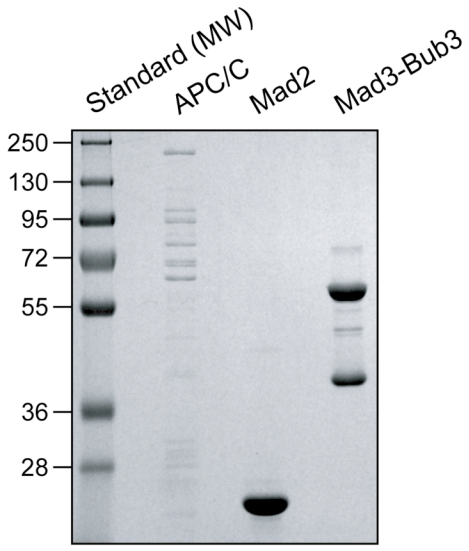

Figure S4. Characterization of Cdc20 lysine mutants

(A) Schematic diagram of budding yeast Cdc20, showing the position of motifs and lysines within the protein. The major vertical lines delineate the 3 segments in which all lysines were changed to arginine (K to R), with the other two segments remaining wild-type: Cdc20-N (N) has the twelve N-terminal lysines mutated; Cdc20-M (M) has the middle eight lysines mutated; and Cdc20-C (C) has the nineteen C-terminal lysines mutated.

(B) Strains with P_{GALL}-*CDC20* on a plasmid and either *cdc20Δ*, *CDC20*, *cdc20-0K*, or *CDC20-5K* at the *CDC20* locus were grown to log phase in minimal media containing galactose and serially diluted onto galactose plates at 30°C or onto dextrose plates at 25°C, 30°C, or 37°C.

(C) The mutants defined in panel (A) were tested in three separate assays. For securin ubiquitination (left panel), purified unlabeled Cdc20 (wild-type or mutant) was incubated with APC/C (5 nM), E1/E2(Ubc4)/methyl-ubiquitin, and purified ^{35}S-securin. For Cdc20 autoubiquitination reactions (middle panel), wild-type or mutant ^{35}S-Cdc20 was incubated with APC/C (5 nM) and E1/E2(Ubc4)/methyl-ubiquitin. For Cdh1-dependent Cdc20 ubiquitination (right panel), reactions included Cdh1, 1 nM APC/C, and E1/E2(Ubc4)/methyl-ubiquitin.

(D) Single lysines within the C-terminal segment were mutated. Purified unlabeled wild-type or mutant Cdc20 was incubated with APC/C (5 nM), purified ^{35}S-securin, and E1/E2(Ubc4)/methyl-ubiquitin.

(E) Substrate ubiquitination reactions with either purified unlabeled wild-type Cdc20 or Cdc20-5K mutant with APC/C (5 nM) and E1/E2(Ubc4)/methyl-ubiquitin. Substrates are ^{35}S-securin, ^{35}S-Clb5-3HA, ^{35}S-Dbf4 (1-236), and ^{35}S-Acm1.

(F) Purified wild-type or mutant ^{35}S-Cdc20 was incubated with APC/C (5 nM) and E1/E2(Ubc4)/methyl-ubiquitin.

Figure S4

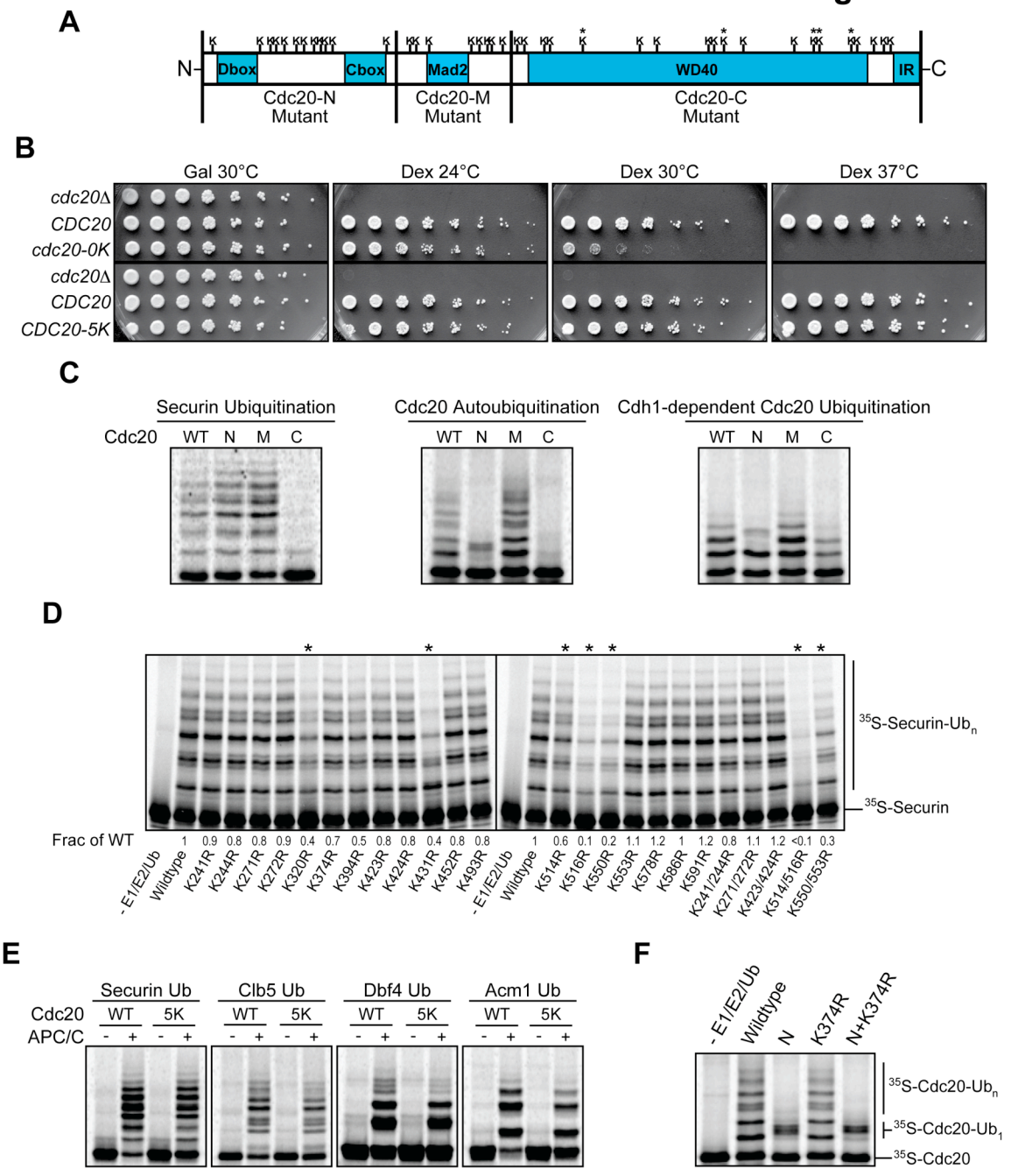
A
N
Dbox
Cbox
Mad2
WD40
IR
C
Cdc20-N Mutant
Cdc20-M Mutant
Cdc20-C Mutant
B
Gal 30°C
Dex 24°C
Dex 30°C
Dex 37°C
cdc20Δ
CDC20
cdc20-0K
cdc20Δ
CDC20
CDC20-5K
C
Securin Ubiquitination
Cdc20 Autoubiquitination
Cdh1-dependent Cdc20 Ubiquitination
Cdc20
WT N M C
D
35S-Securin-Ubn
35S-Securin
Frac of WT
1 0.9 0.8 0.8 0.9 0.4 0.7 0.5 0.8 0.8 0.4 0.8 0.8
1 0.6 0.1 0.2 1.1 1.2 1 1.2 0.8 1.1 1.2 <0.1 0.3
- E1/E2/Ub
Wildtype
K241R
K244R
K271R
K272R
K320R
K374R
K394R
K423R
K424R
K431R
K452R
K493R
- E1/E2/Ub
Wildtype
K514R
K516R
K550R
K553R
K578R
K586R
K591R
K241/244R
K271/272R
K423/424R
K514/516R
K550/553R
E
Securin Ub
Clb5 Ub
Dbf4 Ub
Acm1 Ub
Cdc20
WT 5K
APC/C
- +
F
- E1/E2/Ub
Wildtype
N
K374R
N+K374R
35S-Cdc20-Ubn
35S-Cdc20-Ub1
35S-Cdc20

Figure S5. Stabilized Cdc20 is benomyl-sensitive

Log-phase cultures of *CDC20*, *CDC20-5K*, *mad2Δ*, or *mad3Δ* cells were serially diluted onto a dextrose plate (YPD) or plates containing 10 or 12.5 μg/ml benomyl.

Figure S5

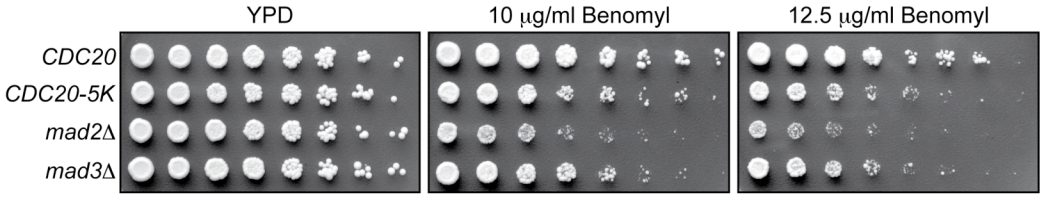
YPD
10 μg/ml Benomyl
12.5 μg/ml Benomyl
CDC20
CDC20-5K
mad2Δ
mad3Δ

Figure S6. Cdc20 autoubiquitination alone does not promote Cdc20 dissociation from the APC/C

(A) Wild-type ^{35}S-Cdc20 in reticulocyte lysate was bound to TAP-APC/C on beads and then incubated with E1/E2(Ubc4 & Ubc1)/ubiquitin mix (+) or buffer as a control (-). Unbound material was removed by washing and bound proteins were eluted with SDS sample buffer. Two representative experiments are shown.

(B) To estimate the rate at which Cdc20 dissociates from the APC/C under different conditions, wild-type ^{35}S-Cdc20 in reticulocyte lysate was bound to TAP-APC/C on beads. For the checkpoint complexes (MCC), the ^{35}S-Cdc20 lysate was pre-incubated with 5 μM Mad2 and 1 μM Mad3-Bub3. Unbound protein was removed by washing, and the beads were incubated with buffer control (left and middle panels) or with ubiquitination components as in panel (A) (right panel). Following the ubiquitination reaction, beads were rapidly washed and then incubated on a rocker in a large volume (10 ml) of buffer (25 mM HEPES pH 7.4, 300 mM NaCl, 0.1% NP-40, 1 mg/ml BSA). Samples were removed at the indicated times and eluted with SDS sample buffer. Estimated final concentrations of APC/C and Cdc20 in the diluted samples were less than 1 nM. In multiple experiments, we did not observe significant dissociation of Cdc20 in any reaction over a one-hour time course, suggesting that Cdc20 binds with very high affinity in the presence or absence of polyubiquitination and checkpoint proteins.

Figure S6

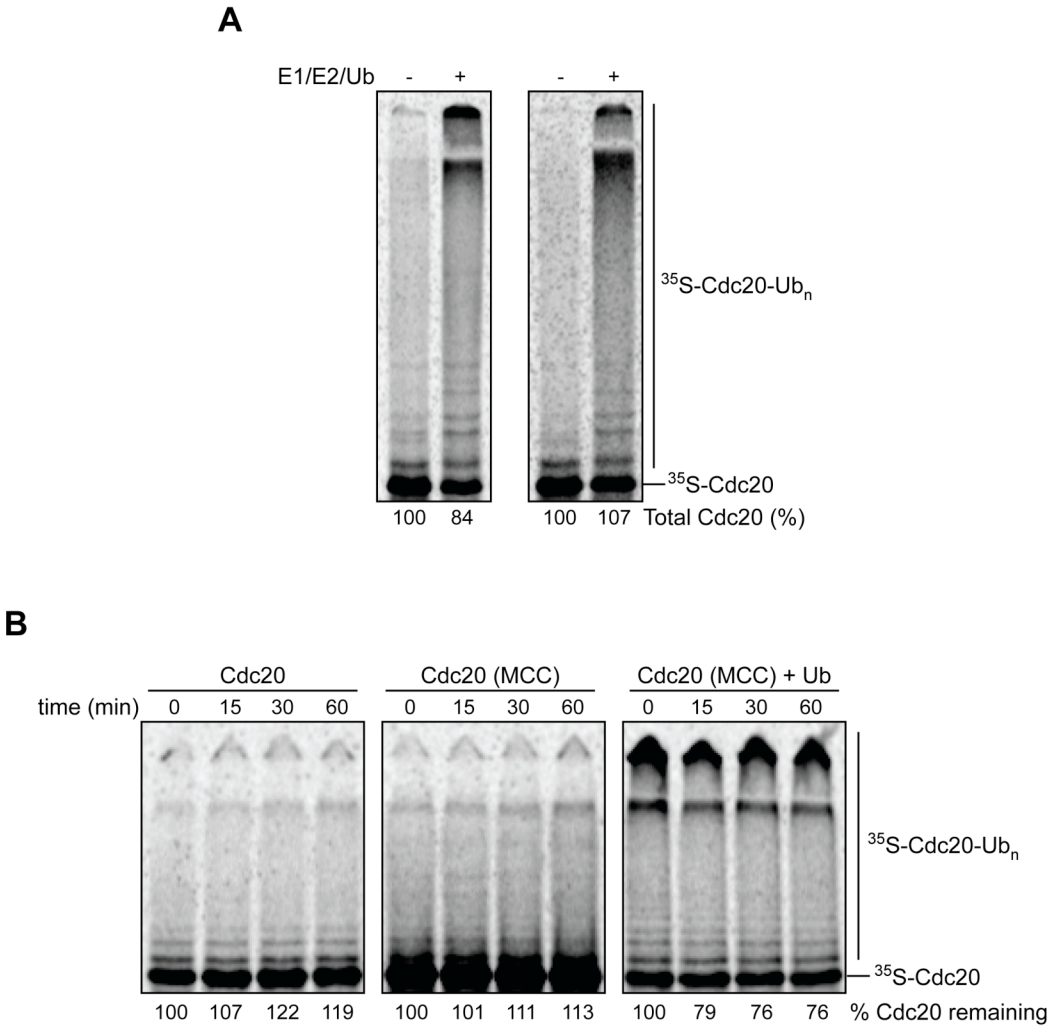
A
E1/E2/Ub - + - +
35S-Cdc20-Ubn
35S-Cdc20
100 84 100 107 Total Cdc20 (%)
B
Cdc20
Cdc20 (MCC)
Cdc20 (MCC) + Ub
time (min) 0 15 30 60 0 15 30 60 0 15 30 60
35S-Cdc20-Ubn
35S-Cdc20
100 107 122 119 100 101 111 113 100 79 76 76 % Cdc20 remaining

ACKNOWLEDGEMENTS

We thank H. Eshelman, M. Galli, J. Girard, L. Holt, M. Matyskiela, M. Lopez, D. Lu, N. Lyons, S. Naylor, M. Rodrigo-Brenni, J. Schaefer, V. Van Voorhis, and G. Yaakov for discussions; M. Lopez and M. Matyskiela for comments on the manuscript; M. Matyskiela for help with assay development and optimization; and D. Lu for help with data processing. This work was supported by funding from the National Institute of General Medical Sciences (GM053270).

REFERENCES

Barford, D. (2011). Structure, function and mechanism of the anaphase promoting complex (APC/C). Q Rev Biophys *44*, 153-190.

Braunstein, I., Miniowitz, S., Moshe, Y., and Hershko, A. (2007). Inhibitory factors associated with anaphase-promoting complex/cylosome in mitotic checkpoint. Proc Natl Acad Sci U S A *104*, 4870-4875.

Burton, J.L., and Solomon, M.J. (2007). Mad3p, a pseudosubstrate inhibitor of APCCdc20 in the spindle assembly checkpoint. Genes Dev *21*, 655-667.

Buschhorn, B.A., Petzold, G., Galova, M., Dube, P., Kraft, C., Herzog, F., Stark, H., and Peters, J.M. (2011). Substrate binding on the APC/C occurs between the coactivator Cdh1 and the processivity factor Doc1. Nat Struct Mol Biol *18*, 6-13.

Carroll, C.W., Enquist-Newman, M., and Morgan, D.O. (2005). The APC subunit Doc1 promotes recognition of the substrate destruction box. Curr Biol *15*, 11-18.

Carroll, C.W., and Morgan, D.O. (2002). The Doc1 subunit is a processivity factor for the anaphase-promoting complex. Nat. Cell Biol. *4*, 880-887.

Carroll, C.W., and Morgan, D.O. (2005). Enzymology of the Anaphase-Promoting Complex. Meth. Enzymol. *398*, 219-230.

Chao, W.C., Kulkarni, K., Zhang, Z., Kong, E.H., and Barford, D. (2012). Structure of the mitotic checkpoint complex. Nature *484*, 208-213.

da Fonseca, P.C., Kong, E.H., Zhang, Z., Schreiber, A., Williams, M.A., Morris, E.P., and Barford, D. (2011). Structures of APC/C(Cdh1) with substrates identify Cdh1 and Apc10 as the D-box co-receptor. Nature *470*, 274-278.

De Antoni, A., Pearson, C.G., Cimini, D., Canman, J.C., Sala, V., Nezi, L., Mapelli, M., Sironi, L., Faretta, M., Salmon, E.D., and Musacchio, A. (2005). The Mad1/Mad2 complex as a template for Mad2 activation in the spindle assembly checkpoint. Curr Biol *15*, 214-225.

Fang, G. (2002). Checkpoint protein BubR1 acts synergistically with Mad2 to inhibit anaphase-promoting complex. Mol Biol Cell *13*, 755-766.

Fang, G., Yu, H., and Kirschner, M.W. (1998). The checkpoint protein MAD2 and the mitotic regulator CDC20 form a ternary complex with the anaphase-promoting complex to control anaphase initiation. Genes Dev. *12*, 1871-1883.

Fava, L.L., Kaulich, M., Nigg, E.A., and Santamaria, A. (2011). Probing the in vivo function of Mad1:C-Mad2 in the spindle assembly checkpoint. EMBO J *30*, 3322-3336.

Foe, I.T., Foster, S.A., Cheung, S.K., Deluca, S.Z., Morgan, D.O., and Toczyski, D.P. (2011). Ubiquitination of Cdc20 by the APC Occurs through an Intramolecular Mechanism. Curr Biol *21*, 1870-1877.

Garnett, M.J., Mansfeld, J., Godwin, C., Matsusaka, T., Wu, J., Russell, P., Pines, J., and Venkitaraman, A.R. (2009). UBE2S elongates ubiquitin chains on APC/C substrates to promote mitotic exit. Nat Cell Biol *11*, 1363-1369.

Ge, S., Skaar, J.R., and Pagano, M. (2009). APC/C- and Mad2-mediated degradation of Cdc20 during spindle checkpoint activation. Cell Cycle *8*, 167-171.

Habu, T., Kim, S.H., Weinstein, J., and Matsumoto, T. (2002). Identification of a MAD2-binding protein, CMT2, and its role in mitosis. EMBO J *21*, 6419-6428.
Hagan, R.S., Manak, M.S., Buch, H.K., Meier, M.G., Meraldi, P., Shah, J.V., and Sorger, P.K. (2011). p31(comet) acts to ensure timely spindle checkpoint silencing subsequent to kinetochore attachment. Mol Biol Cell *22*, 4236-4246.
Hall, M.C., Torres, M.P., Schroeder, G.K., and Borchers, C.H. (2003). Mnd2 and Swm1 are core subunits of the Saccharomyces cerevisiae anaphase-promoting complex. J Biol Chem *278*, 16698-16705.
Hardwick, K.G., Johnston, R.C., Smith, D.L., and Murray, A.W. (2000). MAD3 encodes a novel component of the spindle checkpoint which interacts with Bub3p, Cdc20p, and Mad2p. J Cell Biol *148*, 871-882.
Herzog, F., Primorac, I., Dube, P., Lenart, P., Sander, B., Mechtler, K., Stark, H., and Peters, J.M. (2009). Structure of the anaphase-promoting complex/cyclosome interacting with a mitotic checkpoint complex. Science *323*, 1477-1481.
Hewitt, L., Tighe, A., Santaguida, S., White, A.M., Jones, C.D., Musacchio, A., Green, S., and Taylor, S.S. (2010). Sustained Mps1 activity is required in mitosis to recruit O-Mad2 to the Mad1-C-Mad2 core complex. J Cell Biol *190*, 25-34.
Izawa, D., and Pines, J. (2011). How APC/C-Cdc20 changes its substrate specificity in mitosis. Nat Cell Biol *13*, 223-233.
Jia, L., Li, B., Warrington, R.T., Hao, X., Wang, S., and Yu, H. (2011). Defining pathways of spindle checkpoint silencing: functional redundancy between Cdc20 ubiquitination and p31(comet). Mol Biol Cell *22*, 4227-4235.
King, E.M., van der Sar, S.J., and Hardwick, K.G. (2007). Mad3 KEN boxes mediate both Cdc20 and Mad3 turnover, and are critical for the spindle checkpoint. PLoS One *2*, e342.
Kulukian, A., Han, J.S., and Cleveland, D.W. (2009). Unattached kinetochores catalyze production of an anaphase inhibitor that requires a Mad2 template to prime Cdc20 for BubR1 binding. Dev Cell *16*, 105-117.
Lara-Gonzalez, P., Scott, M.I., Diez, M., Sen, O., and Taylor, S.S. (2011). BubR1 blocks substrate recruitment to the APC/C in a KEN-box-dependent manner. J Cell Sci *124*, 4332-4345.
Larsen, N.A., Al-Bassam, J., Wei, R.R., and Harrison, S.C. (2007). Structural analysis of Bub3 interactions in the mitotic spindle checkpoint. Proc Natl Acad Sci U S A *104*, 1201-1206.
Luo, X., Fang, G., Coldiron, M., Lin, Y., Yu, H., Kirschner, M.W., and Wagner, G. (2000). Structure of the Mad2 spindle assembly checkpoint protein and its interaction with Cdc20. Nat Struct Biol *7*, 224-229.
Luo, X., Tang, Z., Rizo, J., and Yu, H. (2002). The Mad2 spindle checkpoint protein undergoes similar major conformational changes upon binding to either Mad1 or Cdc20. Mol Cell *9*, 59-71.
Ma, H.T., and Poon, R.Y. (2011). Orderly inactivation of the key checkpoint protein mitotic arrest deficient 2 (MAD2) during mitotic progression. J Biol Chem *286*, 13052-13059.
Maldonado, M., and Kapoor, T.M. (2011). Constitutive Mad1 targeting to kinetochores uncouples checkpoint signalling from chromosome biorientation. Nat Cell Biol *13*, 475-482.

Malureanu, L.A., Jeganathan, K.B., Hamada, M., Wasilewski, L., Davenport, J., and van Deursen, J.M. (2009). BubR1 N terminus acts as a soluble inhibitor of cyclin B degradation by APC/C(Cdc20) in interphase. Dev Cell *16*, 118-131.

Mansfeld, J., Collin, P., Collins, M.O., Choudhary, J.S., and Pines, J. (2011). APC15 drives the turnover of MCC-CDC20 to make the spindle assembly checkpoint responsive to kinetochore attachment. Nat Cell Biol *13*, 1234-1243.

Mapelli, M., Filipp, F.V., Rancati, G., Massimiliano, L., Nezi, L., Stier, G., Hagan, R.S., Confalonieri, S., Piatti, S., Sattler, M., and Musacchio, A. (2006). Determinants of conformational dimerization of Mad2 and its inhibition by p31comet. EMBO J *25*, 1273-1284.

Matyskiela, M.E., and Morgan, D.O. (2009). Analysis of activator-binding sites on the APC/C supports a cooperative substrate-binding mechanism. Mol Cell *34*, 68-80.

Miniowitz-Shemtov, S., Teichner, A., Sitry-Shevah, D., and Hershko, A. (2010). ATP is required for the release of the anaphase-promoting complex/cyclosome from inhibition by the mitotic checkpoint. Proc Natl Acad Sci U S A *107*, 5351-5356.

Musacchio, A., and Salmon, E.D. (2007). The spindle-assembly checkpoint in space and time. Nat Rev Mol Cell Biol *8*, 379-393.

Nilsson, J., Yekezare, M., Minshull, J., and Pines, J. (2008). The APC/C maintains the spindle assembly checkpoint by targeting Cdc20 for destruction. Nat Cell Biol *10*, 1411-1420.

Oelschlaegel, T., Schwickart, M., Matos, J., Bogdanova, A., Camasses, A., Havlis, J., Shevchenko, A., and Zachariae, W. (2005). The yeast APC/C subunit Mnd2 prevents premature sister chromatid separation triggered by the meiosis-specific APC/C-Ama1. Cell *120*, 773-788.

Pan, J., and Chen, R.H. (2004). Spindle checkpoint regulates Cdc20p stability in Saccharomyces cerevisiae. Genes Dev *18*, 1439-1451.

Passmore, L.A., McCormack, E.A., Au, S.W., Paul, A., Willison, K.R., Harper, J.W., and Barford, D. (2003). Doc1 mediates the activity of the anaphase-promoting complex by contributing to substrate recognition. Embo J *22*, 786-796.

Penkner, A.M., Prinz, S., Ferscha, S., and Klein, F. (2005). Mnd2, an essential antagonist of the anaphase-promoting complex during meiotic prophase. Cell *120*, 789-801.

Prinz, S., Hwang, E.S., Visintin, R., and Amon, A. (1998). The regulation of Cdc20 proteolysis reveals a role for the APC components Cdc23 and Cdc27 during S phase and early mitosis. Curr. Biol. *8*, 750-760.

Rabitsch, K.P., Toth, A., Galova, M., Schleiffer, A., Schaffner, G., Aigner, E., Rupp, C., Penkner, A.M., Moreno-Borchart, A.C., Primig, M*., et al.* (2001). A screen for genes required for meiosis and spore formation based on whole-genome expression. Curr Biol *11*, 1001-1009.

Reddy, S.K., Rape, M., Margansky, W.A., and Kirschner, M.W. (2007). Ubiquitination by the anaphase-promoting complex drives spindle checkpoint inactivation. Nature *446*, 921-925.

Robbins, J.A., and Cross, F.R. (2011). Regulated degradation of the APC coactivator Cdc20. Cell division *5*, 23.

Rodrigo-Brenni, M., and Morgan, D.O. (2007). Sequential E2s drive polyubiquitin chain assembly on APC targets. Cell *130*, 127-139.

Schreiber, A., Stengel, F., Zhang, Z., Enchev, R.I., Kong, E.H., Morris, E.P., Robinson, C.V., da Fonseca, P.C., and Barford, D. (2011). Structural basis for the subunit assembly of the anaphase-promoting complex. Nature *470*, 227-232.

Shah, J.V., Botvinick, E., Bonday, Z., Furnari, F., Berns, M., and Cleveland, D.W. (2004). Dynamics of centromere and kinetochore proteins; implications for checkpoint signaling and silencing. Curr Biol *14*, 942-952.

Simonetta, M., Manzoni, R., Mosca, R., Mapelli, M., Massimiliano, L., Vink, M., Novak, B., Musacchio, A., and Ciliberto, A. (2009). The influence of catalysis on mad2 activation dynamics. PLoS Biol *7*, e10.

Stegmeier, F., Rape, M., Draviam, V.M., Nalepa, G., Sowa, M.E., Ang, X.L., McDonald, E.R., 3rd, Li, M.Z., Hannon, G.J., Sorger, P.K.*, et al.* (2007). Anaphase initiation is regulated by antagonistic ubiquitination and deubiquitination activities. Nature *446*, 876-881.

Sudakin, V., Chan, G.K., and Yen, T.J. (2001). Checkpoint inhibition of the APC/C in HeLa cells is mediated by a complex of BUBR1, BUB3, CDC20, and MAD2. J Cell Biol *154*, 925-936.

Tang, Z., Bharadwaj, R., Li, B., and Yu, H. (2001). Mad2-Independent inhibition of APCCdc20 by the mitotic checkpoint protein BubR1. Dev Cell *1*, 227-237.

Teichner, A., Eytan, E., Sitry-Shevah, D., Miniowitz-Shemtov, S., Dumin, E., Gromis, J., and Hershko, A. (2011). p31comet Promotes disassembly of the mitotic checkpoint complex in an ATP-dependent process. Proc Natl Acad Sci U S A *108*, 3187-3192.

Thornton, B.R., Ng, T.M., Matyskiela, M.E., Carroll, C.W., Morgan, D.O., and Toczyski, D.P. (2006). An architectural map of the anaphase-promoting complex. Genes Dev *20*, 449-460.

Tipton, A.R., Wang, K., Link, L., Bellizzi, J.J., Huang, H., Yen, T., and Liu, S.T. (2011). BUBR1 and closed MAD2 (C-MAD2) interact directly to assemble a functional mitotic checkpoint complex (MCC). J Biol Chem.

Varetti, G., Guida, C., Santaguida, S., Chiroli, E., and Musacchio, A. (2011). Homeostatic control of mitotic arrest. Mol Cell *44*, 710-720.

Visconti, R., Palazzo, L., and Grieco, D. (2010). Requirement for proteolysis in spindle assembly checkpoint silencing. Cell Cycle *9*, 564-569.

Westhorpe, F.G., Tighe, A., Lara-Gonzalez, P., and Taylor, S.S. (2011). p31comet-mediated extraction of Mad2 from the MCC promotes efficient mitotic exit. J Cell Sci *124*, 3905-3916.

Williamson, A., Wickliffe, K.E., Mellone, B.G., Song, L., Karpen, G.H., and Rape, M. (2009). Identification of a physiological E2 module for the human anaphase-promoting complex. Proc Natl Acad Sci U S A *106*, 18213-18218.

Xia, G., Luo, X., Habu, T., Rizo, J., Matsumoto, T., and Yu, H. (2004). Conformation-specific binding of p31(comet) antagonizes the function of Mad2 in the spindle checkpoint. EMBO J *23*, 3133-3143.

Yang, M., Li, B., Tomchick, D.R., Machius, M., Rizo, J., Yu, H., and Luo, X. (2007). p31comet blocks Mad2 activation through structural mimicry. Cell *131*, 744-755.

Zeng, X., and King, R.W. (2012). An APC/C inhibitor stabilizes cyclin B1 by prematurely terminating ubiquitination. Nat Chem Biol *8*, 383-392.

Zeng, X., Sigoillot, F., Gaur, S., Choi, S., Pfaff, K.L., Oh, D.C., Hathaway, N., Dimova, N., Cuny, G.D., and King, R.W. (2010). Pharmacologic inhibition of the anaphase-

promoting complex induces a spindle checkpoint-dependent mitotic arrest in the absence of spindle damage. Cancer Cell *18*, 382-395.

Chapter 4

Conclusions

Cdc20 Autoubiquitination

It has been clear for some time that the majority of APC/C regulation occurs through the activating subunits Cdc20 or Cdh1. Cdc20 is a highly unstable protein, which is controlled in part through several different APC/C-dependent ubiquitination mechanisms and further enhanced by cell cycle-dependent transcription. These observations made it seem logical that controlling the abundance of Cdc20 was likely the key form of its regulation, and therefore we sought to understand the significance of removing this regulation.

We generated and expressed in yeast a version of Cdc20 that was stabilized throughout the cell cycle (the Cdc20-5K mutant) and we observed a gain of function phenotype. These cells have significantly increased Cdc20 levels and are unable to arrest in the presence of microtubule poisons that activate the Spindle Assembly Checkpoint (SAC). We believe this SAC-bypass phenotype results from the formation of SAC-resistant APC/C-Cdc20 complexes, and not from loss of interaction with SAC components caused by unexpected effects of the mutations.

Somewhat surprisingly, if we instead inhibited the ubiquitination of Cdc20 by more specific means (by deletion of the APC/C subunit Mnd2/Apc15), we observed a loss of function phenotype. Deletion of Mnd2 inhibited only one of the several mechanisms of APC/C-dependent ubiquitination of Cdc20, specifically inhibiting SAC-driven Cdc20 autoubiquitination. Cells with a decreased rate of Cdc20 turnover in the SAC, rather than failing to arrest in the SAC as might have been predicted from Cdc20-5K mutant results, instead decreased the rate at which they recovered from a SAC arrest upon removal of the microtubule poison.

Together these results allowed us to conclude that Cdc20 ubiquitination has multiple and opposing effects on the SAC. Ubiquitination of Cdc20 in late mitosis, which occurs through both an autoubiquitination mechanism and a Cdh1-dependent mechanism, is required to lower Cdc20 levels to allow the cells to establish a SAC arrest in the next cell cycle. Once arrested in the checkpoint, Cdc20 autoubiquitination is not required for the cells to maintain an arrest, but instead increases the rate at which cells inactivate the SAC and recover from the arrest. In particular, observations with the SAC-driven Cdc20 autoubiquitination have raised the following questions. First, how does Mnd2 function to promote this, and only this, APC/C-dependent ubiquitination mechanism? Second, how does autoubiquitination promote SAC inactivation?

Mnd2/Apc15 and SAC-driven Cdc20 Autoubiquitination

Mnd2/Apc15 is specifically required for SAC-driven Cdc20 autoubiquitination, and has no effect on late mitotic Cdc20 autoubiquitination or ubiquitination of any other APC/C-Cdc20 or APC/C-Cdh1 substrate we have tested. So how does Mnd2 contribute to this reaction and achieve this specificity?

The first clue comes from recent experiments conducted by both the Pines and Peters labs (Herzog et al., 2009; Izawa and Pines, 2011), which suggest that Cdc20 repositions on the APC/C when bound to the SAC components. This repositioning appears to move Cdc20 away from Cdc27 and Doc1/Apc10, the position likely required to recognize substrates, and towards Cdc23 and Apc1 (see figure 1). These observations were made by structural and mutational analyses, however, and so the specific binding sites for any of the SAC components have not been mapped. Recent work has suggested

that the Mnd2/Apc15 subunit likely binds the APC/C near Cdc23 and Apc1 (Schreiber et al., 2011; Uzunova et al., 2012), therefore putting it in at least the correct region of the APC/C to have an influence on a SAC-dependent reaction (see figure 1).

This observation suggests that Mnd2/Apc15 directly binds an SAC component, which we suspect from our data is either Mad3 or Bub3. We tested this directly (see Chapter 3 Figure 4D) and concluded that Mnd2 is unlikely to contribute much if anything to binding of the Mad3-Bub3 complex. This led us to the more intriguing conclusion that Mnd2 must either correctly orient Cdc20 within the SAC complex or the APC/C complex itself to allow this reaction to occur. Unfortunately, this model is significantly more difficult to test and will likely require structural analysis to observe such subtle differences.

SAC-driven Cdc20 Autoubiquitination and SAC Inactivation

Recent work in the SAC field has focused on mechanisms of SAC inactivation, and significant evidence has accumulated that Cdc20 autoubiquitination contributes to this process (Jia et al., 2011; Reddy et al., 2007; Uzunova et al., 2012). However, the question remains how the ubiquitination of Cdc20 specifically promotes SAC inactivation, and I will focus here on the simplified system of budding yeast.

We have addressed this question several ways. We have observed that ubiquitination of Cdc20 directly inhibits the recognition of substrates (see figure 2). This implies that upon SAC inactivation, either ubiquitin needs to be removed from Cdc20 by a deubiquitinase or ubiquitinated Cdc20 needs to be removed from the APC/C to allow a fresh Cdc20 to bind the APC/C to promote anaphase. While we have no direct evidence

either for or against a role for a deubiquitinase in SAC inactivation, this model seems unlikely because it does not provide an explanation for how other inhibitory components of the SAC are removed from the deubiquitinated Cdc20 (see figure 1). We have also observed that ubiquitination of Cdc20 does not promote the dissociation of Cdc20 from the APC/C (see Chapter 4 Figure S6). In performing these dissociation experiments, we observed that Cdc20 rapidly dissociates or is extracted if incubated in rabbit reticulocyte lysates (see Figure 3). Interestingly, this rate appears to increase if Cdc20 is polyubiquitinated by the APC/C in the presence of SAC components.

These observations suggested that a Cdc20-dissociating activity exists in these lysates, which prompted us to take a candidate approach to find the activity. Using purified components, we observed that the proteasome is only poorly capable of extracting Cdc20 from the APC/C in the presence of SAC components (see Figure 4). We have also tried extensively, to no avail, to implicate a component upstream of the proteasome, the AAA^+ ATPase Cdc48, in this process. Mounting data from our work and from others suggests that an additional factor functions downstream of Cdc20 autoubiquitination, and identification of this factor is key to a complete mechanistic picture of how the SAC is inactivated.

Conclusion

Studying the ubiquitination of Cdc20 has been a fruitful endeavor and has led to additional interesting questions regarding APC/C enzymology and SAC signaling. As should have been expected, understanding the regulation of this protein is absolutely key

to understanding how cells achieve an accurate anaphase, ensuring the integrity of their genome.

Figure 1. Proposed inhibited APC/C-Cdc20 complex generated in the SAC

During an SAC arrest, Cdc20 is bound by Mad2, Mad3, and Bub3. In the presence of the SAC components, Cdc20 is repositioned on the APC/C towards Cdc23 and Apc1, putting Cdc20 in the proximity of Mnd2/Apc15. Mnd2/Apc15 is required for efficient polyubiquitination in the presence of the SAC components, and this ubiquitinated complex likely represents the final output of the SAC signal that must be resolved upon SAC release.

Figure 1

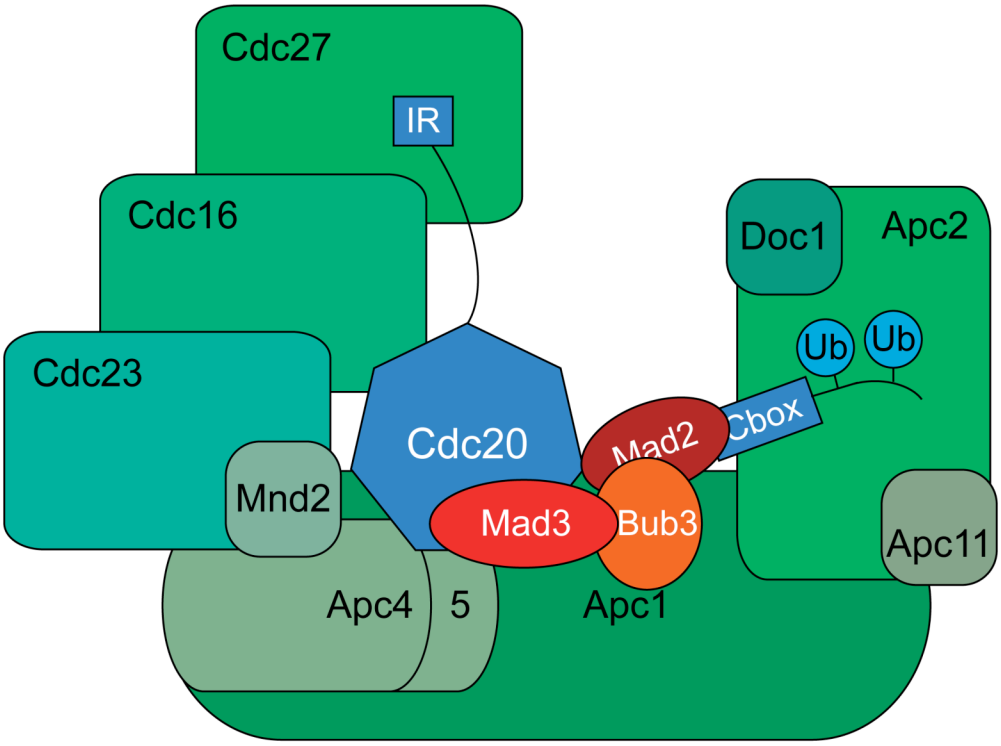
Cdc27
IR
Cdc16
Cdc23
Cdc20
Mnd2
Mad3
Bub3
Mad2
Cbox
Doc1
Apc2
Ub
Ub
Apc11
Apc4
5
Apc1

Figure 2. Autoubiquitination directly inhibits substrate ubiquitination

(A) Unlabeled or ^{35}S-Cdc20 reactions were performed in parallel. Cdc20 wild-type or 5K (see Chapter 3 Figure S4) in reticulocyte lysate was incubated TAP-APC beads and subjected to E1/E2/Ubiquitin mix. Unlabeled Cdc20 reactions were incubated with purified ^{35}S-securin and E1/E2/methyl-ubiquitin mix.

(B) Cdc20 in reticulocyte lysate was incubated TAP-APC beads and subjected to E1/E2/Ubiquitin mix, using either wild-type, K48R, or methyl-ubiquitin. Unlabeled Cdc20 reactions were incubated with purified ^{35}S-securin and E1/E2/methyl-ubiquitin mix.

(C) Cdc20 wildtype or mutant (see Chapter 3 Figure S4) Sin reticulocyte lysate was incubated TAP-APC beads and subjected to E1/E2/methyl-ubiquitin mix. Unlabeled Cdc20 reactions were incubated with purified ^{35}S-securin and E1/E2/methyl-ubiquitin mix.

Figure 2

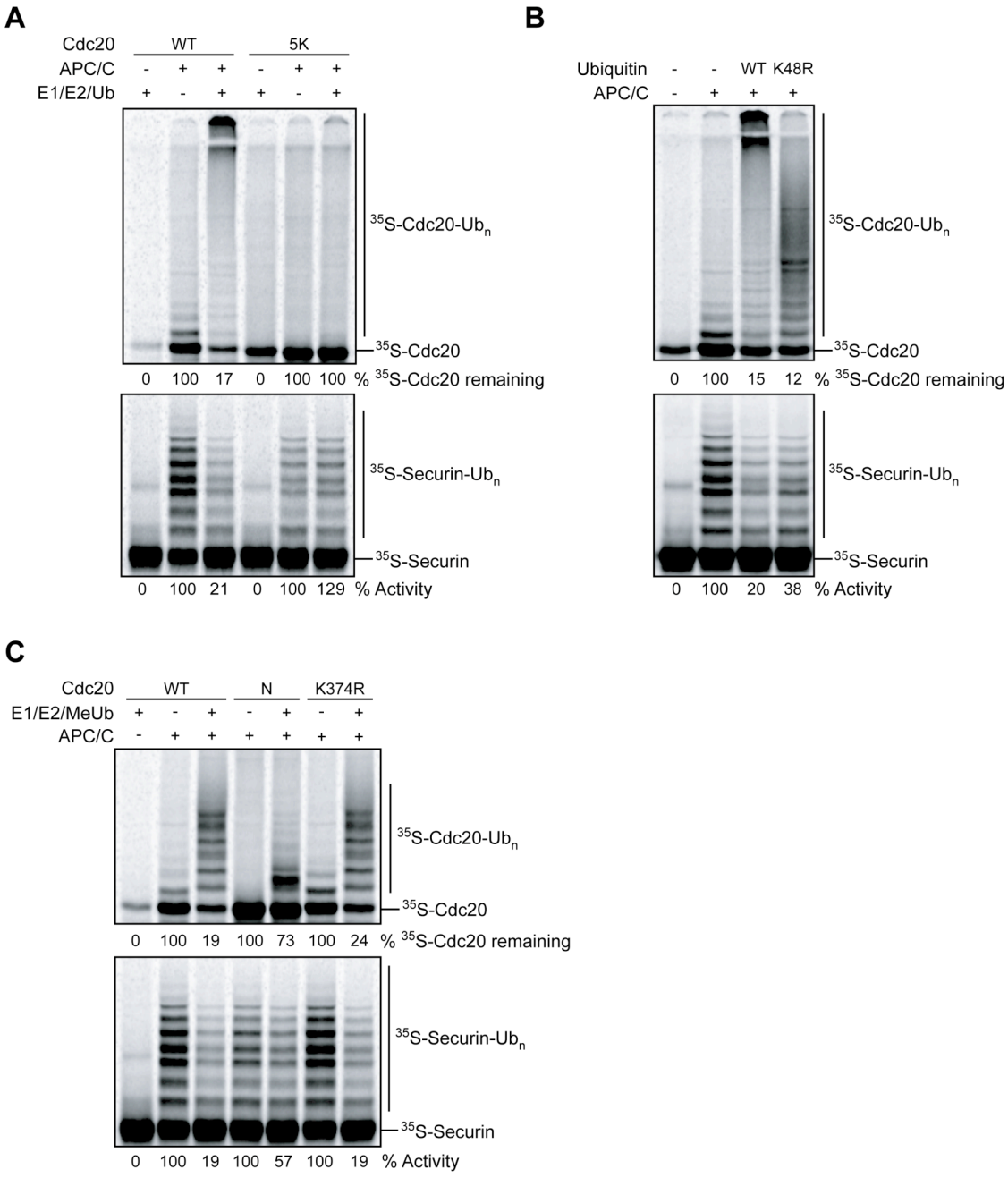
A
Cdc20 WT 5K
APC/C - + + - + +
E1/E2/Ub + - + + - +
35S-Cdc20-Ubn
35S-Cdc20
0 100 17 0 100 100 % 35S-Cdc20 remaining
35S-Securin-Ubn
35S-Securin
0 100 21 0 100 129 % Activity
B
Ubiquitin - - WT K48R
APC/C - + + +
35S-Cdc20-Ubn
35S-Cdc20
0 100 15 12 % 35S-Cdc20 remaining
35S-Securin-Ubn
35S-Securin
0 100 20 38 % Activity
C
Cdc20 WT N K374R
E1/E2/MeUb + - + - + - +
APC/C - + + + + + +
35S-Cdc20-Ubn
35S-Cdc20
0 100 19 100 73 100 24 % 35S-Cdc20 remaining
35S-Securin-Ubn
35S-Securin
0 100 19 100 57 100 19 % Activity

Figure 3. Dissociation or extraction of Cdc20 from the APC/C in lysates

To estimate the rate at which Cdc20 dissociates or is extracted from the APC/C, ^{35}S-Cdc20 in reticulocyte lysate was bound to TAP-APC/C on beads. Unbound protein was removed by washing, and the beads were incubated with a 10-fold excess cold reticulocyte. Upon addition of the excess lysate, samples were removed at the indicated times, washed quickly, and eluted with SDS sample buffer. In the reaction shown, the reticulocyte lysate contained cold Cdc20 to perform a competition experiment (with a ~10-fold excess cold Cdc20 vs ^{35}S-Cdc20). However, similar results were obtained in lysates devoid of cold Cdc20. This suggests, rather than a competitive experiment, the lysate actually contains an activity that is extracting the ^{35}S-Cdc20.

Figure 3

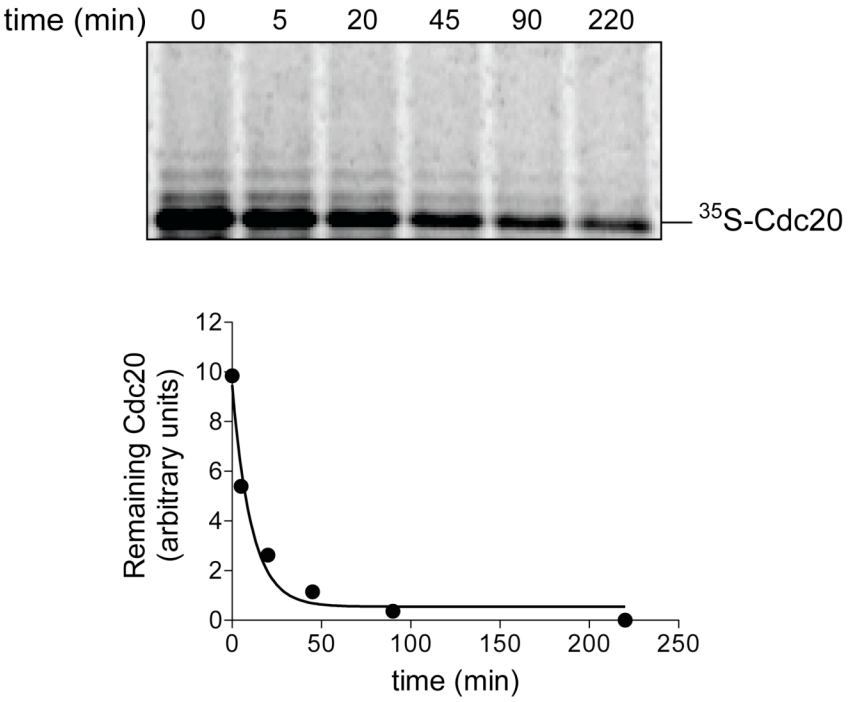
time (min)
0
5
20
45
90
220
35S-Cdc20
Remaining Cdc20
(arbitrary units)
12
10
8
6
4
2
0
0
50
100
150
200
250
time (min)

Figure 4. Purified proteasome is not sufficient to extract ubiquitinated Cdc20 from the APC/C

^{35}S-Cdc20 in reticulocyte lysate was pre-incubated with 5 μM Mad2 and 1 μM Mad3-Bub3 before addition to TAP-APC beads. Unbound material was removed and Cdc20 bound to checkpoint proteins was subjected to E1/E2/ubiquitin mix for 1 h. Polyubiquitinated Cdc20 was exposed to the indicated proteasome concentration. After a 1h reaction, unbound material was removed and the remaining material was eluted with SDS sample buffer.

Figure 4

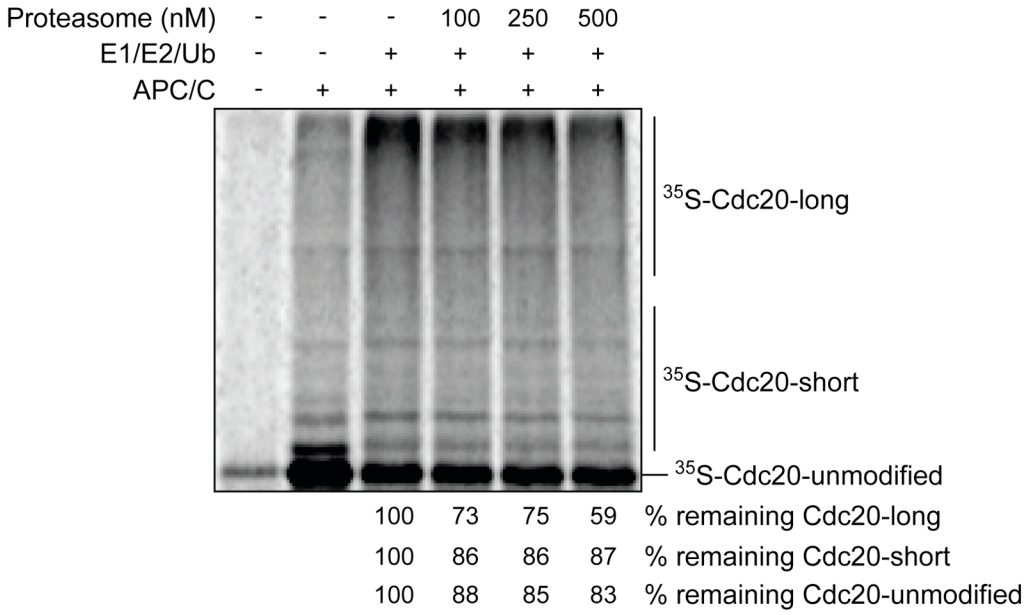
Proteasome (nM) - - - 100 250 500
E1/E2/Ub - - + + + +
APC/C - + + + + +
35S-Cdc20-long
35S-Cdc20-short
35S-Cdc20-unmodified
100 73 75 59 % remaining Cdc20-long
100 86 86 87 % remaining Cdc20-short
100 88 85 83 % remaining Cdc20-unmodified

REFERENCES

Herzog, F., Primorac, I., Dube, P., Lenart, P., Sander, B., Mechtler, K., Stark, H., and Peters, J.M. (2009). Structure of the anaphase-promoting complex/cyclosome interacting with a mitotic checkpoint complex. Science *323*, 1477-1481.

Izawa, D., and Pines, J. (2011). How APC/C-Cdc20 changes its substrate specificity in mitosis. Nat Cell Biol *13*, 223-233.

Jia, L., Li, B., Warrington, R.T., Hao, X., Wang, S., and Yu, H. (2011). Defining pathways of spindle checkpoint silencing: functional redundancy between Cdc20 ubiquitination and p31(comet). Mol Biol Cell *22*, 4227-4235.

Reddy, S.K., Rape, M., Margansky, W.A., and Kirschner, M.W. (2007). Ubiquitination by the anaphase-promoting complex drives spindle checkpoint inactivation. Nature *446*, 921-925.

Schreiber, A., Stengel, F., Zhang, Z., Enchev, R.I., Kong, E.H., Morris, E.P., Robinson, C.V., da Fonseca, P.C., and Barford, D. (2011). Structural basis for the subunit assembly of the anaphase-promoting complex. Nature *470*, 227-232.

Uzunova, K., Dye, B.T., Schutz, H., Ladurner, R., Petzold, G., Toyoda, Y., Jarvis, M.A., Brown, N.G., Poser, I., Novatchkova, M.*, et al.* (2012). APC15 mediates CDC20 autoubiquitylation by APC/C(MCC) and disassembly of the mitotic checkpoint complex. Nat Struct Mol Biol *19*, 1116-1123.

Publishing Agreement

It is the policy of the University to encourage the distribution of all theses, dissertations, and manuscripts. Copies of all UCSF theses, dissertations, and manuscripts will be routed to the library via the Graduate Division. The library will make all theses, dissertations, and manuscripts accessible to the public and will preserve these to the best of their abilities, in perpetuity.

Please sign the following statement:

I hereby grant permission to the Graduate Division of the University of California, San Francisco to release copies of my thesis, dissertation, or manuscript to the Campus Library to provide access and preservation, in whole or in part, in perpetuity.

Scott Fortin
Author Signature

1-8-13
Date